

This item was submitted to Loughborough University as a PhD thesis by the author and is made available in the Institutional Repository (<https://dspace.lboro.ac.uk/>) under the following Creative Commons Licence conditions.



For the full text of this licence, please go to:
<http://creativecommons.org/licenses/by-nc-nd/2.5/>



Department of Chemistry

Polymeric ladderanes; structural
characterization and their application
in synthetic organic chemistry

By Emma Stubbs

Supervisors: Dr B. Buckley, Dr. S. Dann and Prof. H. Heaney

A thesis submitted in partial fulfilment of the requirements for
the award of Doctor of Philosophy at Loughborough University

Abstract

A range of copper(I) alkynyl ladder polymers have been prepared via a simple single step microwave reaction at 100 °C for 2 minutes, using copper hydroxyacetate ($\text{Cu}_2(\text{OH})_3\text{Ac}\cdot\text{H}_2\text{O}$) as the copper source, all with yields in excess of 80 %. A variety of functional groups were chosen ranging from a simple aromatic phenol ring, substituted aromatic groups, groups with a long carbon chain, and an example of 2 alkynyl units in one chain. The polymeric structure of these materials has been elucidated by powder X-ray diffraction, the results of which confirm that by changing the R groups on the copper ladder chains the structure of the ladder itself is altered to accommodate the variety of sizes and shapes. This was further detailed using a series of methyl substituted phenyl rings as the R group (ortho, meta and para), which were further examined by solid state NMR, and Raman spectroscopy. The raman data confirmed that the copper –copper distance in the ladder backbone varied based on the side group present. The NMR results suggest that not only are there variations to copper backbone, but also there are different possible positions for the aromatic group to stack in based on the substitution on the aromatic ring. All data collected indicates the crystallinity of the polymer is strongly affected by the choice of alkyne.

The range of ladder polymers has been used to catalyse a series of dipolar cycloaddition reactions of terminal alkynes and organic azides, with the aim to obtain additional mechanistic information on the alkyne-azide click reactions. These reactions were carried out using a simple microwave method requiring an excess of alkyne (1.5 eq) to azide (1 eq), using 10 mol% of the ladder polymer as catalyst for 10 minutes at 100 °C. These conditions were then modified slightly to allow for “on water” catalysis of the click reactions using copper(I) alkynyl ladder polymers. Triazole products were obtained in excellent yields ranging from approximately 60 -95%. Using similar conditions it was also possible to introduce an iodo group to the triazole product when starting with iodoacetylene rather than a terminal alkyne, with only slightly reduced yields of 50-70%. Flow chemistry was briefly tested and was shown to be a viable option for the synthesis of 1,2,3-triazoles using copper(I) alkynyl ladder polymer catalysts.

The support material copper on carbon was investigated for comparison with the copper(I) alkynyl ladder polymers. The support material was found to actually be a composition of copper hydroxynitrate, a layered material capable of forming copper(I) ladder polymers, and carbon. A series of these materials were made using different supports using the same method as carbon, and all resulted in a mixture of copper hydroxynitrate and support material. An impurity was discovered in specific carbon batches (depending on the carbon preparation method) and was identified as libethenite (copper hydroxyphosphate). A series of click reactions were carried out using these copper hydroxynitrate/carbon mixtures and excellent yields of 80-90% were obtained, the impurity libethenite was also tested but found to not catalyse the click reaction.

Acknowledgments

This work has taken a lot of effort over the past 4 years, but without the help and support of a number of individuals I would never have made it this far!

Firstly I would like to give massive thanks to Dr Ben Buckley and Dr Sandie Dann, for giving me this opportunity, but also for your help and support over the last 4 years. You have both taught me a lot, not just about chemistry but about myself as well. You both kept me going when I thought I was at my wits end, thank you.

I'd like to give a special mention to Dr Caroline Kirk for your extra help with the materials side of things whenever Sandie was away! Also to Dr Mark Edgar for all his hard work and effort helping me with the solid state NMR work, and to Pauline King for all your help with a variety of instruments, especially that pesky XRD!

I would also like to thank all of the people past and current that reside in the lovely labs F009 and F001, you all made coming into the lab every day that little bit less depressing, and my life has been made the better for knowing you all! I feel special thanks should be made to Anish my Buckley group bench buddy for all the great banter we had! Also the lovely ladies Trish, Nat, Tash and Bea at least we managed to keep things a little girly around all those men! Helen and Vicky, whilst we weren't in the same lab (shame) my occasional visits upstairs to see you both made an enormous difference to my state of mind, thank you both!

Adam, you brought happiness back into my life and my heart and gave me the motivation I needed to finish this work, without you I don't think I'd have made it.

Finally a big thanks to all my family for their support and encouragement for the last few years, without you I have no doubt in my mind I would not have made it to where I am today. Laura after this I should finally be able to get a 'real' job!

Mum, Dad, and Laura this final thank you is for you.

Table of Contents

Abstract.....	2
Acknowledgments	3
Abbreviations	6
Introduction	8

Chapter 1

Layered Materials and Metal Alkynyl Complexes	14
Introduction.....	15
Preparation of Ladder Polymers	28
Characterisation of Structures.....	37
Solid State NMR Studies of Copper Ladder Polymers	37
Raman and IR Studies of Copper Ladder Polymers	41
Mixed Metal Polymer Species	48
Chapter 1 Conclusion	51
Chapter 1 Experimental	52

Chapter 2

Catalysis and Click Chemistry	57
Introduction.....	58
Alkynyl Copper Ladder Polymers as Catalysts.....	68
Click “on Water” Reactions	73
Mechanistic Discussion	80
Flow Chemistry.....	81
Chapter 2 Conclusion	83
Chapter 2 Experimental.....	84
General Experimental Details.....	84
Preparation of Azides	84
Preparation of Acetylenes.....	86
Click Reactions	88

Chapter 3

Solid Support Materials	109
Introduction.....	110
Preparation of Copper on Solid Support Materials	115
Identification of the Impurity Phase	119
Click Reactions	122
Further use of Copper on Carbon to Catalysis Organic Reactions.....	125
Ullmann Synthesis.....	125
Heterogeneous Copper-Catalysed Asymmetric Hydrolysatation	127
Chapter 3 Conclusion	129
Chapter 3 Experimental.....	130
General Experimental Details.....	130
Preparation of solid support materials.....	131
Libethenite.....	132
Solid support materials in Click Reactions.....	133
Solid support materials in Ullamnn ether coupling Reactions.....	136
Solid support materials in Asymmetric Hydrolysatation Reactions.....	139
Conclusions	141
Further Work.....	142
Supplementary Work	144
References	145

Abbreviations

Analytical Terms

XRD – X-Ray Diffraction

SEM – Scanning electron microscopy

TEM – Transmission electron microscopy

NMR – Nuclear magnetic resonance

FT-IR – Fourier Transform – Infra Red

MS – Mass spectrometry

TOF-MS – Time of flight mass spectrometry

GC – Gas Chromatography

ESI – Electrospray ionisation

ICP AES – Inductively coupled plasma atomic emission spectroscopy

TGA – Thermogravimetric analysis

TLC – Thin layer chromatography

General Terms

CuAAC – Copper catalysed azide-alkyne cycloaddition

Eq. – Equivalents

Aq. – Aqueous

R.T. – Retention time

m.p – Melting point

UV – Ultra violet

Cat. – Catalyst

qC – Quaternary carbon

Arom. - Aromatic

Solvents / Chemicals

MeCN – Acetonitrile

MeOH – Methanol

CDCl₃ – Chloroform

TMS – Tetramethylsilane

THF – Tetrahydrofuran

EtOAc – Ethyl acetate

NEt₃ – Triethylamine

DMAP – 4-dimethylaminopyridine

DETA - diethylenetriamine

^tBuOH – *tert*-Butylalcohol

Bz – Benzoyl

PMP – *p*-methoxyphenyl

MMPP – Magnesium Monoperoxyphthalate

PMHS - Polymethylhydrosiloxane

Introduction

Ladderanes are typically organic molecules containing two or more fused cyclobutane rings, in a ladder like arrangement. Their geometry is highly strained as the carbon skeleton cannot extend to the desired angle. A variety of synthetic approaches, often using a [2+2] photocycloaddition, have been developed for the synthesis of ladderanes of various lengths. [1] There have been examples of naturally occurring ladderanes, for example ladderanes are a component of the anammoxsome membrane of the anammox bacteria, Planctomycetes. [2]

Ladderanes can be sub classified into linear and closed ladderanes. Linear ladderanes have simpler structures, and have the ability to fold back on themselves. If the first ring and the last ring of a linear ladderane are fused together a closed ladderane is produced. As closed ladderanes contain prismatic structure they are also referred to as [n]-prismanes. [3]

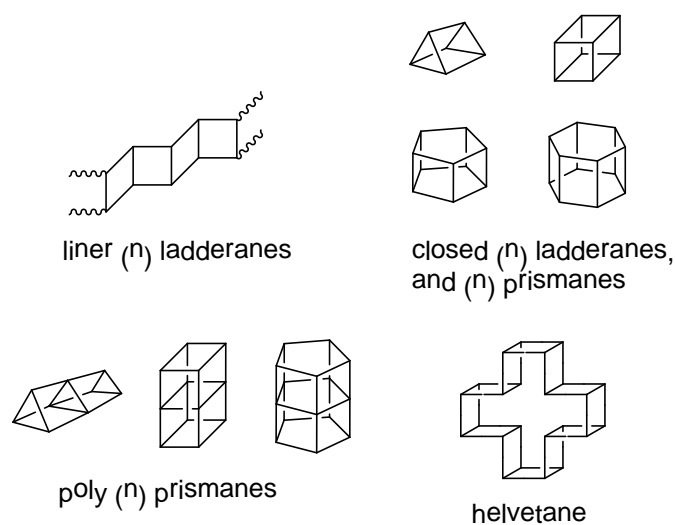


Figure 1: Examples of a variety of ladderane structures [3]

Ladderanes have important applications in material science, due to the ladderanes structural rigidity and electronic properties, they can be functionalised and used as molecular rods, [4] stiff spacers, [5] and molecular devices. [6]

The ladder like structure of ladderanes is not just limited to carbon fused rings. There are examples containing further group 14 elements such as silicon. [7]

The x-ray crystal structure of oligosilane ladders differs notably from the carbon ladderane analogues, which have been reported to have a planar structure, whereas each cyclotetrasilane ring is folded with fold angles of 21.4 – 21.8 °, as shown in Figure 2. [7]

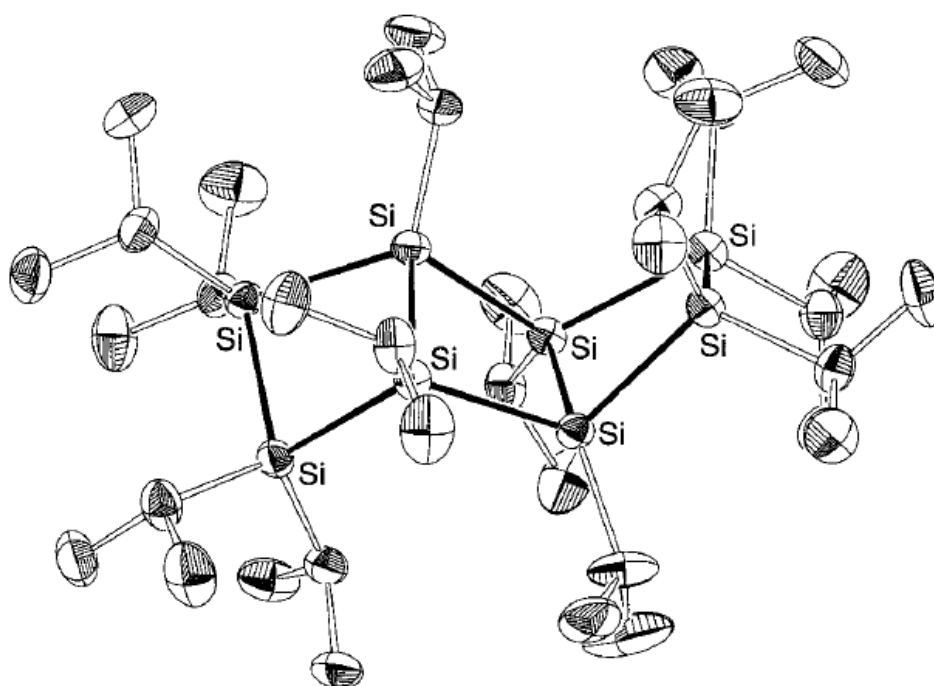


Figure 2: X-ray crystal structure of oligosilane ladder like species (thermal ellipsoids at 30% probability level) [7]

There are also examples of heavier metal atoms forming ladder like structures. One example is a simple tin species $[\text{C}_6\text{N}_2\text{H}_{18}]^{2+}2[\text{SnPO}_4]^-$, the structure involves edge sharing of 4 membered $\text{Sn}_2\text{P}_2\text{O}_4$ rings which form one dimensional chains in the form of ladders, this is shown in Figure 3. [8]

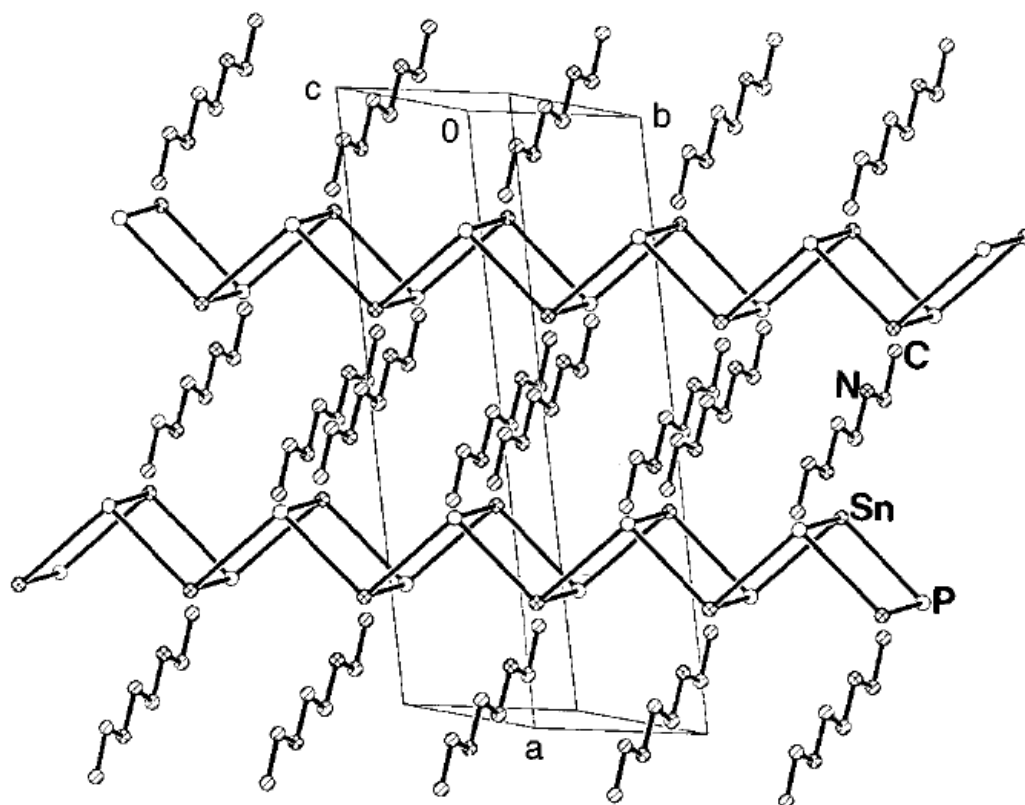


Figure 3: Structure of $[\text{C}_6\text{N}_2\text{H}_{18}]^{2+}2[\text{SnPO}_4]^-$ showing the ladders and the amine. [8]

Another Example is a zinc phosphate species consisting of ladder like layers. ^[9] $[\text{NH}_3(\text{CH}_2)_2\text{NH}(\text{CH}_2)_2\text{NH}_3]^{2+} 2[\text{Zn}_2\text{PO}_4(\text{HPO}_4)]^-$ has a framework structure made from the tetrahedral linkage between ZnO_4 and PO_4 moieties sharing the vertices. Connectivity between these units forms anion layers, with a doubly protonated structure directing agent (DETA) between them. Therefore the structure can be considered to be made up of alternating anionic (inorganic) and cationic (organic) layers. These layers are connected by chains formed from the connectivity between the ZnO_4 and PO_4 units, forming a layer with ladder like steps, shown in Figure 4. ^[9]

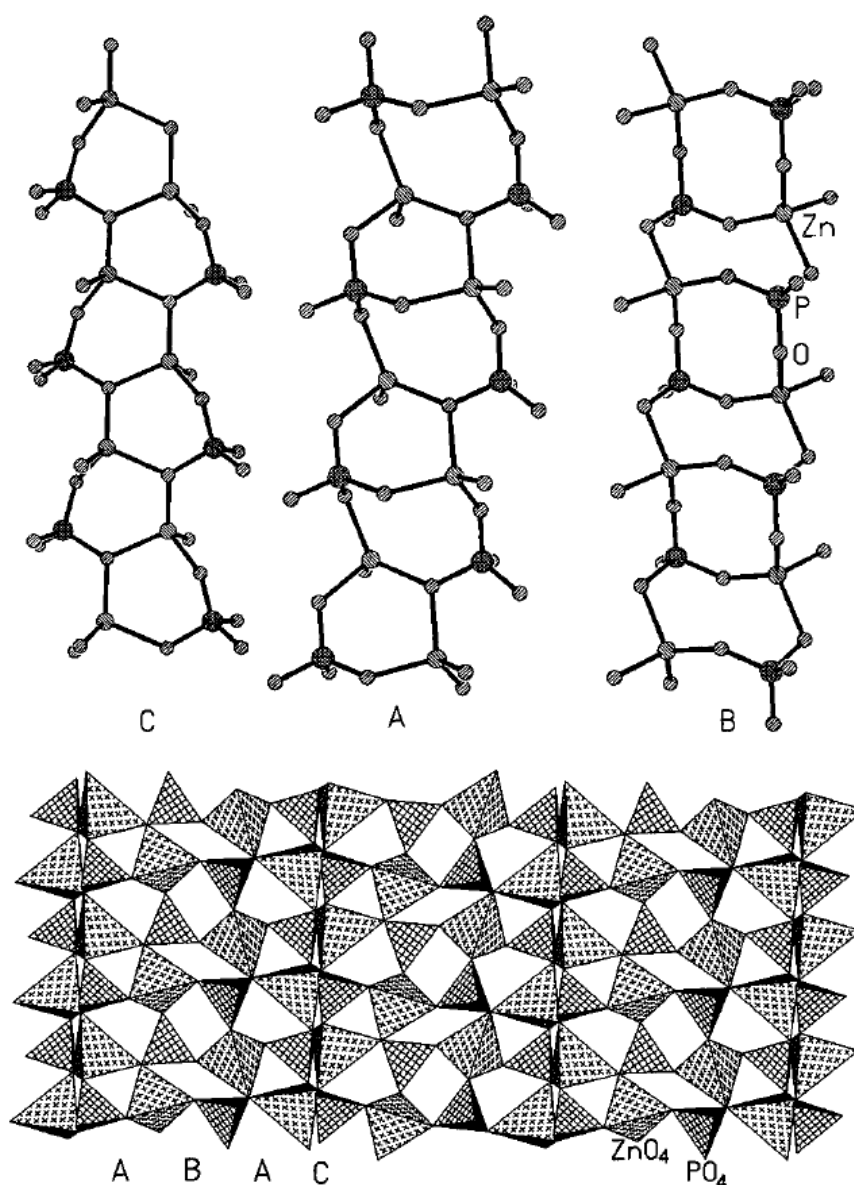


Figure 4: The different type of chain arrangements that are seen in $[\text{NH}_3(\text{CH}_2)_2\text{NH}(\text{CH}_2)_2\text{NH}_3]^{2+} 2[\text{Zn}_2\text{PO}_4(\text{HPO}_4)]^-$ (Top), Polyhedral view along the [010] direction showing the layers, the various chains, and the connectivity between them. ^[9]

There are a limited number of examples of ladder like structures involving copper atoms within the backbone. In 1966 Corfield and Shearer reported the crystal structure of phenylethynyl(trimethylphosphine)copper(I).^[10] The structure is shown in Figure 5 where it is possible to see a ladder like copper backbone.

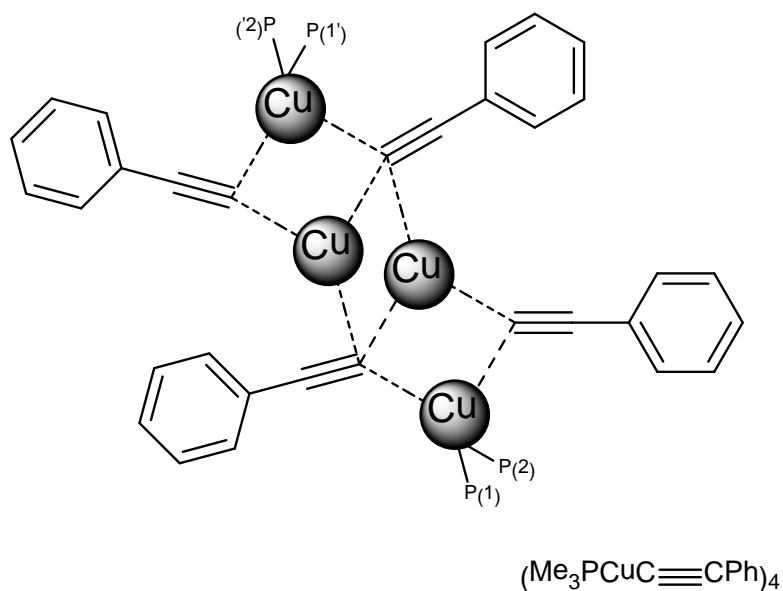


Figure 5: crystal structure of phenylethynyl(trimethylphosphine)copper(I).^[10]

The research detailed in this thesis will revolve around a species similar to that shown in Figure 5, an alkynyl copper(I) ladder polymer, whose structure is a copper ladder chain backbone with an alkynyl side group.

Chapter 1 contains information regarding the structural characterisation of the ladder polymers using powder XRD, Raman and solid state NMR, as well as a brief introduction to the possibility of mixed metal ladder species.

Chapter 2 explains the use of alkynyl copper(I) ladder polymers as catalysts in the copper catalysed azide-alkyne cycloaddition (CuAAC) reaction, looks into the use of “on water” conditions from greener chemistry, the addition of iodoalkanes, and the use of flow chemistry.

Chapter 3 details the comparison of a series of solid support materials with alkynyl copper(I) ladder polymers, comparing structural properties and potential as catalysts in the CuAAC reaction.

Finally the published work with regards to this thesis is listed at the end in the supplementary work.

Chapter 1

Layered Materials and Metal Alkynyl Complexes

Introduction

Layered materials have been the subject of great interest over that past decade due to the various possible chemical applications in fields such as separation science, ^[11] drug delivery, ^[12] and catalysis. ^[13,14] The most salient feature of layered materials is the ability to modify and control their interlayer spacing, which allows chemists to tailor their physical properties to a specific application, therefore making them excellent substrates for advanced material design.

Layered double hydroxides (LDH) and layered hydroxide salts (LHS) are types of layered materials which consist of positively charged layers with charge balancing anions between the layers. ^[15] These structures may be considered as modifications of the mineral brucite, $\text{Mg}(\text{OH})_2$. The brucite structure is based on individual layers of Mg^{2+} centered octahedra with hydroxide groups located on the vertices. Each $\cdot\text{OH}$ is surrounded by three metal cations resulting in neutral layers this can be seen in Figure 6. ^[16]

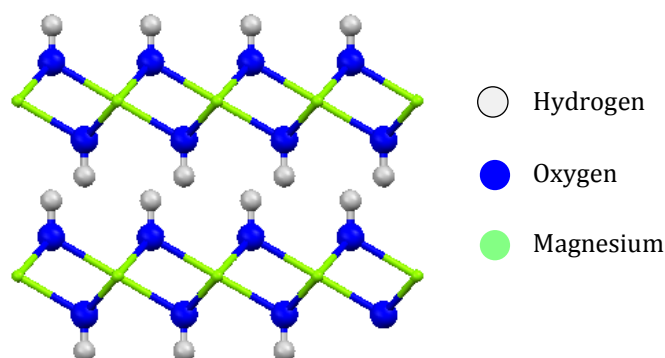


Figure 6: General schematic of the brucite structure, with the space group $p3m1$.

Layered double hydroxides (LDH) are formed by modifying the brucite structure, replacing some of the Mg^{2+} cations with a trivalent cation (M^{3+}), forming a positively charged brucite like layered compound. An anion lying within the interlayer spacing provides charge compensation. LDH's can be represented by the general formula $[\text{M}^{2+}_{1-x}\text{M}^{3+}_x(\text{OH})_2]^{x+}(\text{A}^{m-})_{x/m}\cdot n\text{H}_2\text{O}$ where M^{3+} and M^{2+} are metal cations and A is a counter anion with m^- charge. As can be shown in the formula, there are also some water molecules within the interlayer spacing. An example of a naturally occurring LDH is hydrotalcite, which consists of Mg^{2+} , Al^{3+} , and CO_3^{2-} , a generic LDH is shown in Figure 7.

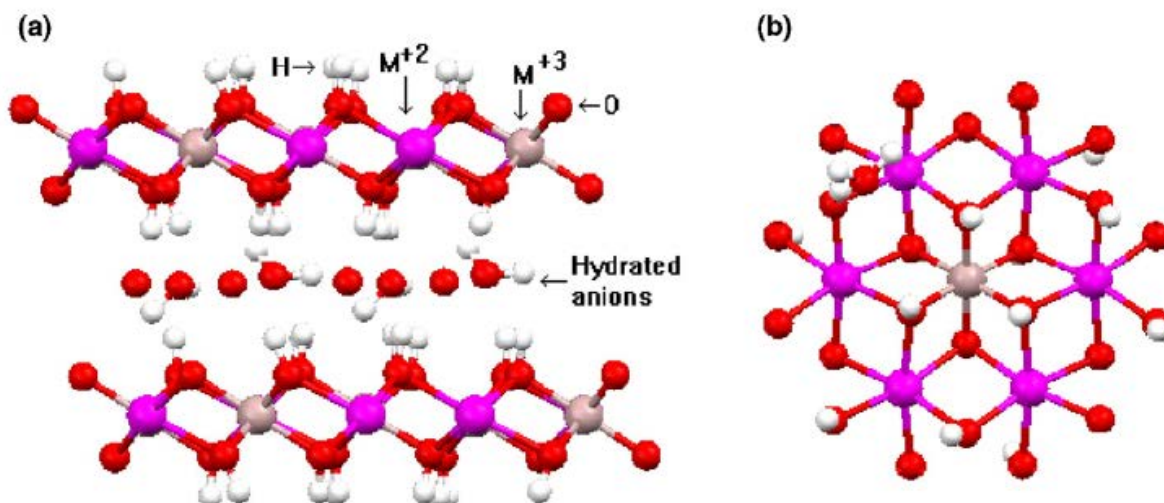


Figure 7: Schematic representation of the structure of a generic LDH. (a) Side and (b) top view [16]

Hydroxy double salts (HDS) have a similar structure to that of layered double hydroxides, with the key difference being the presence of two types of divalent cation. This type of layered material can be given the general formula $[(M_{1-x}^{2+}Me_{1-x}^{2+})(OH)_{3(1-y)}]^{+}A_{(1+3y)/n}^{-}.zH_2O$ where the anions of variable negative charge can compensate for the positive charge within the layer. [17]

Another possible modification to the brucite structure is the isomorphic substitution of cations in the layers or substitution of part of the hydroxide groups by appropriate anions or water molecules. [16] This type of modification forms layered hydroxide salts (LHS) with the general formula $M^{2+}(OH)_{2-x}(A^{m-})_{x/m}.nH_2O$ where M^{2+} is the metal cation and A^{m-} is the counter ion. An example LHS, copper hydroxide sulfate, is shown in Figure 8.

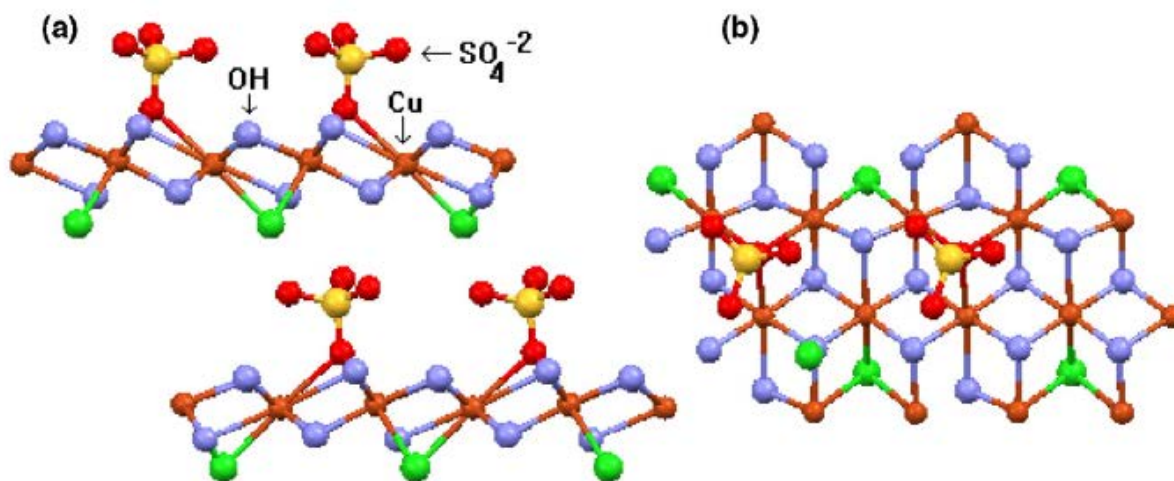


Figure 8: Structure of copper hydroxide sulfate, an example LHS, (a) side and (b) top view [16]

Structure-property relationships exist in nearly all facets of materials chemistry and therefore it is essential to carefully characterise materials in order to improve their properties. This applies not only to the synthesis steps themselves but also to slight alterations in chemical composition. For the study of these layer type structures, characteristic techniques of particular importance are powder X-ray diffractometry (PXRD) and vibrational spectroscopy (both Fourier transform infrared spectroscopy (FTIR) and Raman spectroscopy). Electron microscopy (SEM/TEM) is often used to investigate the periodicity and faults in the layers, and thermal analysis (TG/DTA/DSC) can be used to assess structural stability.

Powder XRD is one of the preferred techniques for analysis of layered materials. The XRD patterns normally exhibit a low angle reflection which is directly related to the interlayer distance, which is then normally followed by the other 001 reflections, shown simply in Figure 9, which tend to be strong in reflection mode measurements due to preferred orientation of the lamellar type crystallites, although these are dependent on the quality of the long range order of the layer packing. [16]



Figure 9: Simple diagram of LDH reflections which align in a plane to give much stronger reflections than would otherwise be observed.

FTIR is both a powerful and practical method of obtaining information pertaining to functional groups. For layered materials the pertinent information is mainly derived from the counter ions within the interlayer spaces. In layered materials it is also possible to observe vibrations originating from the main lattice of metal to oxygen bonds, which are detected in the low wave number region (typically 400-800 cm^{-1}).

For example the lattice vibrations for the layered copper hydroxynitrate phase $\text{Cu}_2(\text{OH})_3\text{NO}_3$ for which 3 absorptions were recorded for the Cu-O-H bending modes at 876, 784 and 673 cm^{-1} , the variation in frequencies for the same vibrational mode was attributed to the various degrees of hydrogen bonding available. [18] The ability to identify the counteranion within the layers of these materials is essential as atmospheric carbon dioxide can generate carbonate anions in solutions which can be intercalated in the interlayer spacing. Some of these carbonate species occur naturally as minerals, such as malachite, which are extremely stable. The presence of carbonate in layered hydroxysalts as an impurity effects reactivity and the presence of carbonate during synthesis in solution has been monitored by FTIR. [19]

Thermal decomposition profiles of layered materials are generally made up of two isolated thermal events. Firstly the loss of water of hydration, followed by decomposition to the metal oxide which releases water from dehydroxylation and sometimes gas from the counter ions if the materials contain anions which can decompose (e.g. acetate, nitrate). Figure 10 shows an example TG profile for α -cobalt hydroxide nitrate. It can be seen that hydration water is gradually lost until 200 $^\circ\text{C}$ followed by the decomposition of the nitrate from 200-500 $^\circ\text{C}$. [16]

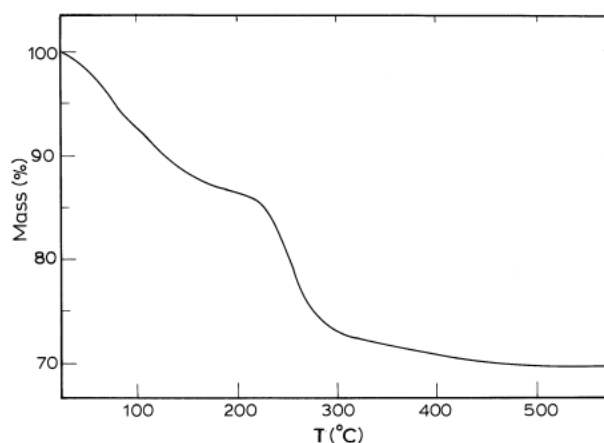


Figure 10: Thermogravimetric profile of α -cobalt(II) hydroxide with intercalated nitrate ions [16]

The natural mineral gerhardtite ($\text{Cu}_2(\text{OH})_3\text{NO}_3$) is a type of layered material from a family of copper hydroxy salts, which can be given the formula $\text{Cu}_2(\text{OH})_3\text{X}$ where X is a monovalent anion such as NO_3^- or CH_3COO^- . Gerhardtite has gained specific attention due to its synthetic analogue being used in vehicle airbags. [18] Synthetic gerhardtite can be prepared through direct reaction of $\text{Cu}(\text{NO}_3)_2$ and NaOH aqueous solutions, [20] or by the digestion of CuO in $\text{Cu}(\text{NO}_3)_2$ concentrated aqueous solutions. [21] The naturally occurring and synthetic forms of copper hydroxy nitrate exist as two different polymorphs, gerhardtite which has an orthorhombic cell ($a=6.087(2)$, $b=13.813(4)$, $c=5.597(2)$ Å), [22] or the synthetic version which is obtained as a monoclinic metastable phase ($a=5.596(2)$, $b=6.079(2)$, $c=6.925(3)$ Å). It is possible to distinguish the two types of copper centres for both polymorphs. In both cases the copper ions co-ordinate to four hydroxide ions in the equatorial position, however in one case the copper co-ordinates to one nitrate and one hydroxide ion, and in the other case to two nitrate ions in the axial positions. [22] These [4+2] and [4+1+1] distorted octahedral arrangements are examples of Jahn-Teller distortions related to the $3d^9$ configurations of copper(II). [23] This can be seen in Figure 11.

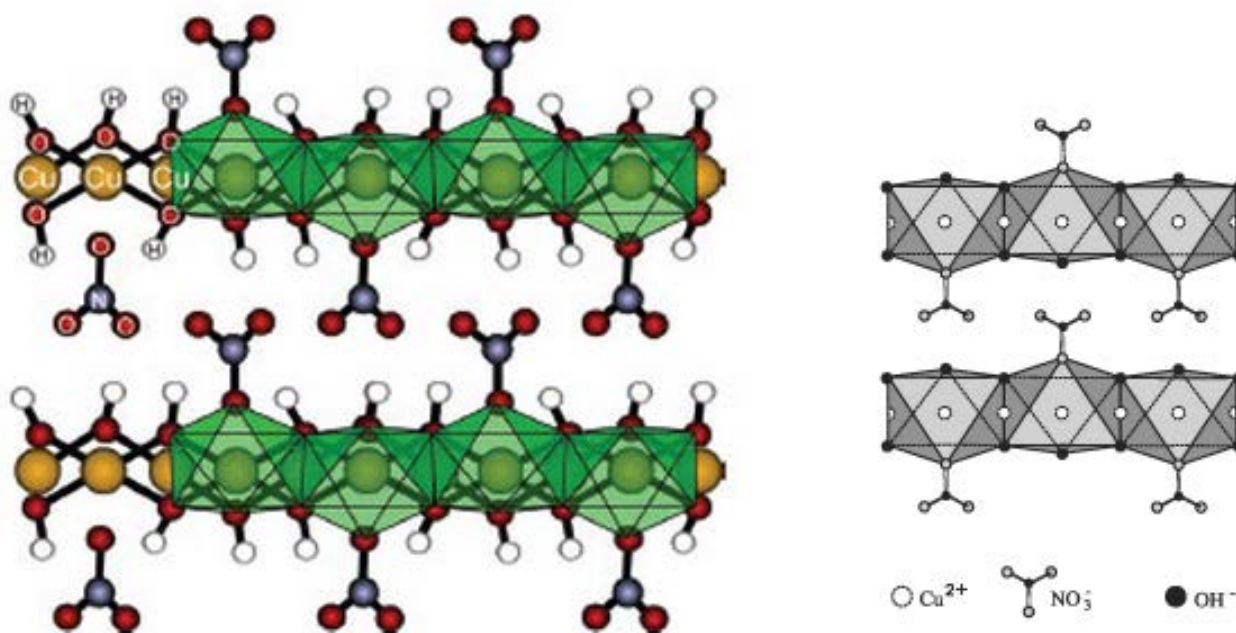


Figure 11: Layered structure of copper hydroxy nitrate, where 1/4 of the sites are occupied by nitrate ions

[23,24]

Pereira and co-workers explored the complementary structural information obtained by XRD, FTIR, and Raman to contribute to the understanding of the copper hydroxy salt family. [23] Figure 12 shows the powder XRD patterns obtained for 3 types of copper hydroxy salts, copper hydroxy nitrate ($\text{Cu}_2(\text{OH})_3\text{NO}_3$), copper hydroxy acetate ($\text{Cu}_2(\text{OH})_3\text{OAc}$), and copper hydroxy perchlorate ($\text{Cu}_2(\text{OH})_3\text{ClO}_4$). The basal spacing increases from 6.81 Å to 7.28 Å to 9.42 Å as the nitrate anion is replaced by the larger anions, perchlorate and acetate respectively causing an increase in the interlayer spacing.

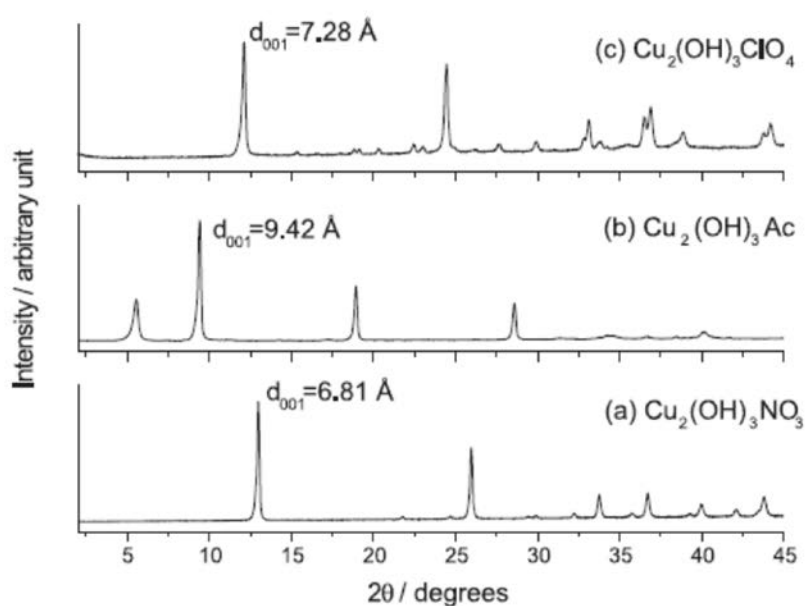


Figure 12: XRD patterns of: (a) copper hydroxy nitrate, (b) copper hydroxy acetate, (c) copper hydroxy perchlorate [23]

The authors also obtained thermogravimetric curves (TGA and DTG) for both copper hydroxy nitrate and acetate (Figure 13).

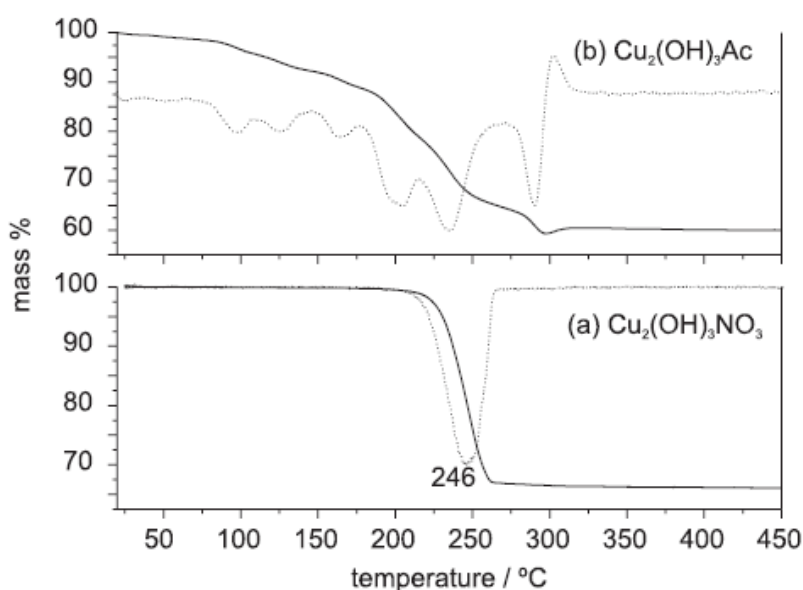
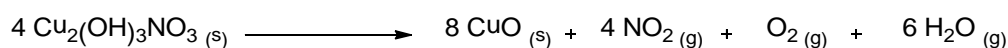


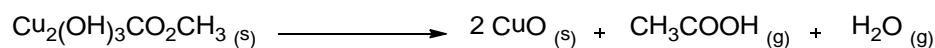
Figure 13: TGA (full) and DTG (dashed) for copper hydroxy nitrate (a) and acetate (b) [23]

The decomposition of the hydroxy nitrate occurs in one step to form CuO via the following equation (Scheme 1). [21]



Scheme 1: Decomposition of hydroxy nitrate to copper oxide [21]

There is no loss of water observed due to the material being anhydrous. In the acetate case, water is lost from the interlayer space in two steps up to 145 °C, followed by decomposition to CuO via the following equation (Scheme 2) [23]



Scheme 2: Decomposition of hydroxy acetate to copper oxide [23]

Information was also obtained by Pereira and co-workers from the Raman and IR spectra for copper hydroxy nitrate (Figure 14). [23] The Raman spectra showed four weak modes at 258, 408, 455, and 505 cm^{-1} , which agree with previously reported data. [25,26] However, there is some disagreement between the authors as to the band assignments of these modes. The modes relating to the nitrate ion are of particular interest, as these provide information on the ions symmetry. In its free state the nitrate ion belongs to the point group D_{3h} with irreducible representation for internal modes $\Gamma = A'_1 + A''_2 + 2E'$, originating four normal modes ν_1, ν_2, ν_3 and ν_4 . If the ion symmetry is lowered to C_{2v} or C_s the degeneracies of the E' representations are removed and splitting of the originally degenerate modes are observed. [23]

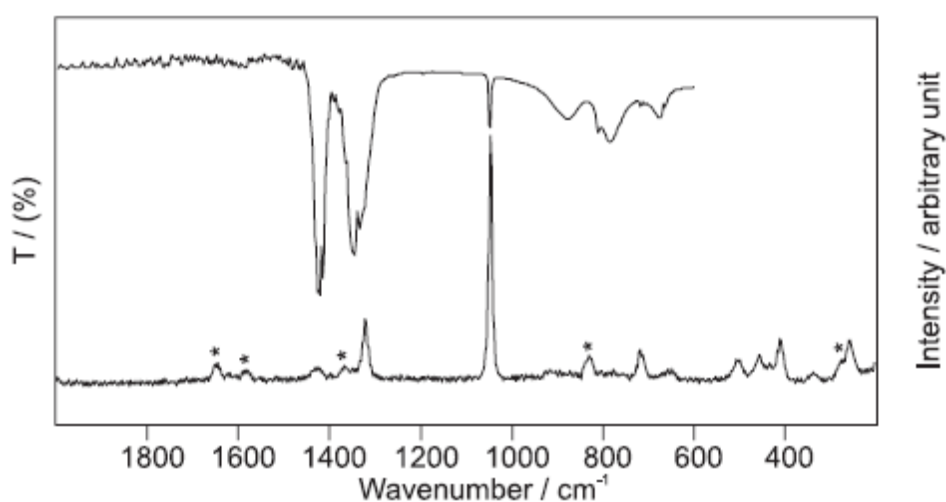


Figure 14: FTIR and Raman spectra of $\text{Cu}_2(\text{OH})_3\text{NO}_3$ [23]

The splitting of the ν_3 mode can be clearly seen in Figure 14, with bands at 1335, 1346, 1416, and 1421 cm^{-1} . The weak splitting (86 cm^{-1}) indicates a weak interaction between the nitrate ion and the layers of the lattice. A similar effect was expected for the ν_4 mode, but this was not evident in either Raman or IR spectra, the same is true for other studies in the literature. [26,27] The sharp band at 1049 cm^{-1} corresponds to the ν_1 mode and confirms the loss of degeneracy as this band would not be IR active if the ion still had D_{3h} symmetry. From these data the authors concluded that the nitrate ion coordinates to copper through a relatively weak interaction, with bidentate coordination not supported (as the ν_3 splitting would be much larger for bidentate coordination). [23]

The planar morphologies of these layered materials are also of interest as they can be used in the assembly of nanoribbons, of various compositions, which can be used in areas such as nanodevices. [28] Zhu and co-workers describe an approach to growing single-crystalline $\text{Cu}_2(\text{OH})_3\text{Cl}$ nanoribbons and their characterisation using a variety of electron microscopy techniques to examine the morphology of the crystals and powder XRD data to confirm the crystal structures of their products. [29] Figure 15 shows a micrograph of the morphologies collected on a field emission SEM of the $\text{Cu}_2(\text{OH})_3\text{Cl}$ nanoribbons. The average width of a ribbon was found to be 50 nm and up to several micrometers in length.

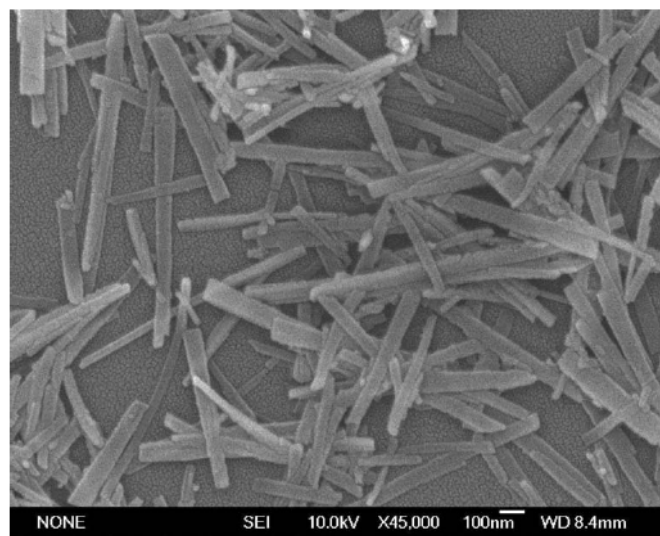


Figure 15: Field emission SEM image of the $\text{Cu}_2(\text{OH})_3\text{Cl}$ nanoribbons [29]

Metal alkynyl complexes are another group of materials which are of interest in both synthetic and materials chemistry, with a vast amount of research being reported since the mid 1980's ranging from complexes with just one alkynyl group bound to a metal centre, to polymeric species which can contain as many as 10,000 M-C≡C- linkages. The species can be applied to various purposes, due to the inclusion of both a transition metal centre which can provide redox, [30] optical, [31] and magnetic [32] properties, and the alkynyl species which can sometimes provide luminescence, [33, 34, 35, 36] non-linear optic effects, [37] and electronic communication. [38] Both the alkynyl group and the metal can each have catalytic relevance in various types of syntheses.

These transition metal alkynyl complexes can be regarded as complexes of the HC≡C- ligand, which is isoelectronic with CN⁻, CO and N₂. [39] The complexes stoichiometry, colour, and magnetic properties are closely related to the corresponding cyanide complexes. Alkynyl and cyanide ligands share a simple frontier-orbital relationship, wide ranging spectroscopic and magnetic studies have shown both ligands occupy similar "strong-field" positions in the spectrochemical series. [39]

Metal alkynyl complexes can generally be synthesized by either the reaction of metal halides with anionic alkynylating agents, such as copper(I) [40] or magnesium [41] or by direct dehydrohalogenation. [42]

A metal alkynyl complex of particular importance is the electron rich d¹⁰ acetylides, due to their impressive structural diversity [43] and their possible photoluminescent properties [44], along with applications in organic optoelectronics [45] and luminescence signalling. [46] Che and co-workers have reported the structures of a number of these homoleptic d¹⁰ metal alkynyl complexes. [47]

The first species observed showed a Cu_{20} cluster, from powder X-ray and single crystal diffraction data, the ORTEP diagram of the molecular structure is shown in Figure 16. The structure has twenty ${}^t\text{BuC}\equiv\text{CCu}$ units which are crystallographically independent, and can be seen as an interlocking of a distorted Cu_8 ring with two puckered hexagonal Cu_6 rings. The single crystal data were then used as a starting model for the Rietveld refinement of the powder XRD data, which afforded good agreement ($R_p=5.27\%$, $R_{wp}=7.68\%$) between the experimental and calculated data. [47]

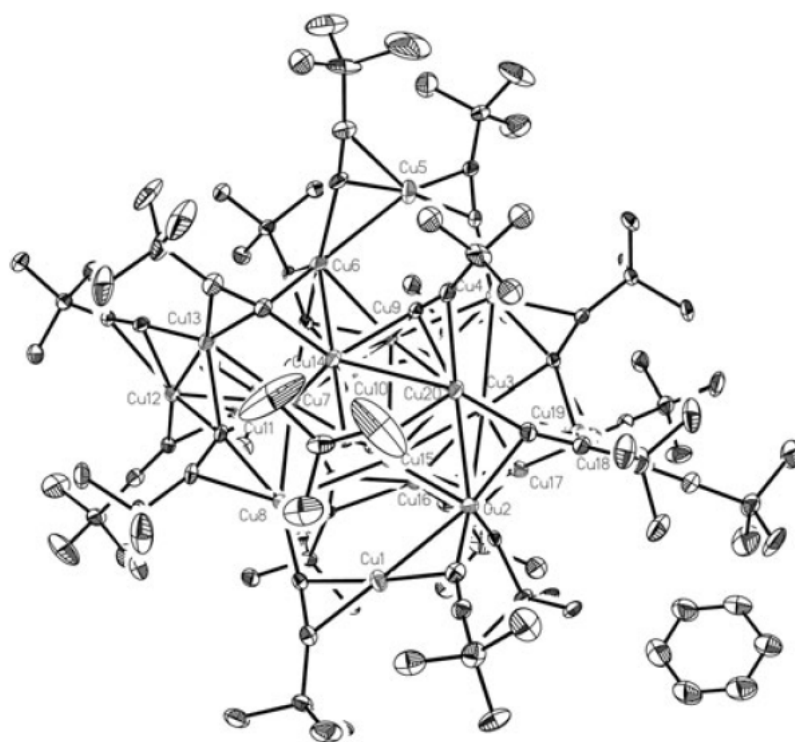


Figure 16: ORTEP diagram of crystal structure of Cu_{20} molecular cluster [47]

By changing the $t\text{BuC}\equiv\text{C}$ group to a $\text{PhC}\equiv\text{C}$ species the authors were able to form the polymeric species $[\{\text{PhC}\equiv\text{CCu}\}_\infty]$ shown in Figure 17. They found that a crystallographic 21 screw axis parallel to the polymer chain bisected Cu-Cu so that the $\text{PhC}\equiv\text{C}$ groups were projecting alternatively up and down along the chain. The group was able to show that the refined Cu-Cu distances were 2.49(4)-2.83(2) Å, and the Cu-C distances were 1.95(1)-2.63(1) Å. [47] This type of ladder like topology had not been reported in previous literature examples. [48,49]

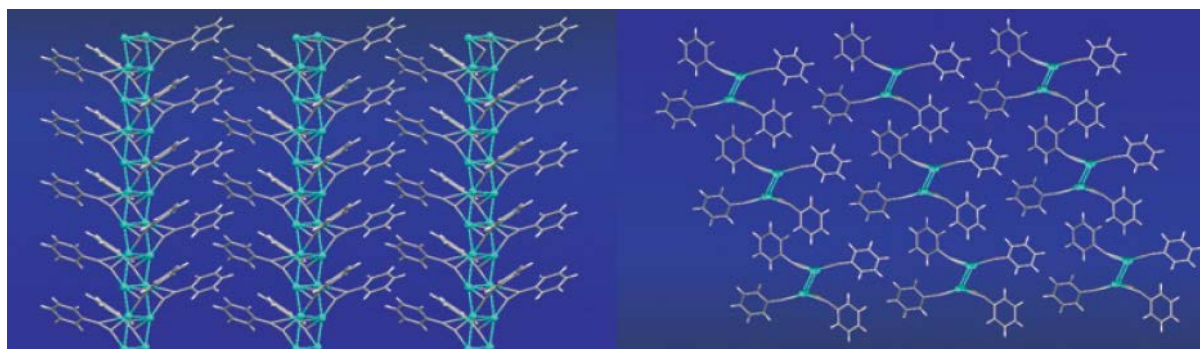


Figure 17: (Left) ladder like polymeric structure of $[\{\text{PhC}\equiv\text{CCu}\}_\infty]$ (right) perspective view of solid state packing in [010] direction [47]

Long range intermolecular interactions between the aromatic rings can also be observed, with weak $\text{C-H}\cdots\pi$ interaction ($d>3.35\text{Å}$) and insignificant $\pi\cdots\pi$ stacks ($d>3.7\text{Å}$) noted. [47]

When Che and co-workers examined the corresponding silver complexes, they observed similarities within the powder XRD patterns, with the first three reflections having similar intensities but shifted to a lower 2θ angle. When indexed the silver species showed a monoclinic cell parameter similar to that of the copper species, but with a larger cell volume, all of which suggests that the silver species resembled the structure of the copper ladder like polymer, $[\{\text{PhC}\equiv\text{CAg}\}_\infty]$. [47] The refined structure is shown in Figure 18.

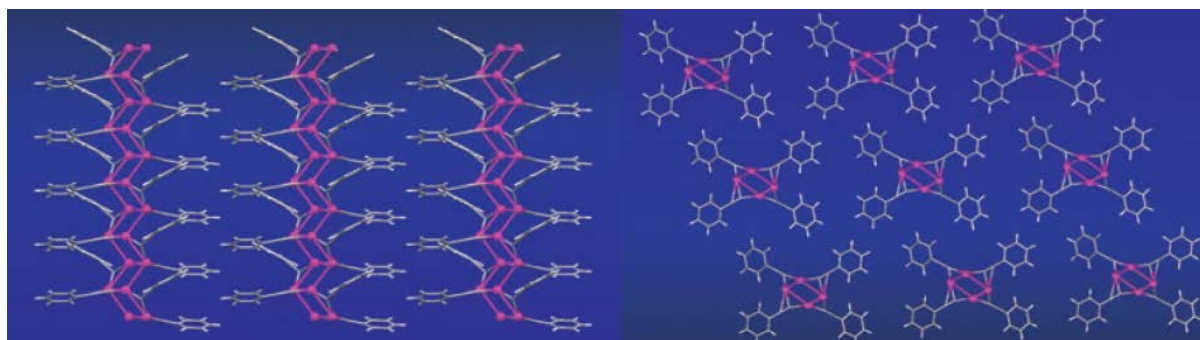


Figure 18: (Left) ladder like structure of $[\{\text{PhC}\equiv\text{CAg}\}_\infty]$ showing a higher degree of folding compared with its copper counterpart. (Right) perspective view of solid state packing in $[010]$ direction ^[47]

An increase of zig-zag folding of the ladder was observed in the silver species compared to the copper, though this makes sense due to the difference in M-M-M bond angles (105.2° for Ag and 163.5° for Cu), the refined Ag-Ag distance was approximately 3.13 \AA , ^[47] falling between the metallic radius (2.89 \AA) and the sum of van der Waals radii of two silver atoms (3.4 \AA). ^[50] The paper concludes with the formation of a gold analogue $[\{\text{PhC}\equiv\text{CAu}\}_\infty]$. The refinement data from the powder XRD showed a structure different to the silver and copper analogues with a layered network of $\text{Au}\bullet\bullet\bullet\text{Au}$ with $\text{PhC}\equiv\text{C}$ pillars in a honeycomb like network, shown in Figure 19. The refined $\text{Au}\bullet\bullet\bullet\text{Au}$ distances were $2.98(1)\text{-}3.27(1) \text{ \AA}$, ^[47] which is longer than the metallic radius of gold (2.88 \AA), ^[50] which suggests that the gold atoms are weakly intercalating within the sheet. ^[51]

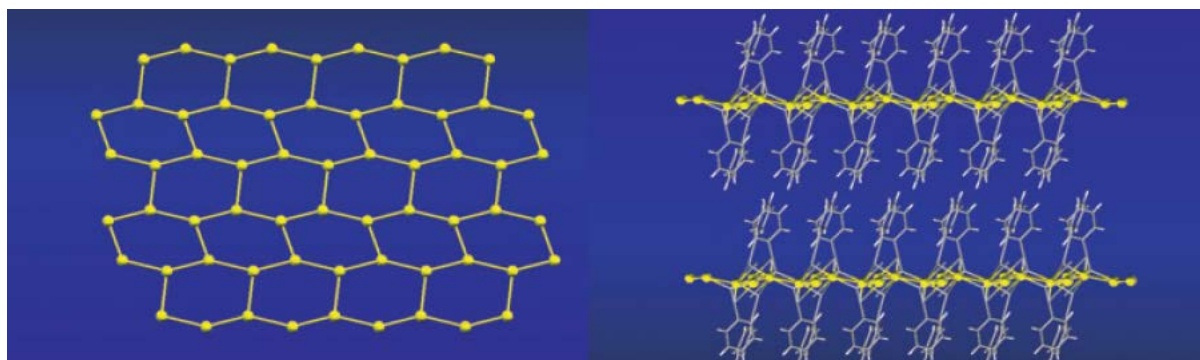


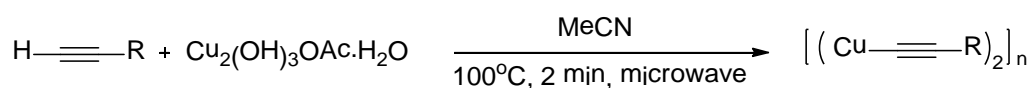
Figure 19: (Left) depiction of the gold honeycomb network. (Right) pillared network of $\text{PhC}\equiv\text{C}$ groups ^[47]

Table 1: Crystal structure information for the copper, silver, and gold ladder species. ^[47]

	$[\{\text{PhC}\equiv\text{CCu}\}_\infty]$	$[\{\text{PhC}\equiv\text{CAg}\}_\infty]$	$[\{\text{PhC}\equiv\text{CAu}\}_\infty]$
Crystal system	monoclinic	monoclinic	triclinic
Space group	$P2_1$	$P2_1$	$P1$
$a \text{ (\AA)}$	15.451(3)	18.512(4)	6.238(1)
$b \text{ (\AA)}$	5.287(2)	4.971(1)	7.531(1)
$c \text{ (\AA)}$	10.283(2)	13.413(3)	15.017(1)

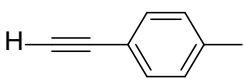
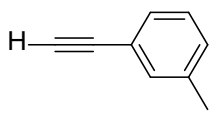
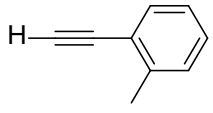
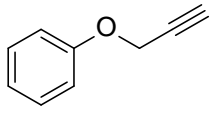
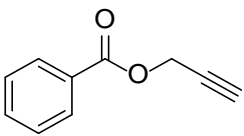
Preparation of Ladder Polymers

In an effort to further investigate the packing behaviour of the alkynyl copper(I) ladder polymers, a range of ladders were synthesised using various R groups by the general method shown in Scheme 3. Different R groups were chosen varying in their bulk and/or arrangement of substituted groups on the organic group attached to the copper backbone, for example, closely related species (**2**, **3**, and **4**). The R groups prepared have been summarised in Table 2.



Scheme 3: General reaction for the formation of copper(I) ladder polymers shown in Table 2

Table 2: Variety of synthesised copper(I) ladder polymers a with the corresponding alkyne starting materials.

Alkyne	Product
$\text{H}-\text{C}\equiv\text{C}-\text{Ph}$	$[(\text{Cu}-\text{C}\equiv\text{C}-\text{Ph})_2]_n$ 1
	$[(\text{Cu}-\text{C}\equiv\text{C}-\text{C}_6\text{H}_4)_2]_n$ 2
	$[(\text{Cu}-\text{C}\equiv\text{C}-\text{C}_6\text{H}_4)_2]_n$ 3
	$[(\text{Cu}-\text{C}\equiv\text{C}-\text{C}_6\text{H}_4)_2]_n$ 4
$\text{H}-\text{C}\equiv\text{C}-\text{CH}_2\text{OH}$	$[(\text{Cu}-\text{C}\equiv\text{C}-\text{CH}_2\text{OH})_2]_n$ 5
	$[(\text{C}_6\text{H}_4\text{O}-\text{C}\equiv\text{C}-\text{Cu})_2]_n$ 6
	$[(\text{C}_6\text{H}_4\text{O}-\text{C}(=\text{O})-\text{O}-\text{C}\equiv\text{C}-\text{Cu})_2]_n$ 7

Alkyne	Product
	$\left[\left(\text{C}_9\text{H}_{17}\text{Cu} \right)_2 \right]_n$ 8
	$\left[\left(\text{C}_6\text{H}_8\text{Cu} \right)_2 \right]_n$ 9
	$\left[\left(\text{C}_{10}\text{H}_7\text{Cu} \right)_2 \right]_n$ 10 <i>Not Formed</i>
	$\left[\left(\text{Cu-Si} \right)_2 \right]_n$ 11 <i>Not Formed</i>
	$\left[\left(\text{C}_{14}\text{H}_{19}\text{Cu} \right)_2 \right]_n$ 12

General conditions: Cu₂(OH)₃OAc (0.5 eq.), alkyne (3.0 eq.), MeCN, 100°C microwave, 2 min.

Entry **10** could not be investigated, as the preparation of the starting alkyne material was unsuccessful. Entry **11** did not form a copper ladder polymer either but is discussed further on page 35.

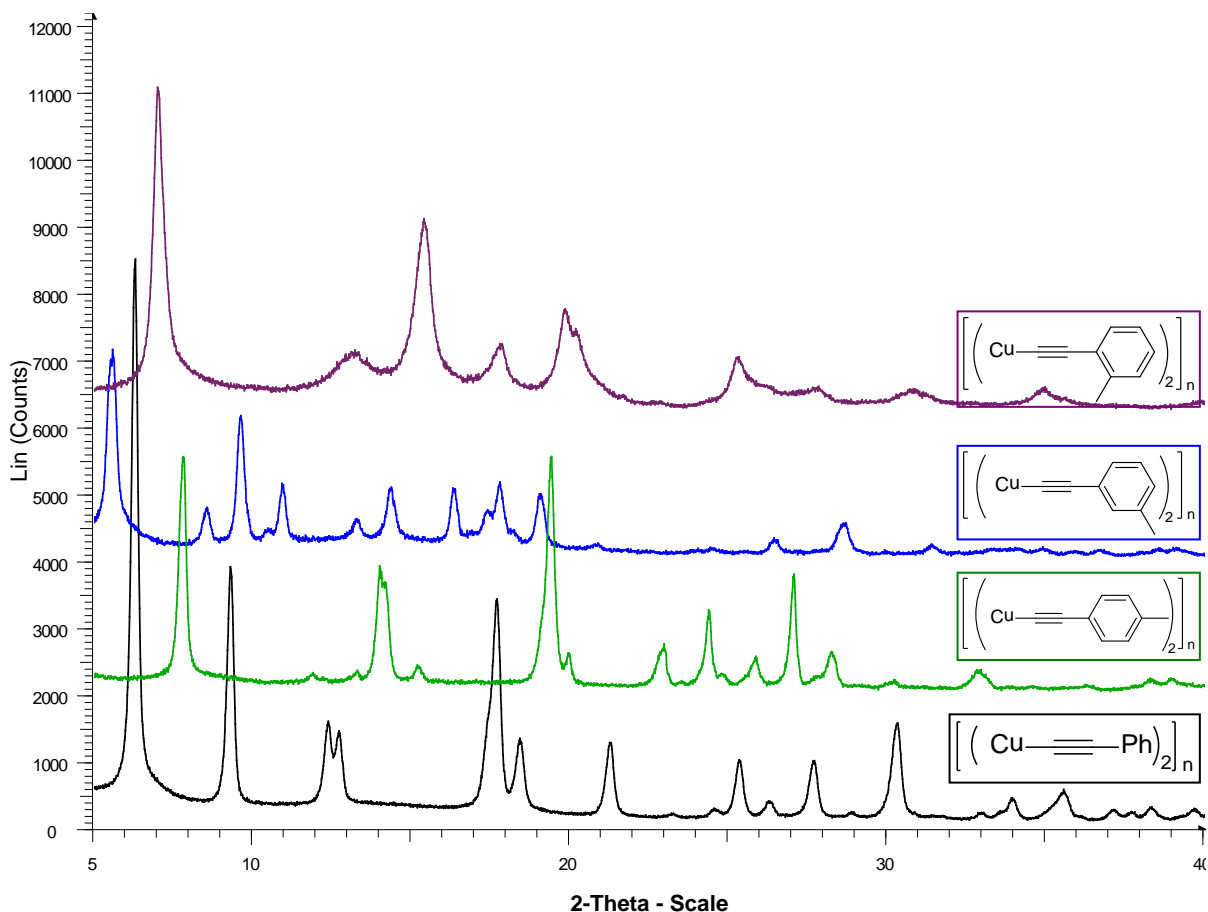


Figure 20: Powder XRD patterns for ladder polymers with various aromatic functionalization

Entries **1-4** all worked well and show variation in the XRD patterns, which show that the position of the methyl group on the aromatic ring affects the ladders spacial packing. XRD patterns for these species are shown in Figure 20, and indicate a variation in the size of the particles as the two theta width of the reflections at half maximum height varies markedly. For example, the broadness of the reflections in entry **4** (re. Debye Scherer equation) ^[52] indicates much poorer long range order than that of entry **1**.

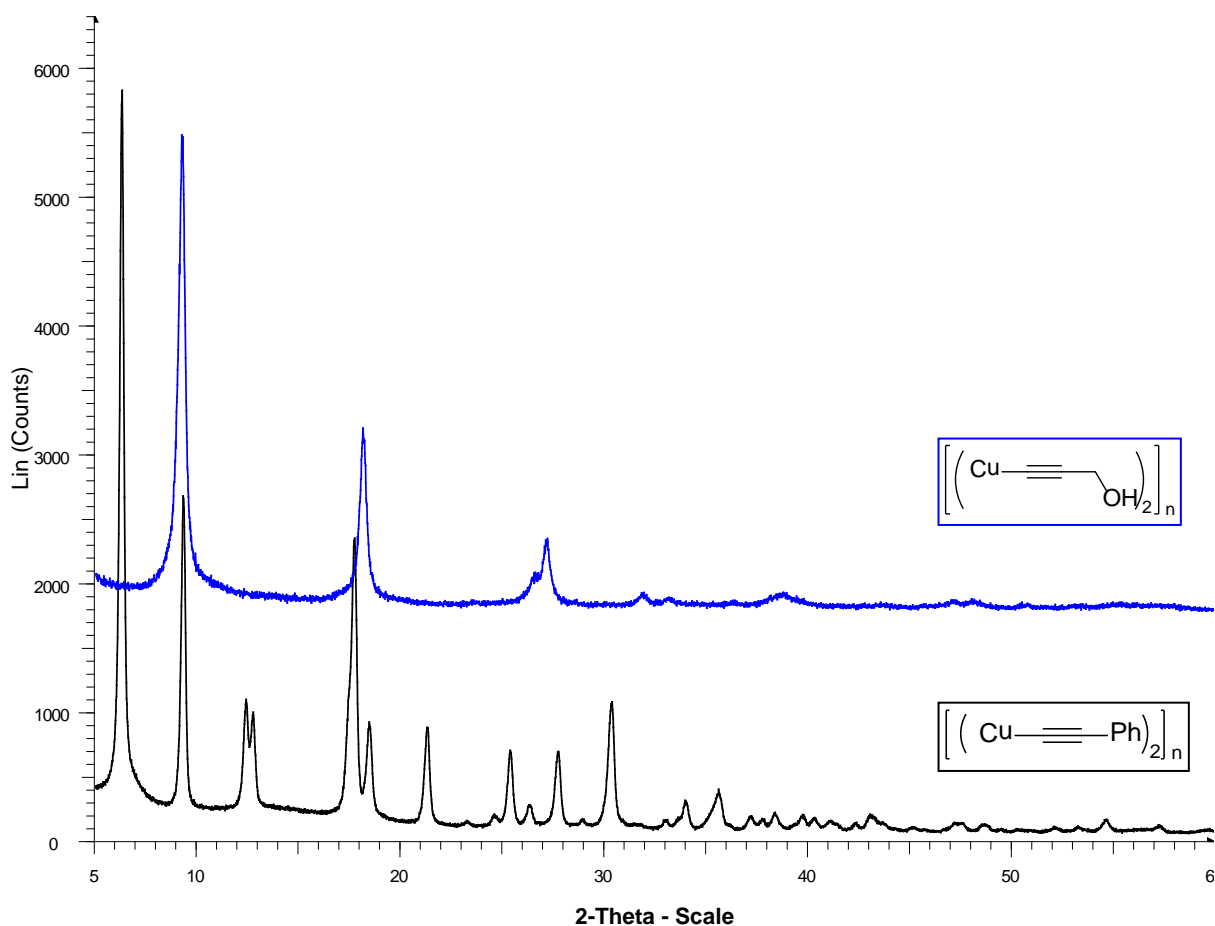


Figure 21: Powder XRD comparison of an aromatic ring and an alcohol group on the copper(I) ladder polymers. The alcohol example shows a larger distance between the reflections suggesting shorter Cu-Cu bonds

Entry 5 produced a ladder polymer that was a darker orange/yellow colour which suggests a shorter copper – copper bond distance in the ladder, which is plausible as the alcohol group is much smaller than the aromatic groups, the XRD pattern shown in Figure 21, supports this theory as the reflections are spaced much further apart and shifted to higher 2 theta values.

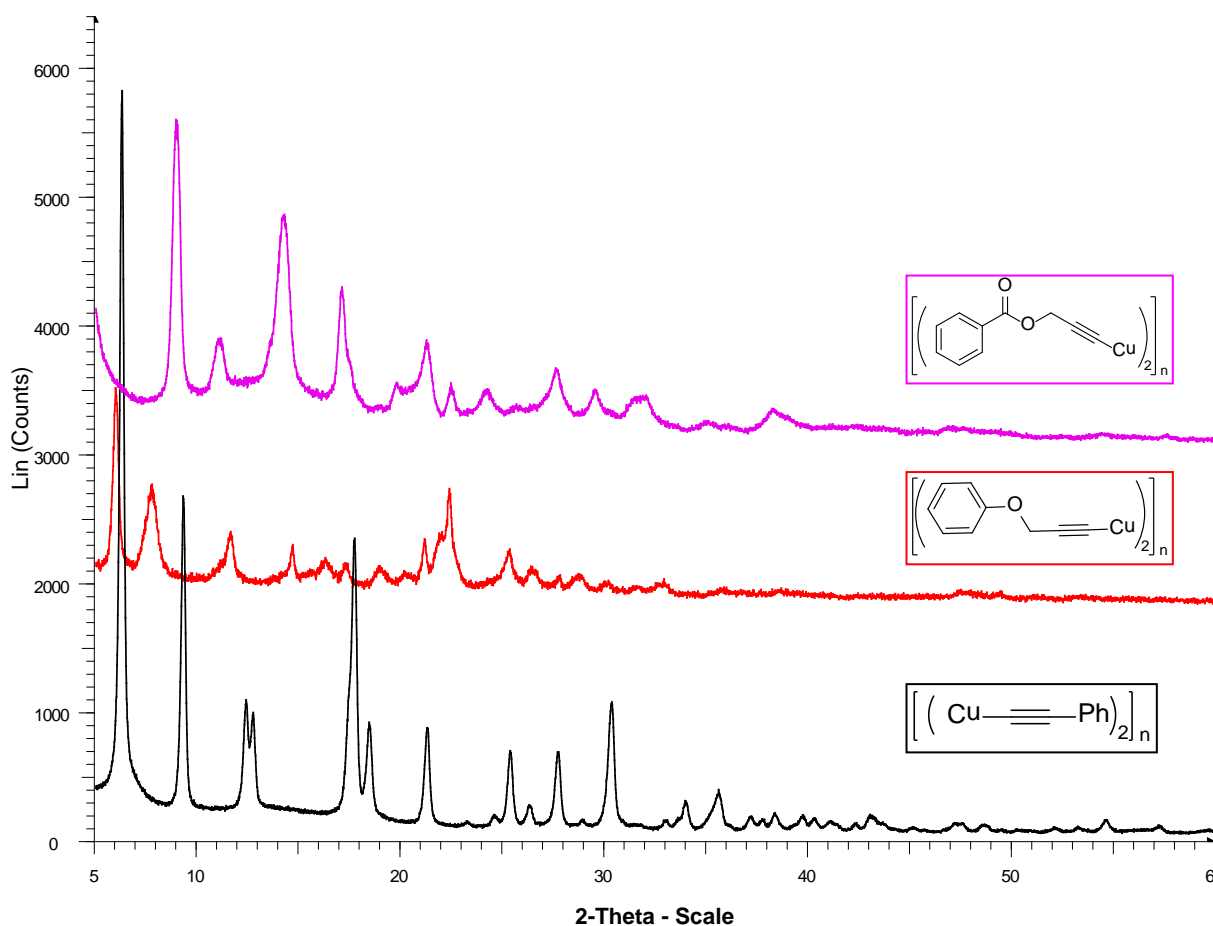


Figure 22: Powder XRD patterns of two extended aromatic structures attached to the copper chain (Red and Purple) compared to phenylethynyl copper(I) ladder polymer

Entries **6** and **7** produced ladder polymers which we know are able to catalyse the CuAAC reactions (the CuAAC reaction is discussed in more detail in chapter 2), however they show more amorphous content in their XRD patterns, which will make them harder to fully characterise. This is probably due to the extended structure between the aromatic ring and the triple bond, which means the stacking of functional groups within the ladder will be more complex. The XRD patterns are shown in Figure 22, compared to that of the phenylethynyl-copper(I) ladder.

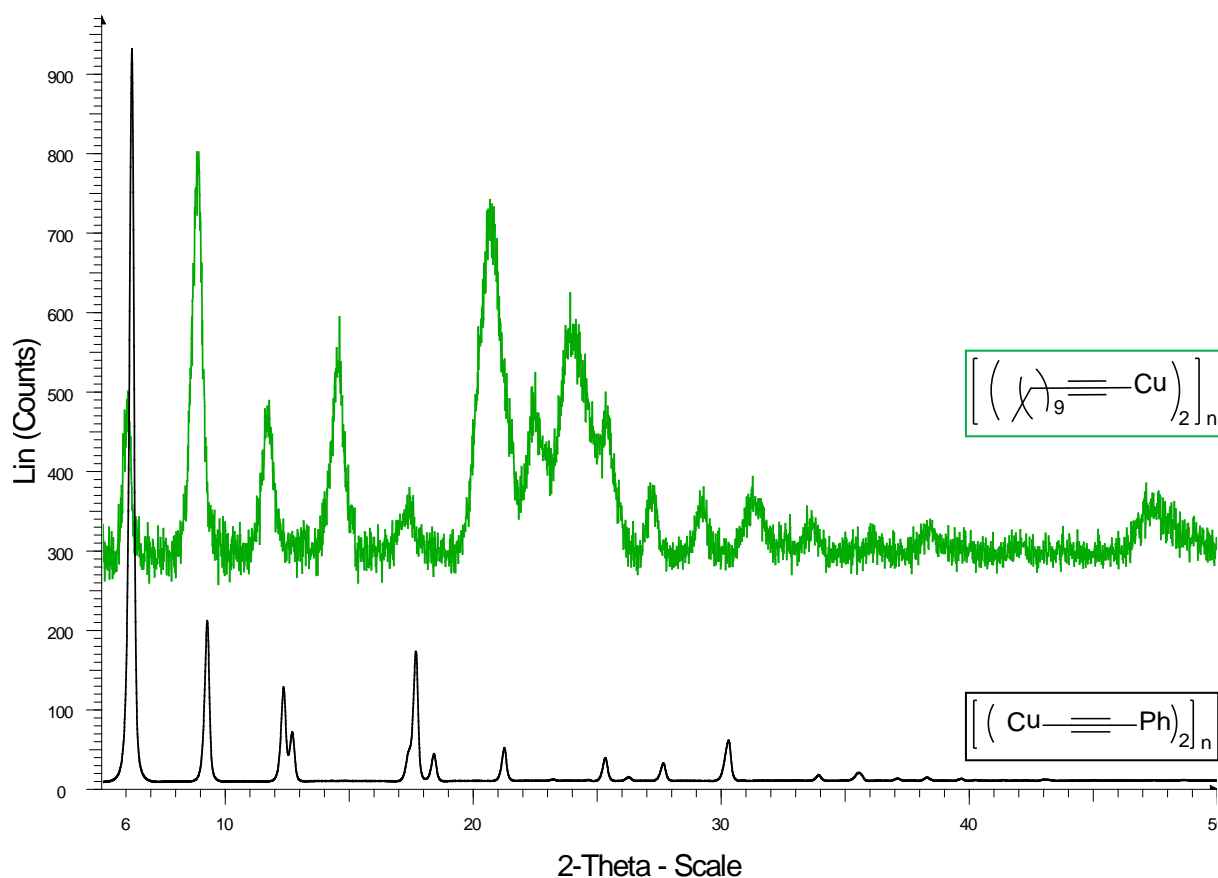


Figure 23: Powder XRD patterns of the long aliphatic chain species (green), compared to the phenylethynyl copper(I) ladder polymer.

Entry **8** did not form a yellow material typical of the copper(I) ladder polymers, rather made an insoluble green material, which when filtered was a brownish colour. XRD results suggest that the material is at least partially ladder like (Figure 23). The problems with **8** are probably due to the length of the aliphatic chain causing difficulty in the arrangement of the copper ladder backbone.

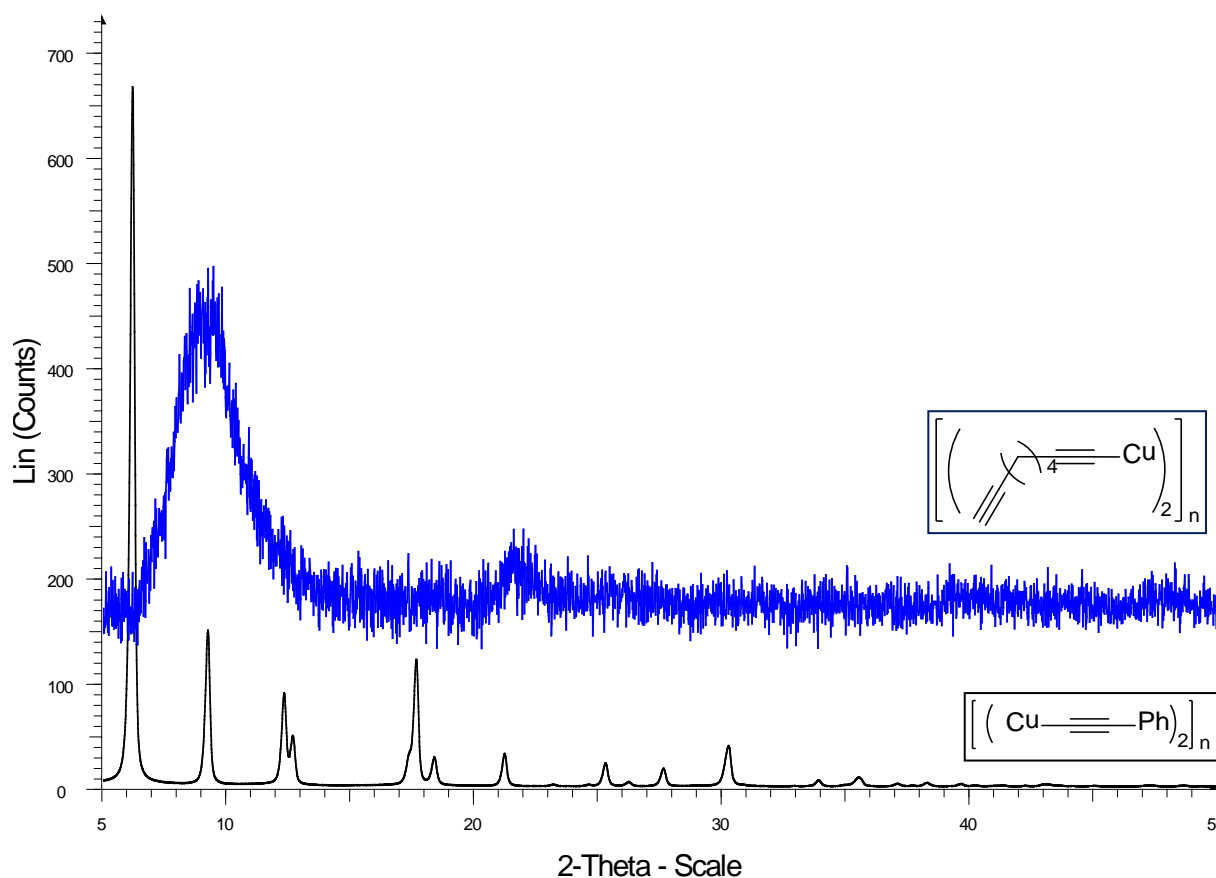


Figure 24: Powder XRD patterns of the double alkyne tether, Octadyene species (blue) compared to the phenylethynyl copper(I) ladder polymer.

Entry **9** formed a yellow material of similar appearance to the known copper(I) ladder polymers. This species has catalysed the CuAAC reaction. However, a clear XRD pattern for this species was not obtained. Only a broad amorphous hump was observed, shown in Figure 24, which could indicate a lack of long range order in the structure.

Previous experience unravelling the poor crystallinity behaviour of entry **1** suggests that careful washing/drying of the polymer can lead to larger crystals and more easily characterised product. Application of these techniques to entry **9** did not improve the quality of the diffraction pattern.

This could suggest that the presence of two alkyne groups within the chain is not only creating crystallinity issues but also creating a species more complex than the other ladder polymers studied.

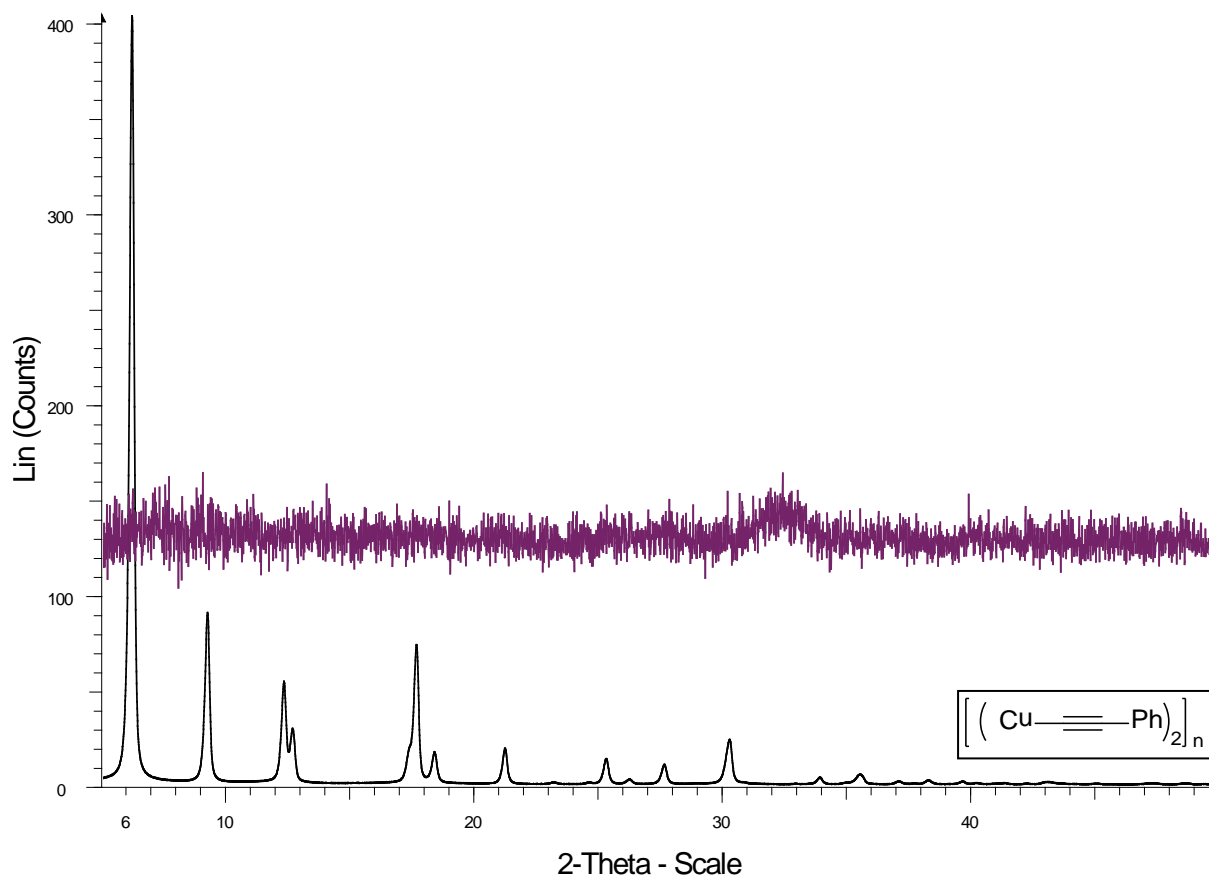


Figure 25: Powder XRD patterns of the silicon species (purple) compared to the phenylethynyl copper(I) ladder polymer.

Entry **11** did not form a yellow ladder polymer, which can be seen clearly in the diffraction pattern, Figure 25, as there are no obvious reflections at all. This is probably due to the silicon atom being too large to stack correctly within the space of a ladder backbone. Interestingly a copper mirror formed around the side of the microwave vessel at the end of the reaction, which could provide second explanation for the lack any ladder polymer formed if the mirror was the preferential product with the silicon starting material present.

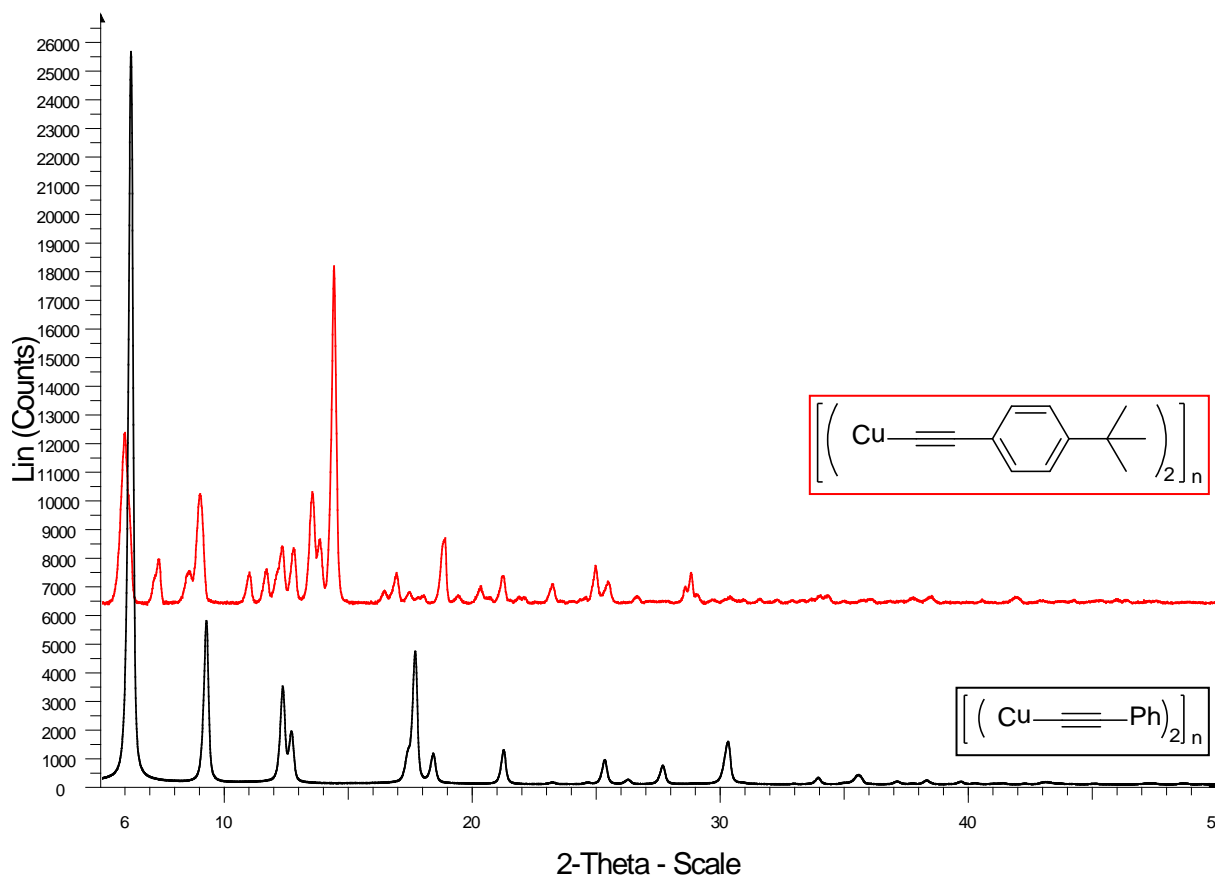


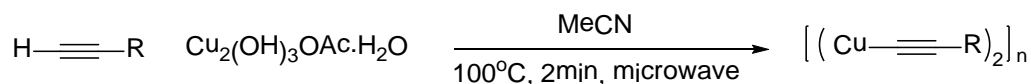
Figure 26: Powder XRD patterns of the large tertiary protected aromatic species (red) compared to the phenylethynyl copper(I) ladder polymer.

Entry **12** produced a yellow ladder polymer. The XRD (Figure 26) show a much more complicated pattern to that of the phenyl ladder (**1**). These results suggest a ladder which is packed much more loosely as the reflections are spaced much closer together and shifted to lower 2 theta values. These results correspond to the structure of the R group as the tertiary butyl group on the aromatic ring would be very bulky and harder to accommodate within a copper ladder without a large amount of space.

Characterisation of Structures

Solid State NMR Studies of Copper Ladder Polymers

The *ortho* (**4**), *meta* (**3**), *para* (**2**), and phenyl (**1**) ladder series was studied further by solid state ^{13}C NMR spectroscopy. Each ladder was prepared by the standard method (Scheme 4), and run as a solid sample on the Bruker 500 MHz spectrometer. The results are shown in Figure 27.



Scheme 4: General reaction for the formation of Copper(I) ladder polymers

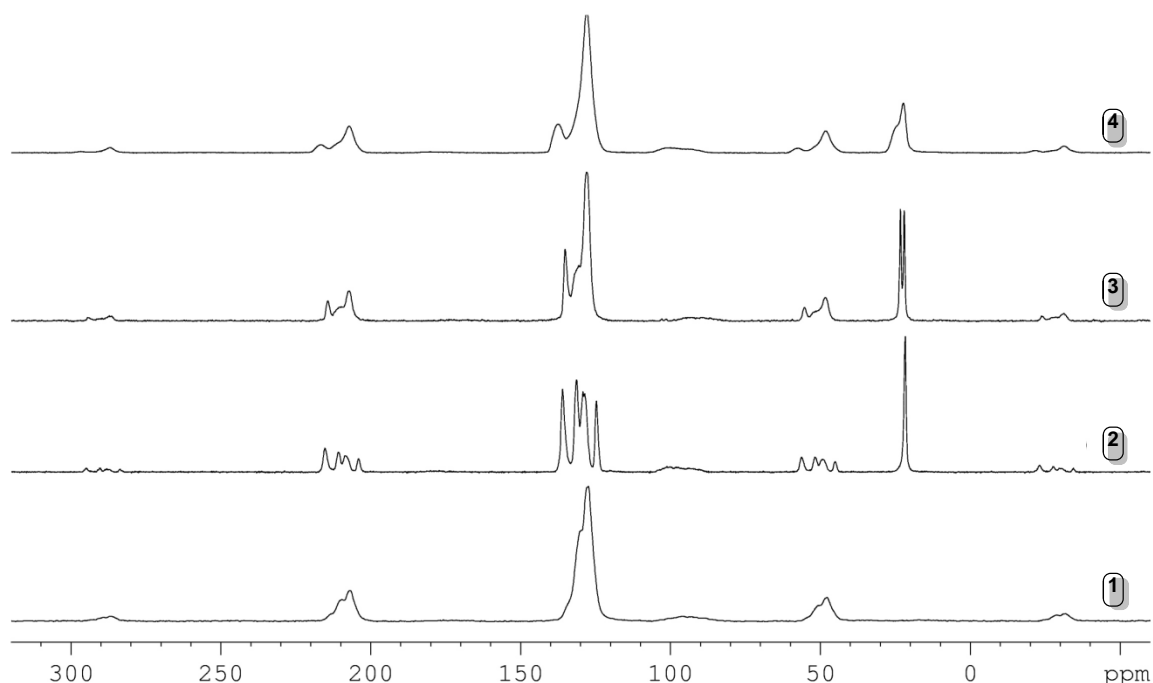


Figure 27: Solid State ^{13}C NMR results of the *ortho* (**4**), *meta* (**3**), *para* (**2**) methyl substituted and phenyl (**1**) ring series

Each ladder species shows a distinct peak at ≈ 130 ppm with corresponding spinning side bands at ≈ 210 and 50 ppm. This signal is due to the carbons in the aromatic ring groups of the ladders. Each species shows a degree of splitting in the aromatic peaks, with the *para*-methyl substituted sample showing four resonances, which is typical for a substituted aromatic ring. This suggests that the packing of the *para*-methyl ladder has little effect on its long range order. Whereas the signals of the *ortho*-methyl and *meta*-methyl samples are much broader implying that being packed in a ladder chain causes the aromatic signals to become less resolved, due to poor long range ordering of the

chains. These data are in good agreement with the powder XRD previously discussed for the series which show similar broadening associated with poor crystallinity (long range order).

A broad peak at ≈ 95 ppm corresponds to the alkyne carbons, the peak at ≈ 30 ppm appears in the *ortho*, *meta*, *para* species which corresponds to the carbon in the methyl group, the *meta* species being split in two, possibly indicating the presence of two possible environments for the *meta* species methyl group.

Due to the interesting nature of the behaviour of the ladder polymers with solvent, it was believed that solvent was incorporated between the layers causing them to swell, it was deemed necessary to examine the solvated ladders by SS-NMR.

However, to do this a slightly different sample introductory system had to be used. A set of NMR 'bottles' were prepared from standard 3 mm NMR tubes, which were cut down to length and re-sealed at the bottom using a flame torch. Aliquots of solvated ladder polymer were taken directly from the microwave tube they were prepared in before any drying or filtration steps had occurred, and transferred directly into the 3 mm bottles. The samples compacted as much as possible by centrifugation and additional sample was added until the bottle was fully packed. This had to be accomplished quickly to minimise the possibility of the sample drying out. The bottles were then sealed with the epoxy resin, Araldite.



Figure 28: SS-NMR Bottles, filled (left), empty (right)

However, when acetonitrile was used as the solvent for ladder preparation, the resin did not harden fully therefore not sealing the bottle correctly which lead to the samples drying out before analysis could be carried out. The preparation method was altered slightly to use ethanol as a solvent to circumvent this problem. Despite packing the samples into the bottles as fully as possible via centrifugation the initial results suffered

from a very poor signal to noise ratio, with the only peaks observed in the spectra arising from the ethanol. To obtain interpretable results from the solid phase rather than just the solvent the spectra were acquired with a greater number of scans to improve the signal to noise. The results for the phenyl ladder species are shown in Figure 29.

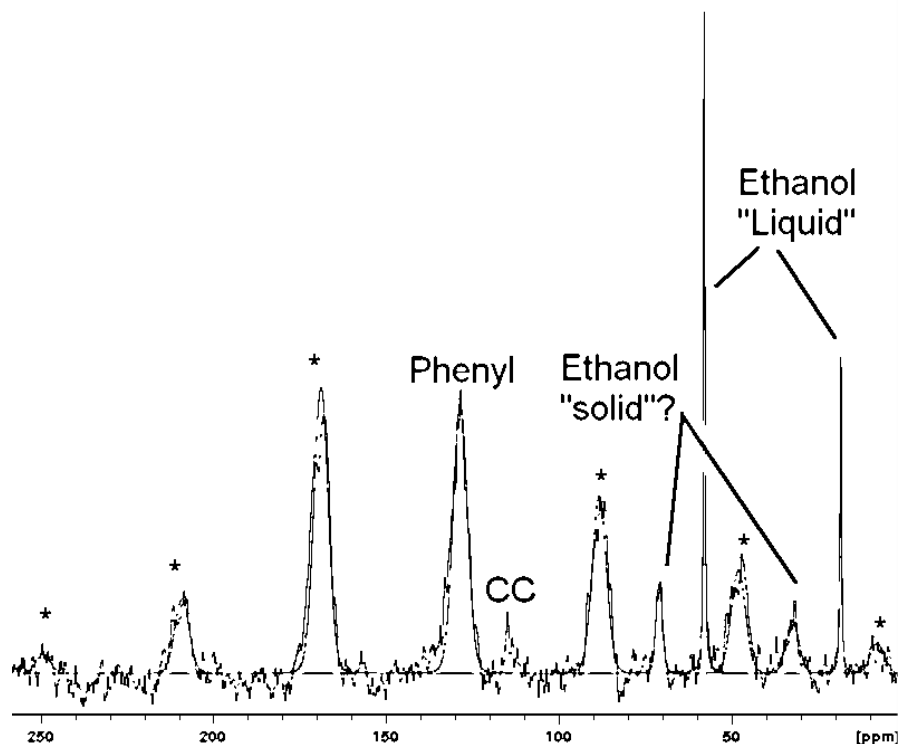


Figure 29: Solid State NMR results for solvated phenylethynyl copper(I) ladder polymer

The aromatic signal occurs at ≈ 130 ppm which is in the same region as the previously analysed solid sample with spinning side bands at 170/90 and 210/50 ppm. The alkyne carbons can be seen just above the signal to noise to the right of the aromatic peak at ≈ 115 ppm. The two sharp signals at 20 and 60 ppm are from the ethanol solvent in the bottle, however two slightly shifted, broader peaks at 30 and 70 ppm can be seen. It is possible that these resonances are caused by ethanol that has been bound between the layers of the ladder polymer, which could be responsible for the swelling behaviour observed.

Data on the rest of the series have yet to be collected. However, it is believed that the nature of the interaction between polymer and solvent can be defined via solid state NMR and XRD providing a full crystal structure, which would lead to a better understanding of not only the structure but also possibly provide a clearer understanding of the ladder polymers catalytic behaviour.

Raman and IR Studies of Copper Ladder Polymers

To provide further insight into the structure of the ladder polymers, complementary Raman and Infrared data were collected, as described in the experimental section at the end of the chapter. Figure 30 shows the Raman spectra for the phenyl ladder polymer (1), with a summary of the observed bands and the corresponding literature values and assignments given in Table 3.

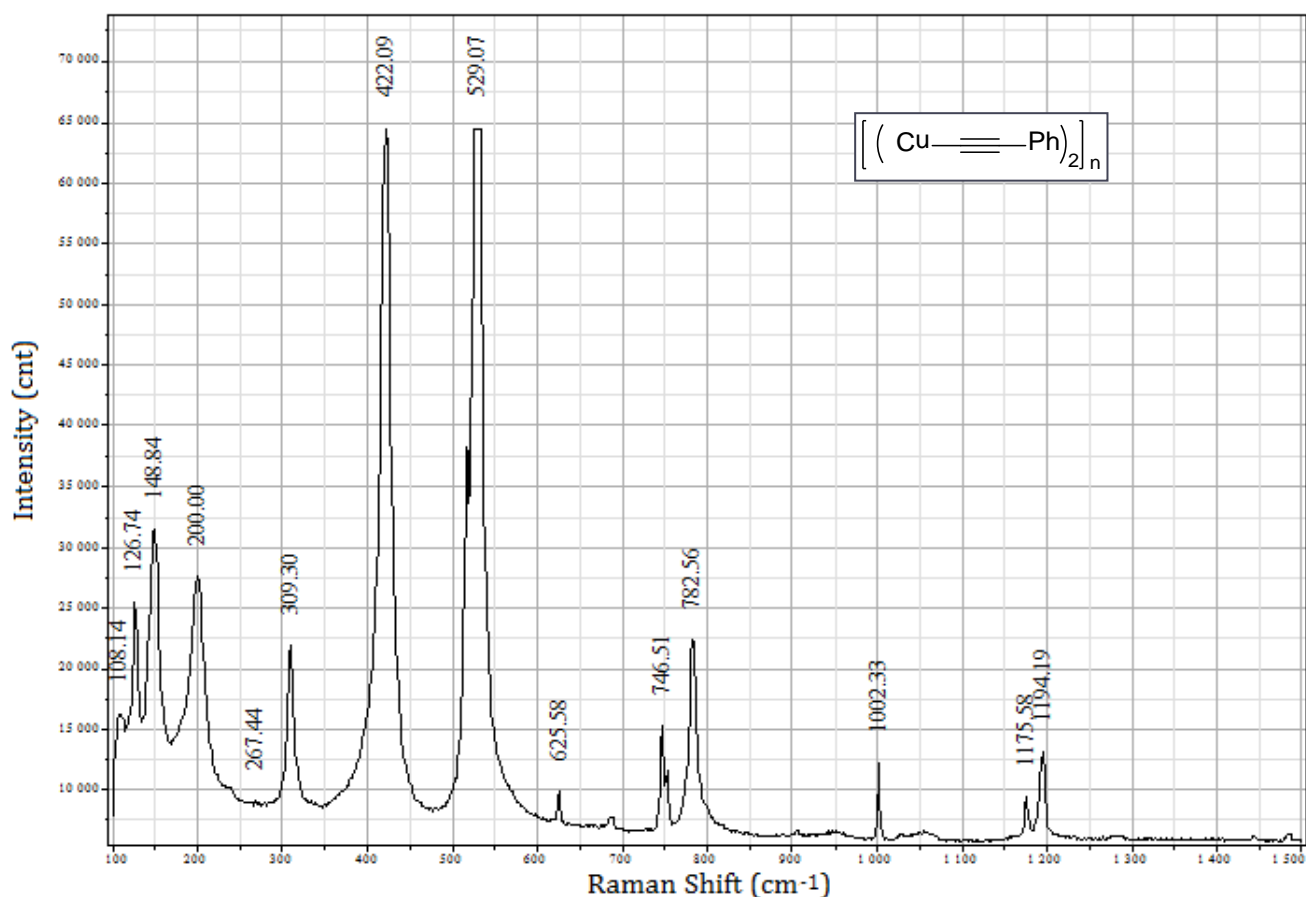


Figure 30: Raman data obtained for phenylethynyl copper(I) ladder polymer

The majority of the bands at higher frequencies can be attributed to the organic functional groups in the side chains on the ladder polymers. To better understand the basic structure of the ladder polymers backbone it is of more interest to examine the bands at the lower frequencies. In the case of the phenyl ladder there are two prominent bands at 422 and 529 cm⁻¹, which according to the Garbusova group [54] correspond to copper – ligand bond vibration.

There are also a number of bands at lower frequencies between 120 and 300 cm^{-1} . These are believed to correspond to the copper – copper interactions between the copper atoms within the ladder chains. Raman data obtained for a pair of dicopper cryptates provides evidence of copper – copper bond formation, with bands in the ranges 140-181 and 240-290 cm^{-1} ,^[53] which are consistent with the data collected on the phenyl ladder polymer (**1**).

Table 3: Observed bands from the Raman spectrum compared to literature values^[54] with possible assignments of the bands

<i>Observed Bands</i>	<i>Literature Bands</i>	<i>Assignment</i>
108		
127		
149	150	Copper – Copper Interactions
200	200	
309	308	
422	422	Copper – Carbon Bond Participation
529	529	
626		Various Aromatic/Alkyne Conjugation, Stretching, and Ring Breathing
747		
783	780	
1002	999	
1176		
1194	1192	

It was believed that the carbon – carbon interactions within the ladder chains would vary depending upon the side chain attached to the copper, for example a smaller R-group would mean that the copper – copper distances would decrease due to the chain being able to pack closer together than if a bulky side chain was attached.

Data were collected on the *ortho* (**4**), *meta* (**3**), *para* (**2**)-methyl ladder series for comparison with the non-methyl substituted phenyl ladder. Figure 31 shows the results, and Figure 32 shows all four species together for comparison of band shifts.

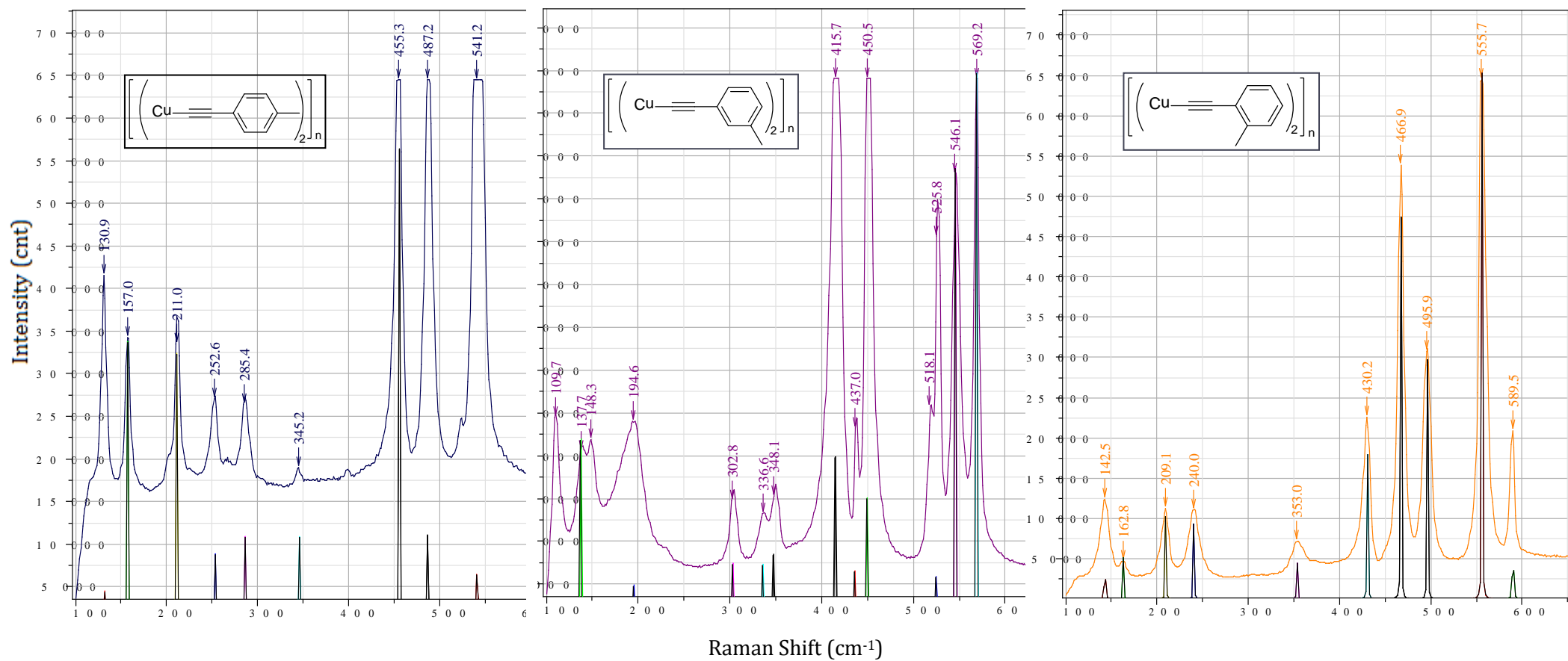


Figure 31: Raman data obtained for para (2) (left), meta (3) (middle) and ortho (4) (right) copper(I) ladder polymers

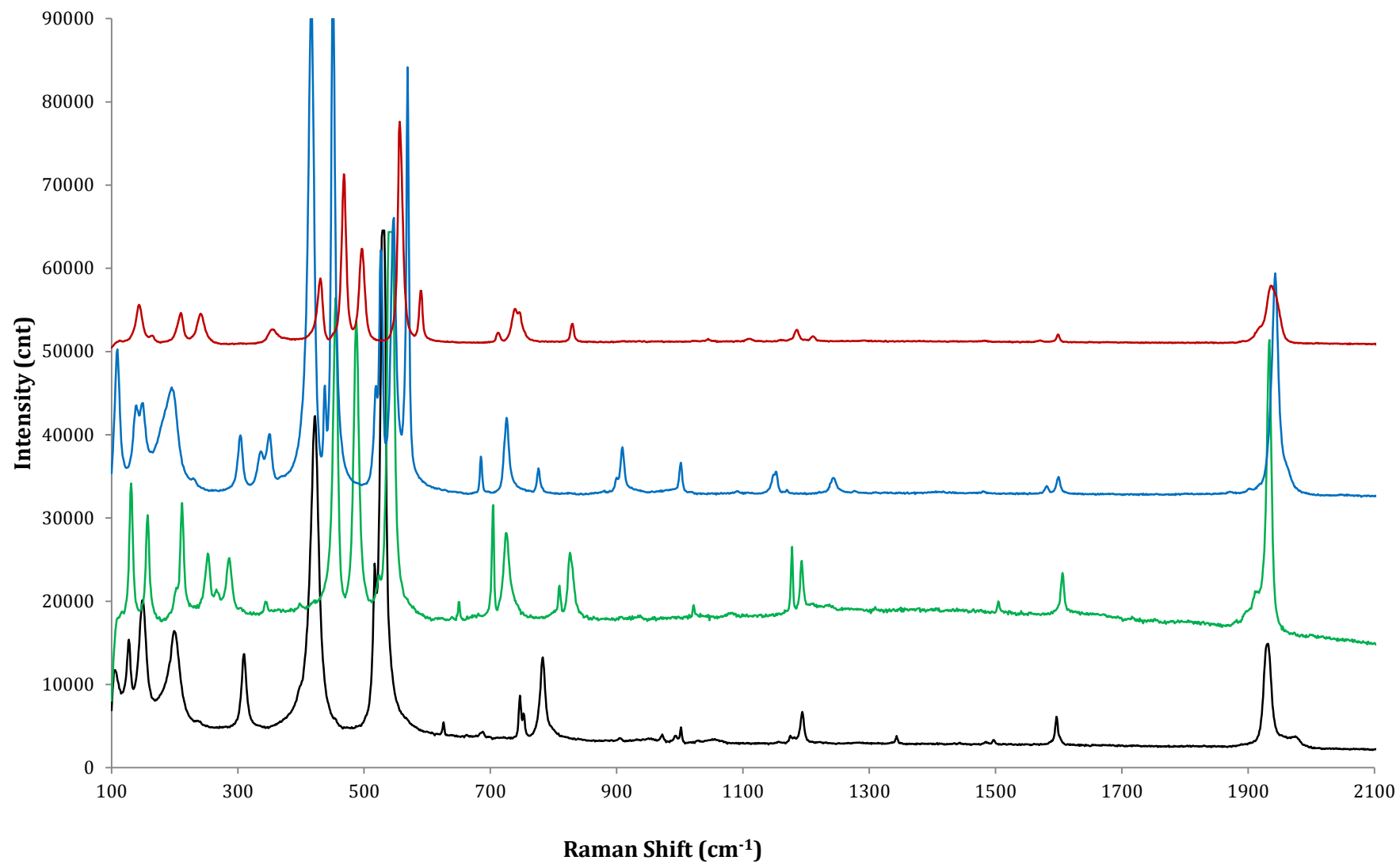


Figure 32: Full Scan Raman of the phenyl [1] (black), ortho [4] (red), meta [3] (blue), para [2] (green) ladder polymer series.

Table 4: Observed low frequency bands for the *ortho*, *meta*, *para*-methyl ladders compared to the phenylethynyl copper(I) ladder polymer

<i>Phenyl</i>	<i>Para-methyl</i>	<i>Meta-methyl</i>	<i>Ortho-methyl</i>
127	131	110	143
149	157	138	209
200	211	195	240
309	253	303	353

Table 4 shows the observed bands at low frequencies, which are believed to correspond to copper – copper interactions within the chain, for the four ring species. It is possible to see a general pattern emerging between the series with the meta species having bands which are shifted to lower frequencies than the phenyl ladder. Whereas the para and ortho species have shifted to higher frequencies than the phenyl ladder. These results could be indicative of the variable copper – copper distances within the ladders, with the meta ladder stacking in such a way that the copper – copper distances are shorter than in the cases of the other ladders. There is also a degree of splitting in the bands, which is particularly noticeable in the meta and ortho species. Table 5 shows the observed bands for the copper – ligand interactions for the four ring species.

Table 5: Observed bands for the *ortho*, *meta*, and *para*-methyl ladders compared to phenylethynyl copper(I) ladder polymer.

<i>Phenyl</i>	<i>Para-methyl</i>	<i>Meta-methyl</i>	<i>Ortho-methyl</i>
422	455	416	430
529	541	526	556

phenylethynyl-copper(I) ladder polymer

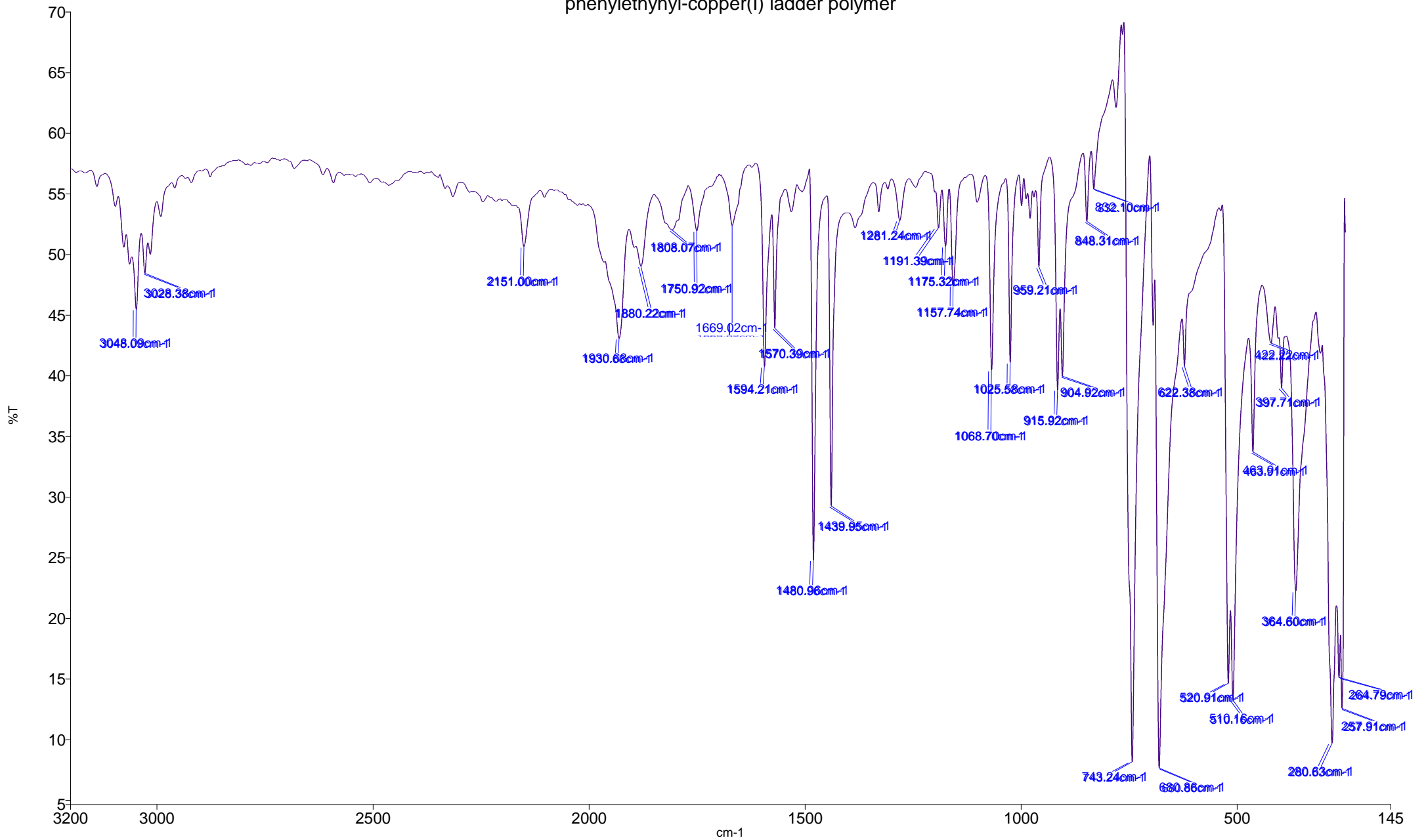


Figure 33: FT-IR data obtained for phenylethynyl copper(I) ladder polymer

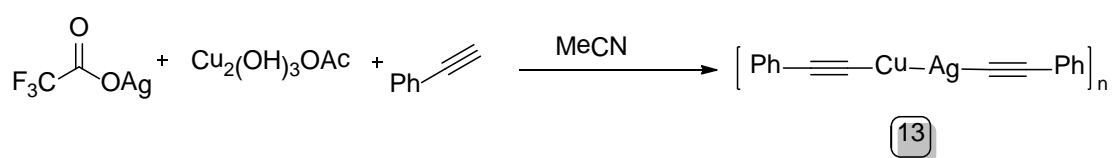
Table 6: Observed bands from the FT-IR spectrum compared to literature values ^[54] with possible assignments of the bands

<i>Observed Bands</i>	<i>Literature Bands</i>	<i>Assignment</i>
281		
365		
510	515	
521	525	
681	685	
743		
916	915	
1026	1026	
1481	1481	C-C
1594	1594	(C≡C)-(Ph) Conjugation
1931	1930	C≡C stretch
3000-3100		C-H

As the research currently stands the IR spectra have not been characterised, although it is believed that the copper – copper interactions will be observed at the lower frequencies similarly to the Raman data. The characterisation method could still be used as a method of comparison between ladder polymers with varying side chain groups, until further work into this characterisation is carried out.

Mixed Metal Polymer Species

Alkynyl copper, silver, and gold species are all known and have been discussed in the introduction section. The potential of these species meant that it would be of interest to prepare an alkynyl ladder with two different metal centres, as a polymer with two different metal atoms contained in its structure may be capable of catalysing different reactions in a one pot synthesis. To begin with an attempt was made to prepare a copper-silver ladder polymer using copper(II) hydroxyacetate (1 mmol), silver trifluoroacetate (2 mmol), and phenylacetylene (10 mmol) in acetonitrile (10 mL), as shown in Scheme 5.



Scheme 5: Preparation method for a copper – silver mixed metal ladder complex

The reaction mixture was left to stir at room temperature for 3 days. The product was then examined by powder XRD, and the pattern compared to those from $[(\text{CuC}\equiv\text{CPh})_2]_n$ and $[(\text{AgC}\equiv\text{CPh})_2]_n$ from previous work, see Figure 34.

The red pattern shows the mixed metal ladder, whilst some reflections correspond to copper or silver ladder, there are some reflections which do not, this suggests that a mixed metal ladder has actually formed and not just a mixture of the copper and silver ladders.

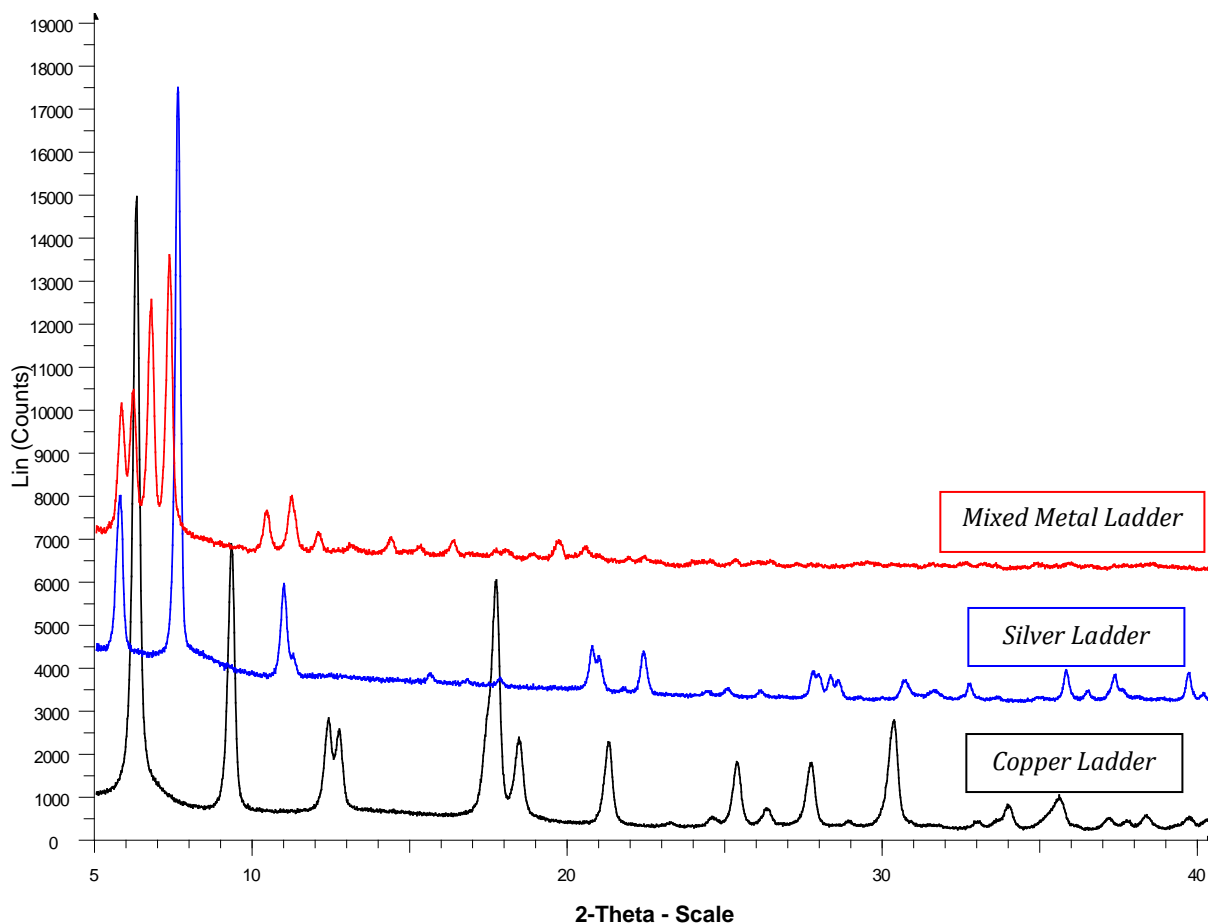


Figure 34: Powder XRD comparison of copper(I) (Black) silver (Blue) and a mixture of copper(I) and silver(I) (Red) ladder polymers

This was followed by a series of reactions similar to those shown in Scheme 5, but varying the reaction time, the powder XRD results are shown in Figure 35. One reaction was left for 15 min at room temperature (black pattern), which shows just silver alkynyl ladder formation. Another reaction was left for 2 weeks stirring at room temperature (blue pattern) and a reaction was carried out in the microwave for 10 min at 100 °C (green pattern). Both the 2 week and microwave reaction show formation of mainly mixed metal ladder, however the intensity of the first two major reflections is switched between the two samples which suggests there could be a difference in the ordering of the copper and silver atoms in the ladder depending on the method of formation. Further work would be required to fully understand this behaviour.

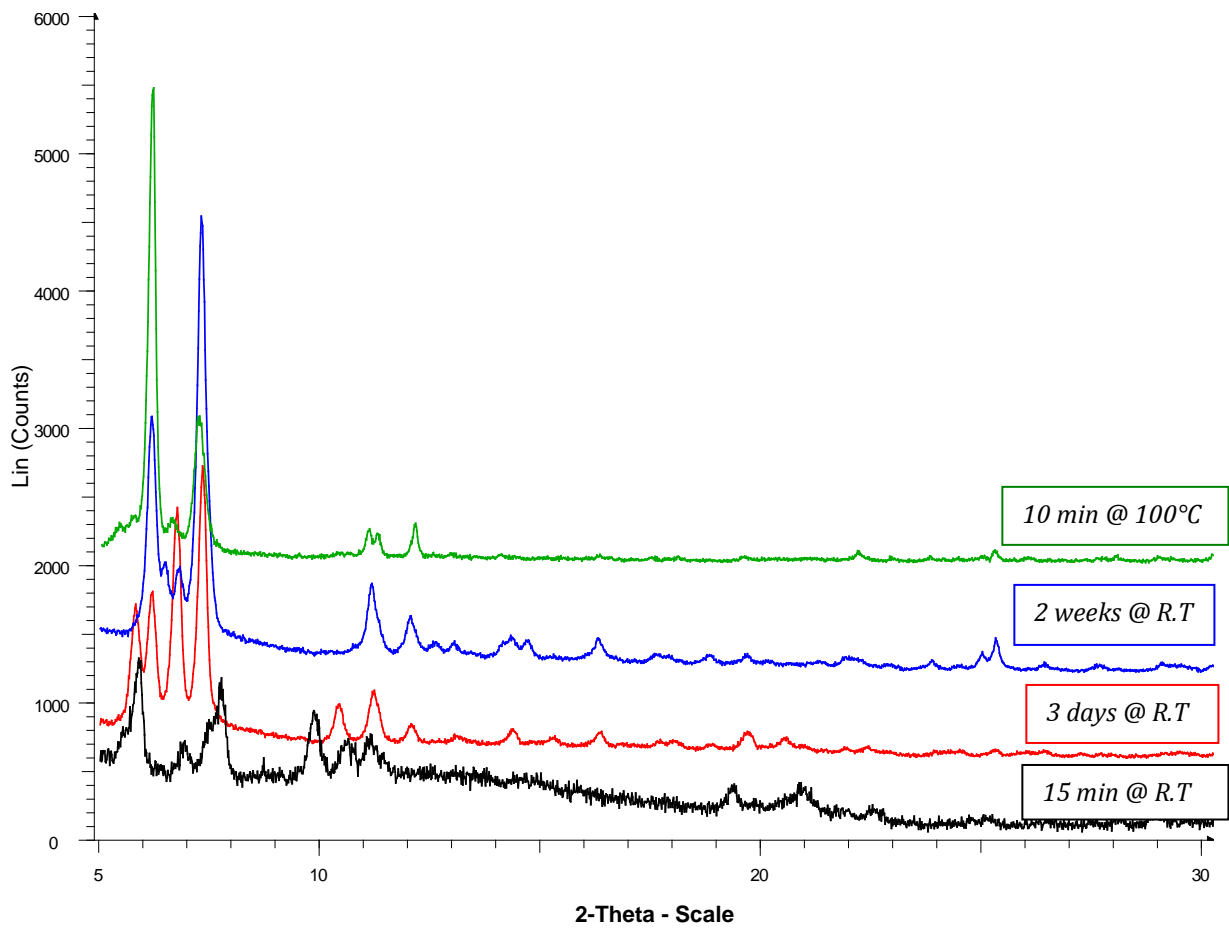


Figure 35: powder XRD patterns for the various time controlled experiments to form the mixed metal copper(I) - silver(I) ladder polymer

Chapter 1 Conclusion

The work carried out in this chapter has demonstrated the preparation of a variety of alkynyl copper(I) ladder polymers via the copper(II) acetate method. By using a variety of alkyne starting materials, the structural characteristics of the prepared ladder polymer species vary greatly. This was shown in the various powder XRD patterns obtained. The data was able to show that smaller R groups such as the alcohol species (**5**) formed short copper-copper bonds within the ladder backbone. The R groups, which allowed π - π stacking of aromatic groups, for example the phenyl group of entry (**1**), produced the best XRD pattern indicating the best long range order. The R groups with chains before the aromatic ring (**7**) were unable to stack as well, therefore the XRD patterns showed poorer long range order.

The packing of the alkynyl copper(I) ladders was further examined by SS-NMR, Raman, and FT-IR, using the *ortho* (**4**), *meta* (**3**), *para* (**2**)-methyl, and phenyl (**1**) ladders for comparison. The results showed that, by only changing the position of the methyl group on an aromatic ring, it is possible to alter both the long range order of the ladder, and also the distance between the copper atoms within the ladders backbone. For example the *ortho* (**4**) species has the poorest long range order of the samples, and the copper bond distances are shortest in the *meta* (**3**) sample, and longest in *ortho* sample (**4**).

By understanding which side groups affect the copper chain in certain ways, it is possible to tailor the copper(I) ladder polymers to have specific properties, which may be advantageous to catalyse different reactions. A longer copper-copper bond length could provide more space within the polymer to allow large reagents in during a reaction, whereas a smaller copper-copper bond length could exclude larger reactants during a reaction.

Finally some work was also carried out on the preparation of a mixed metal ladder species (**13**), which was successful at the inclusion of the two metals into the chain. However, a method of determining the exact ordering of the metals has yet to be found, so the exact structure is still unknown. This mixed metal ladders are of great interest due to the possibility of catalysing multicomponent one pot reactions.

Chapter 1 Experimental

X-Ray Diffraction Data:

A Bruker D8 powder diffractometer operating with $\text{Cu}_{K\alpha 1}$ (1.5406Å) radiation, using a 2θ range of 5° - 60° , with a step size of 0.0147° with a step time of 1s for 1 hour was used for the collection of the X-ray data presented here in this work. The detectors used in the collection of data were a Braun position sensitive detector and a Lynxeye position sensitive detector that allows a range of scattering angles to be measured increasing signal detection and reducing noise. The collected data were then analysed in the EVA program using ICDD to identify and determine sample purity.

Solid-State NMR Data:

Solid-state NMR spectra were recorded on Bruker Avance 500MHz NMR spectrometer, equipped with a 4mm MAS HX probe, 100W proton amplifier and 500W X amplifier. Cross-polarisation used a 1H pulse of 2 μ s (at -5.5 dB), a ramped proton CP pulse of 2ms (at -4.0 dB) and a carbon CP pulse of 2ms (at -3.1 dB). TPPM15 proton decoupling was applied during the 30ms acquisition time. FIDs contain 3k data points which were Fourier transformed into 16k data points, an exponential function of 20 Hz was applied to the FID using Bruker TOPSPIN(1.3) software. Spectra were referenced to external TMS via adamantane for ^{13}C , and the magic angle was set up using KBr. Magic angle spinning of 10kHz was used for powders and 3kHz - 5kHz for glass-inserts containing sample and solvent.

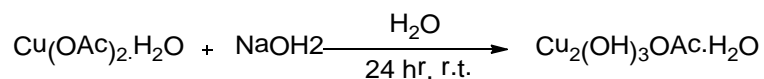
Raman Data:

Data were collected on a Horiba John Yvon LabRAM HR800 spectrometer using a 632.8 nm HeNe laser with 600 grating, 100x objective, 300 μm hole size and a 150 μm slit aperture. Data were collected across a 100 – 4000 cm^{-1} range in collection sets of 500 cm^{-1} with 10 accumulations of 10s exposures. The data were analysed using LabSpec software v5.25 and Microsoft Excel.

FT-IR Data:

Data were collected between ranges 150-32000 cm^{-1} using a Perkin Elmer Spectrum 100 FT-IR spectrometer with an ATR accessory fitted. Data were analysed using Perkin Elmer Spectrum, Microsoft Excel and Essential FTIR.

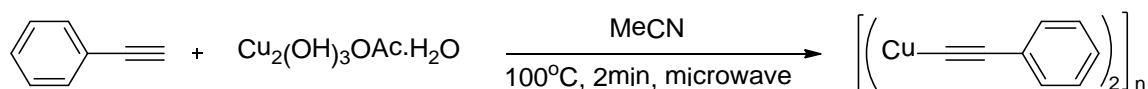
Preparation of copper hydroxyacetate



In a typical procedure $\text{Cu}^{\text{II}}(\text{OAc})_2 \cdot \text{H}_2\text{O}$ (4.0 g, 20.1 mmol) was added to distilled water (200 mL) in a 500 mL conical flask. Sodium hydroxide (0.1M, 200 mL) was titrated in slowly with vigorous stirring. After addition the reaction was left to stir for 24 hours. The precipitate was then collected by centrifugation 5 min at 2,000 RPM, and the solid then washed with distilled water (100 mL), ethanol (100 mL) and dichloromethane (100 mL). The solid was left to dry and then ground into a fine powder using a pestle and mortar. Pale blue solid (1.5g, 59%) was obtained, and analysed by powder XRD.

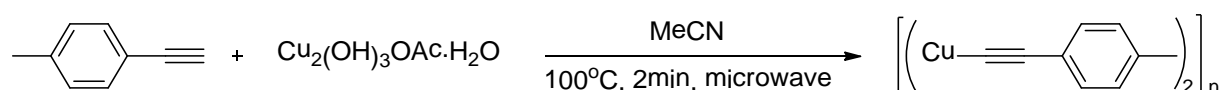
Representative method for the preparation of copper(I) ladder polymer species

Preparation of phenylethynyl copper(I) ladder polymer - (1)



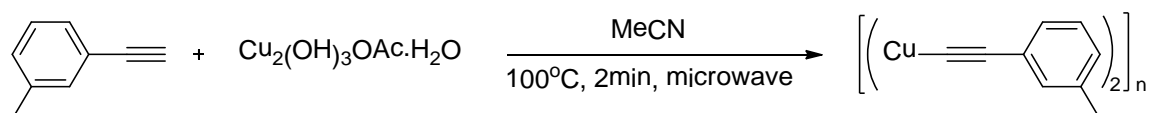
$\text{Cu}_2(\text{OH})_3\text{OAc}$ (0.12 g, 0.5 mmol) was added to a 2-5 mL microwave tube fitted with a magnetic stirrer bar. Phenylacetylene (0.15 g, 1.5 mmol) and MeCN (5 mL) were added and the mixture heated in the microwave for 2 min at 100 °C. The solid formed was then collected by gravity filtration, and washed with a series of H_2O (20 mL), MeOH (20 mL), and diethyl ether (20 mL). The sample was then left to dry overnight. Bright yellow solid (0.15 g, 92%) was obtained, and analysed by powder XRD, in agreement with the literature. [46]

Preparation of *para*-methyl phenylethynyl copper(I) ladder polymer - (2)



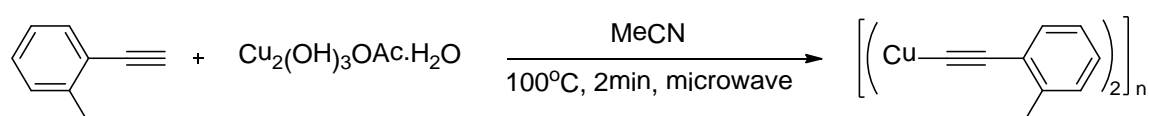
Prepared using the representative procedure from $\text{Cu}_2(\text{OH})_3\text{OAc}$ (0.15 g, 0.58 mmol) and *p*-tolylacetylene (0.18 g, 1.5 mmol). Bright yellow solid (0.19, 87%) was obtained, and analysed by powder XRD.

Preparation of *meta*-methyl phenylethynyl copper(I) ladder polymer - (3)



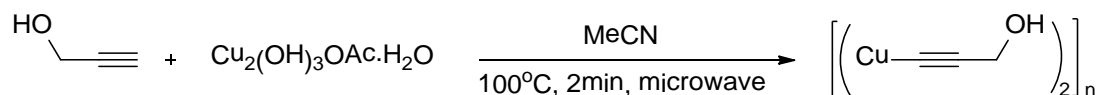
Prepared using the representative procedure from $\text{Cu}_2(\text{OH})_3\text{OAc}$ (0.14 g, 0.55 mmol) and *m*-tolylacetylene (0.18 g, 1.6 mmol). Bright yellow solid (0.16 g, 82%) was obtained, and analysed by powder XRD.

Preparation of *ortho*-methyl phenylethynyl copper(I) ladder polymer - (4)



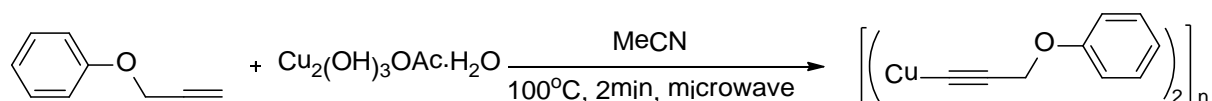
Prepared using the representative procedure from $\text{Cu}_2(\text{OH})_3\text{OAc}$ (0.14 g, 0.55 mmol) and *o*-tolylacetylene (0.17 g, 1.5 mmol). Bright yellow solid (0.14 g, 71%) was obtained, and analysed by powder XRD.

Preparation of propargyl alcohol copper(I) ladder polymer - (5)



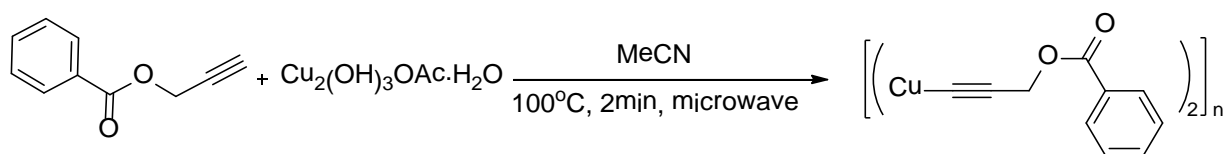
Prepared using the representative procedure from $\text{Cu}_2(\text{OH})_3\text{OAc}$ (0.12 g, 0.5 mmol) and propargyl alcohol (0.10 g, 1.8 mmol). Orangey-yellow solid (0.05 g, 42%) was obtained, and analysed by powder XRD.

Preparation of prop-2-yn-1-yloxy benzene copper(I) ladder polymer - (6)



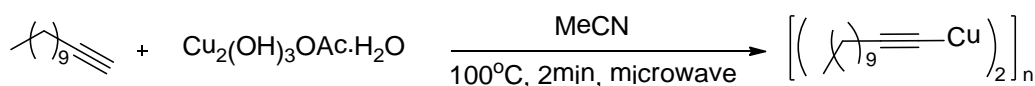
Prepared using the representative procedure from $\text{Cu}_2(\text{OH})_3\text{OAc}$ (0.13 g, 0.5 mmol) and (prop-2-yn-1-yloxy)benzene (0.19 g, 1.5 mmol). Dark yellow solid (0.19 g, 83%) was obtained, and analysed by powder XRD.

Preparation of prop-2-yn-1-yl benzoate copper(I) ladder polymer - (7)



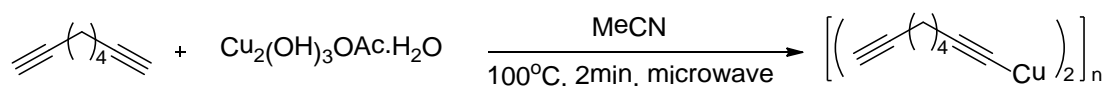
Prepared using the representative procedure from $\text{Cu}_2(\text{OH})_3\text{OAc}$ (0.30 g, 1.2 mmol) and prop-2-yn-1-yl benzoate (0.48 g, 3.0 mmol). Dark yellow solid (0.37 g, 70%) was obtained, and analysed by powder XRD.

Preparation of 1-dodecyne copper(I) ladder polymer - (8)



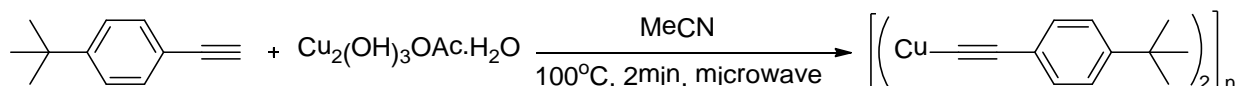
Prepared using the representative procedure from $\text{Cu}_2(\text{OH})_3\text{OAc}$ (0.13 g, 0.5 mmol) and 1-dodecyne (0.24 g, 1.4 mmol). Brownish-yellow solid (0.11 g, 48%) was obtained, and analysed by powder XRD.

Preparation of octadiyne copper(I) ladder polymer - (9)



Prepared using the representative procedure from $\text{Cu}_2(\text{OH})_3\text{OAc}$ (0.13 g, 0.5 mmol) and octadiyne (0.15 g, 1.4 mmol). Bright yellow solid (0.13 g, 77%) was obtained, and analysed by powder XRD.

Preparation of 4-t-butylphenylethynyl copper(I) ladder polymer - (12)

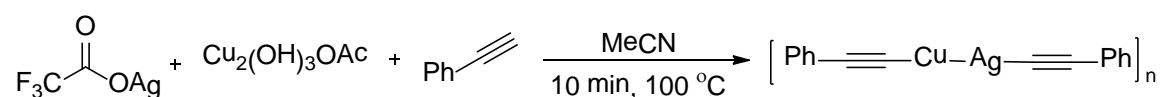


Prepared using the representative procedure from $\text{Cu}_2(\text{OH})_3\text{OAc}$ (0.13 g, 0.5 mmol) and 4-t-butylphenylethynyl (0.24 g, 1.5 mmol). Bright yellow solid (0.19 g, 86%) was obtained, and analysed by powder XRD.

Preparation of alkynyl copper(I) ladder polymers for SS-NMR

In a typical procedure Cu(II)(OAc)₂.H₂O (0.10 g, 0.02 mmol) was added to a 2-5 mL microwave tube fitted with a magnetic stirrer bar, which was then dispersed in ethanol (5 mL). To this alkyne (2 mmol) was added. The mixture was heated in the microwave with stirring for 2 min at 100 °C. The reaction was then allowed to cool to room temperature and the reaction mixture transferred directly to an NMR bottle (prepared from a 3 mm NMR tube). The bottle was centrifuged for 2 min at 2,000 RPM to pack the sample into the bottle, then sealed with Araldite.

Preparation of alkynyl copper-silver ladder polymer - (13)



Copper hydroxyacetate (0.3 g, 1.3 mmol) and silvertrifluoroacetate (0.5 g, 2.3 mmol) were added to a 10-20 mL microwave vial fitted with a magnetic stirrer bar. Phenylacetylene (1.0 g, 10 mmol) and MeCN (20 mL) were then added and the reaction heated in the microwave for 10 min at 100 °C. The sample was collected by gravity filtration and washed with H₂O (50 mL). The sample was dried during filtration then analysed by powder XRD. Sample was stored in a sample vial wrapped in foil to prevent sample degradation by light.

Chapter 2

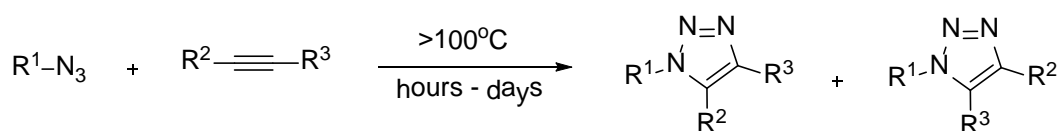
Catalysis and Click Chemistry

Introduction

One area that is currently of particular interest in synthetic chemistry is the application of click chemistry. [55, 56, 57] Click chemistry has been applied in a variety of different areas of synthesis, including drug discovery and material science. The term click chemistry can be described as a set of near perfect bond forming reactions useful for rapid assembly of molecules with a desired function. [58]

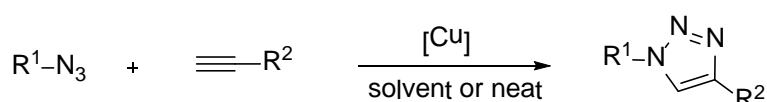
One reaction in particular stands out as being an excellent example of a click reaction, the Huisgen 1,3-dipolar cycloaddition of alkynes and azides to form 1,2,3-triazoles, with organic azides proving particularly effective due to their highly energetic and selective nature. The original reaction suffered from a low reaction rate, which was later solved by the introduction of a copper(I) catalyst, which was reported independently by both Meldal in Denmark [59] and Fokin and Sharpless in America. [60]

A: 1,3-Dipolar cycloaddition of azides and alkynes



reactions are faster when R², R³ are electron withdrawing groups

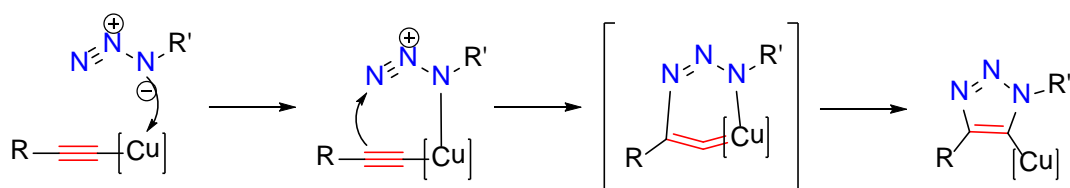
B: Copper catalyzed azide-alkyne cycloaddition (CuAAC)



Scheme 6: General reactions schemes comparing both the non catalysed (A) and copper(I) catalysed click reaction (B) [61] where a single isomer was isolated.

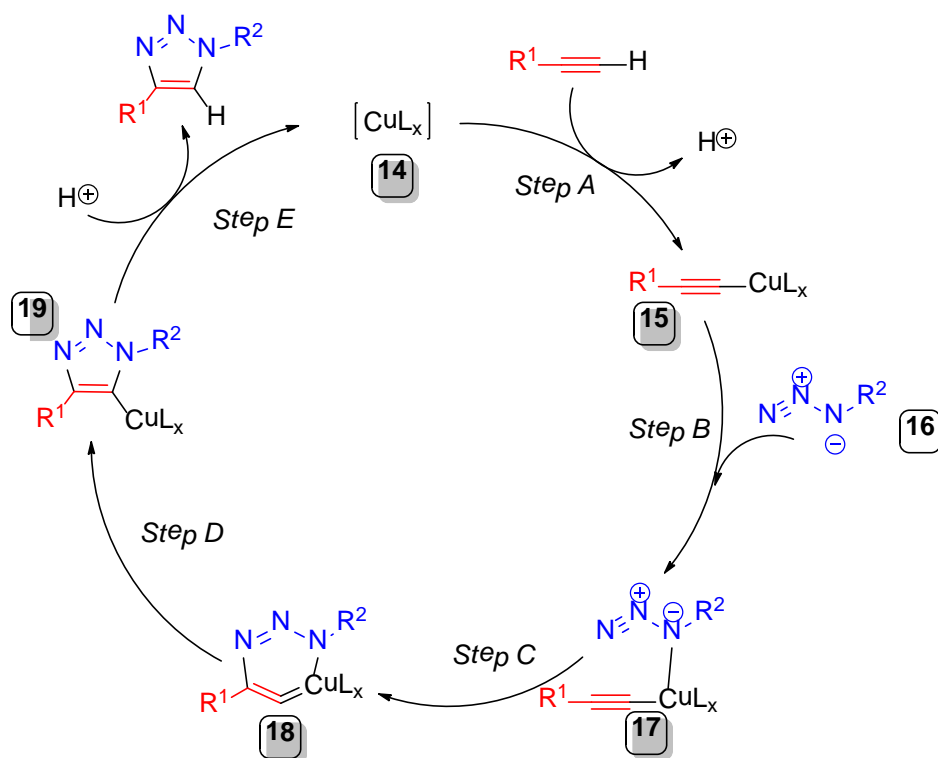
The copper catalyzed azide alkyne cycloaddition (CuAAC) reaction has been regularly reviewed over the last few years. [62,63,64] The thermal reaction between azides and alkynes has been known for over a century, for example when Michael and co-workers synthesized a 1,2,3-triazole from phenylacetylene and diethyl acetylene-dicarboxylate in 1893. [65] This reaction was studied later by Huisgen and co-workers during their research into the larger family of 1,3-dipolar cycloaddition reactions. [66] It was shown that although the reaction is highly exothermic (ΔH° between -50 and -65 kcal⁻¹) the

reaction has a large activation barrier which causes low rates of reaction even at high temperature. Furthermore a mixture of regioisomeric 1,2,3-triazole products are formed if the alkyne is unsymmetrically substituted, which is a result of the difference of HOMO-LUMO energy levels for the azide and alkyne being a similar size, and both pathways being used during the reaction. By using a copper catalyst, the reaction mechanism is drastically changed, and it was originally postulated to include the formation of a 5-triazole copper intermediate, shown in Scheme 7. [40]



Scheme 7: Simplified representation of the proposed bond making and breaking steps [61]

The copper catalyst increases the rate of the reaction typically by a factor of 100 relative to the thermal process. [67] The steric and electronic properties of the alkyne or azide groups, does not significantly impact on the reaction, it is also possible to use a wide variety of solvents either protic or aprotic. The 1,2,3-triazole product has a high chemical stability, which allow it to be used for various purposes, an interesting example being the replacement of an amide bond. The reaction mechanism for the CuAAC reaction has been studied in depth by Hien and Fokin in a recent review of click chemistry. [61]



Scheme 8: An early proposed catalytic cycle from Fokin and co-workers. ^[61]

Scheme 8 shows a catalytic cycle of the CuAAC reaction based upon initial DFT calculations, which focused on mononuclear copper(I) acetylides and organic azide reaction pathways. Hien and Fokin calculated that the formation of the copper(I) acetylide (**15**) was exothermic by 48.95 KJmol⁻¹. The azide is activated by coordination with the copper forming intermediate (**17**). This is followed by the first C-N bond forming to produce a strained copper metallacycle (**18**). Meldal and Tornøe proposed that the coordination of the azide to the copper proceeded via the terminal nitrogen although they had no supporting experimental evidence, ^[64] and was later disproved by Hien and Fokin. ^[61]

If the CuAAC mechanism takes into account the involvement of dinuclear copper(I)acetylides, a drop in the activation barrier is observed. [68] This led to the idea that a transition state existed where a second copper(I) atom interacted strongly with the acetylide carbons, indicated by short Cu-C distances of 1.93 and 1.90 Å, shown in Figure 36. It is also worth noting that dinuclear intermediates are favoured over tetranuclear complexes, which has been shown by Straub. [69]

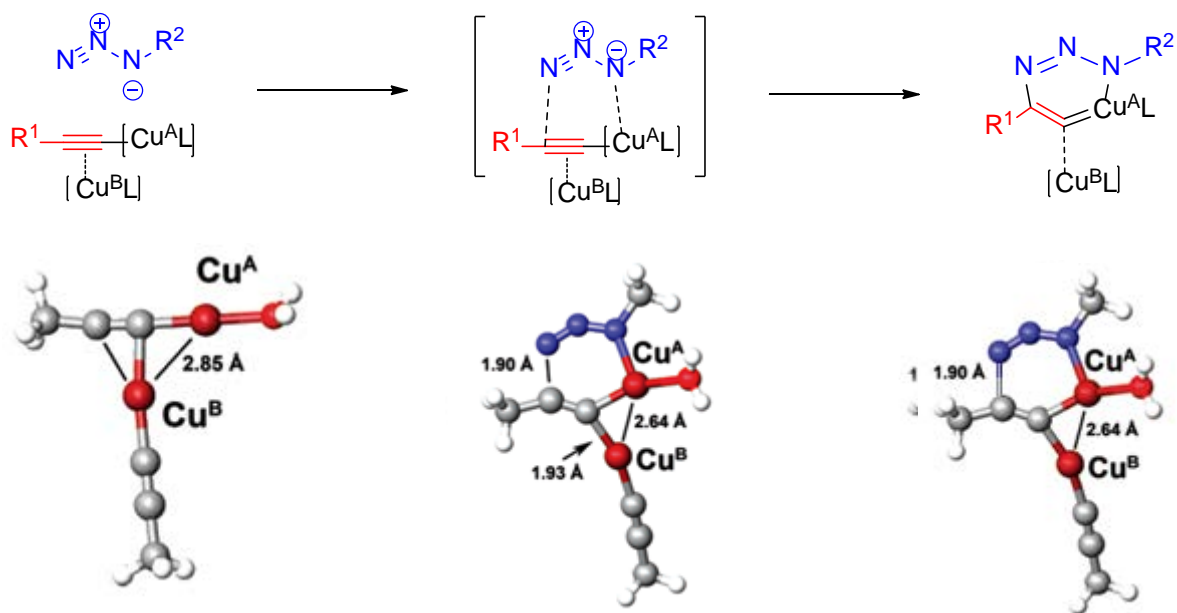
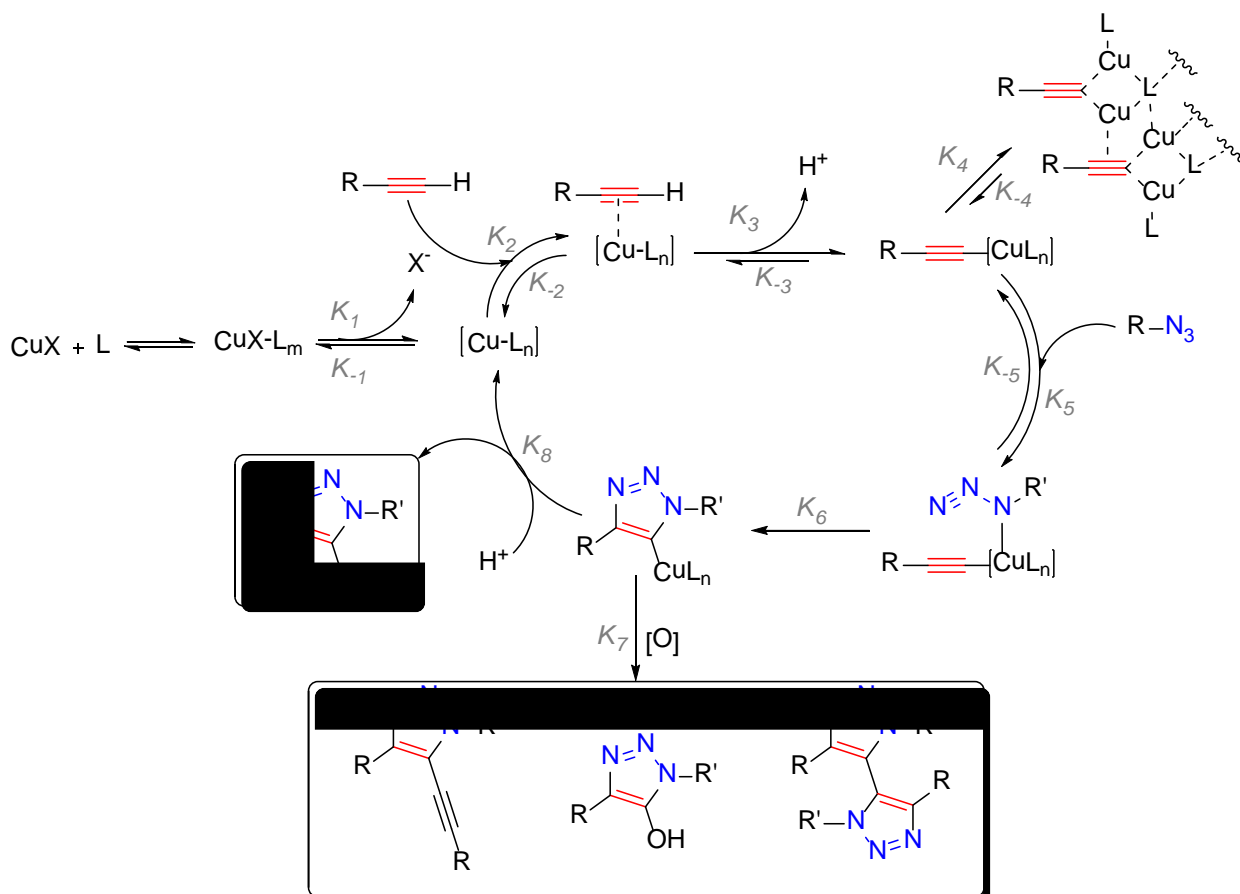


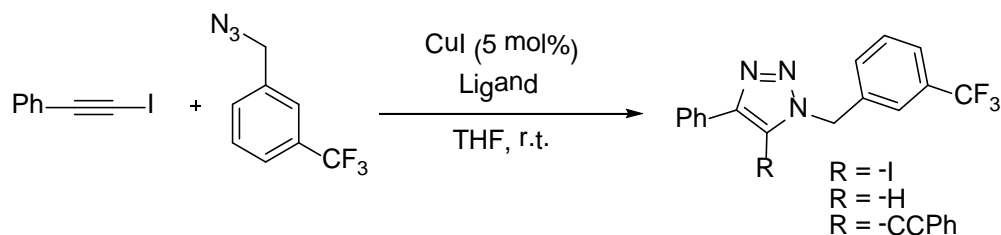
Figure 36: Proposed transition state for the copper(I)alkyne from Fokin et al. [61]

After further kinetic studies, the transition state was altered to incorporate a second copper atom of a specific bond distance from the first. The previously proposed bond-making and breaking steps remaining the same, but a better understanding of the catalyst activation and deactivation pathways and their effects on the entire mechanism, is shown in Scheme 11. [60]



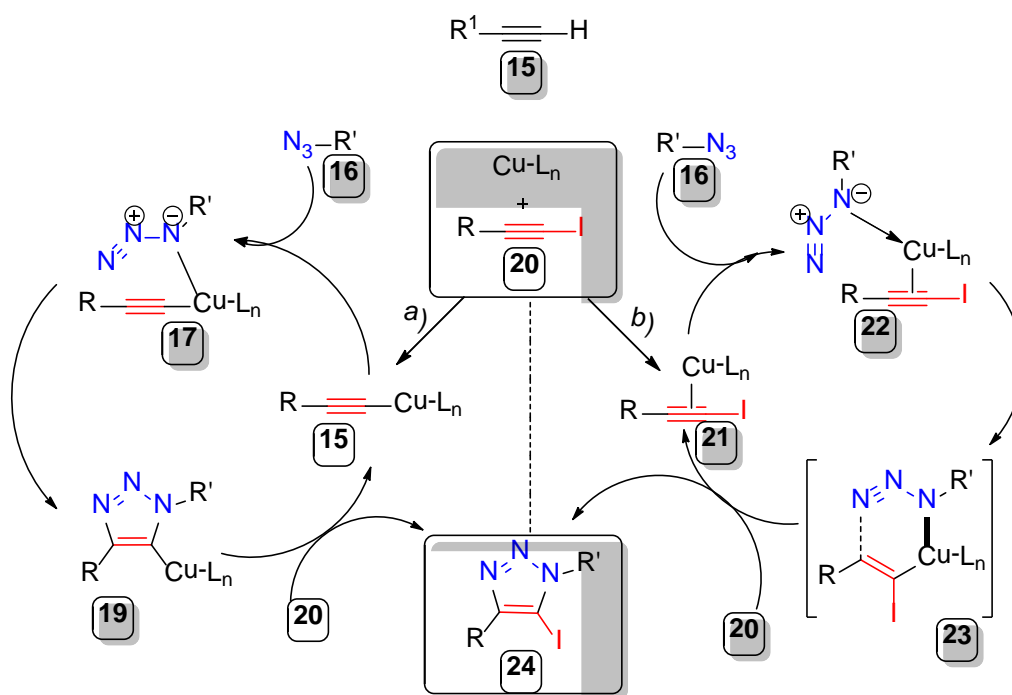
Scheme 9: Catalytic cycle from Fokin and co-workers, showing key equilibria and possible irreversible off cycle pathways which can affect the productivity of the CuAAC catalytic cycle [61]

Iodoalkynes can also be used in a similar way to the terminal alkynes used in the previous click reactions. 1-iodoalkynes are stable and readily accessible internal acetylenes, which can be prepared by treating a terminal acetylene with *N*-iodomorpholine with copper iodide as a catalyst; after about 30 to 60 minutes the corresponding 1-Iodoalkyne is formed. When reacted with organic azides 5-iodo-1,2,3-triazole products are formed, which can be useful synthetic intermediates for further functionalization (Scheme 10). [70]



Scheme 10: Iodoalkyne version of the CuAAC reaction [61]

Sharpless and Fokin claim that this system produces the 5-iodotriazoles as the exclusive products, with no dehalogenation of either the iodoalkyne or triazole product. Due to the mild reaction conditions, high selectivity and low catalyst loading, these reactions are also relatively simple to work up. Fokin and Hein have also proposed two possible mechanistic pathways along which the reaction may occur, shown in Scheme 11. [61]

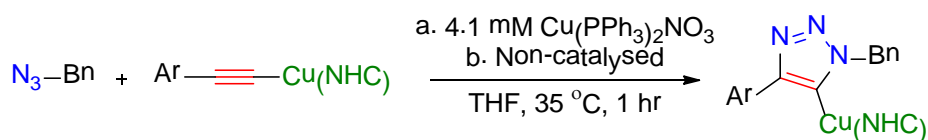


Scheme 11: Proposed mechanistic pathways for the Cu(I)-catalyzed azide-iodoalkyne cycloaddition [61]

Pathway (a) is similar to that proposed for the CuAAC reaction, with the first key intermediate being the σ -acetylide complex (15) formation, followed by the activation and coordination of the azide to the copper acetylides as previously discussed for the CuAAC mechanism. The cycle is completed by the exchange of the copper iodide with the iodoalkyne (20) through a σ -bond metathesis, forming the triazole product (24) and recovering the acetylide (15). [60] Pathway (b) involves the activation of the iodoalkyne by forming a π -complex with the copper (21), which then interacts with the azide to form the complex (22). Cyclisation occurs to produce the vinylidene-like intermediate (23) and to give the triazole product (24). It is of particular interest to note that the copper-iodide bond is never broken during this pathway. [60]

Fokin and Hein proposed that pathway (b) was the preferred of the two routes. The main reason for this proposal was the exclusive formation of the 5-iodotriazole product, even if the reaction is carried out in protic solvents or with substrates with acidic protons. If pathway (a) were followed they postulate that a mixture of 5-iodo and 5-prototriazoles would be formed. [61]

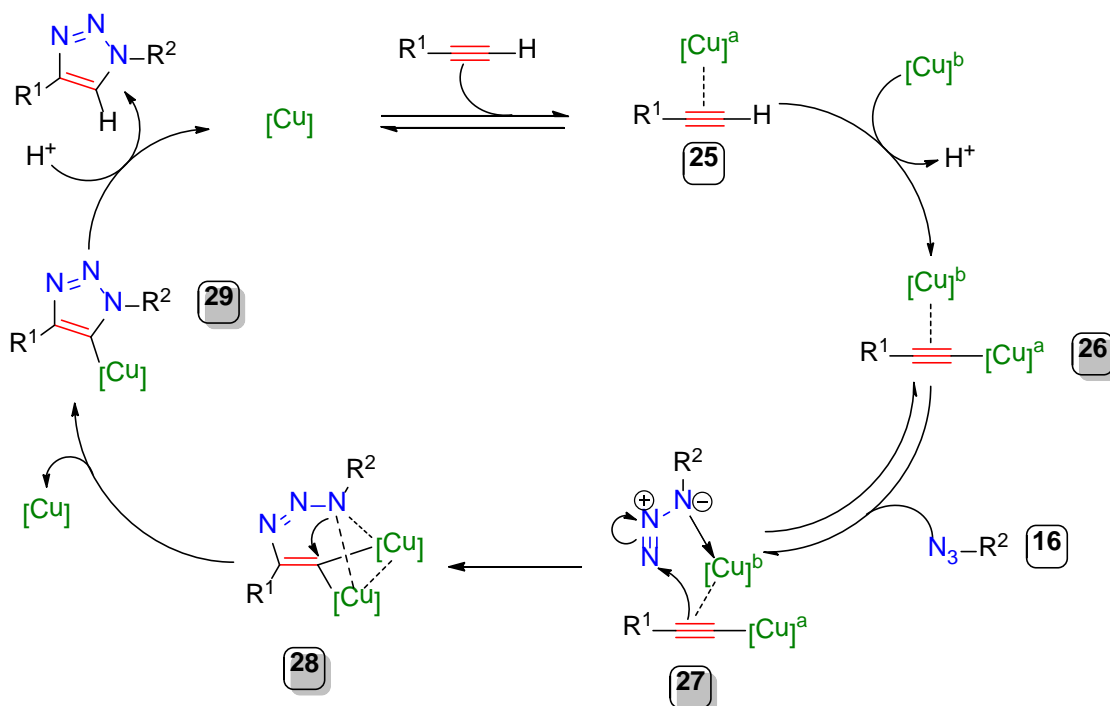
Fokin's latest paper provides further direct evidence of a dinuclear copper intermediate in the CuAAC reaction. [71] They began by establishing the necessity for a second copper atom within the active cycloaddition complex. This was achieved via a reaction of a σ -bound copper(I) acetylide treated with a stoichiometric amount of organic azide in the presence of an added copper(I) catalyst (Scheme 12), which was monitored by real-time heat-flow reaction calorimetry.



Scheme 12: CuAAC reaction carried out by Fokin and co-workers, both catalysed and uncatalysed. [71]
 Bn, benzyl; Ar, *p*-^tBuPh, ^tBu; NHC, 1,3-bis(2,6-diisopropyl)phenyl-4,5-dihydroimidazol-2-ylidene

They found that the catalysed reaction reached completion much quicker than the non-catalysed reaction, and by lowering the catalyst concentration a decrease in the maximum reaction rate was observed. This showed a positive-order dependence on the exogenous copper species. [71]

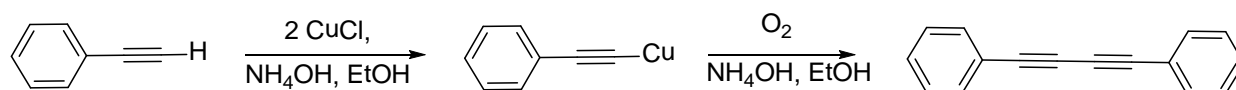
Fokin and his co-workers then sought to establish the respective roles of each copper atom. Their previous work had suggested that the first copper atom acted purely as a strongly σ -bound ligand, and the second copper atom operated through weak π complexation (Figure 36). By using a series of isotopic enriched reactions and analysing them by TOF-MS they found this previous transition state to be incorrect. Fokin proposed the following mechanistic interpretation to account for their new results (Scheme 13).^[71]



Scheme 13: Proposed catalytic model for the CuAAC with two copper atoms.^[71]

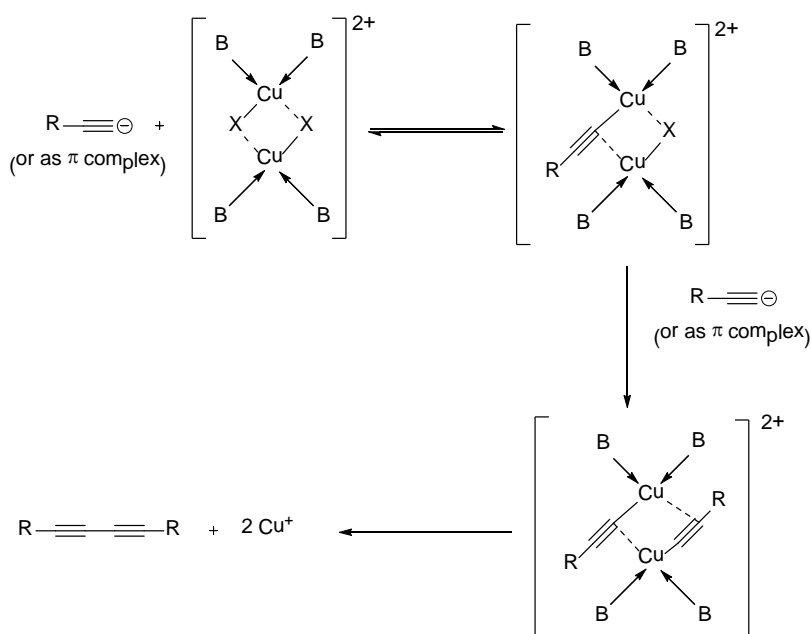
The mechanism now includes the second copper atom (**26**) which acts as a stabilising donor ligand to the unstable mononuclear metacycle intermediate (**28**). They conclude that there is a reactivity trend in which any σ -acetylide that can effectively recruit a π bound copper atom will undergo annulation with a compatible dipolar partner.^[71]

Acetylenic coupling is another area of synthetic chemistry which is currently receiving a lot of interest. The di- and oligo-acetylene products are frequently found in natural products, and can be useful in synthetic receptors for molecular recognition. A recent review by Siemsen and co-workers covers the area in great depth. [72] The original acetylenic coupling was first observed by Carl Glaser in 1896, [73] where he observed copper(I) phenylacetylide, when exposed to air, underwent oxidative dimerization to diphenyldiacetylene (Scheme 14).



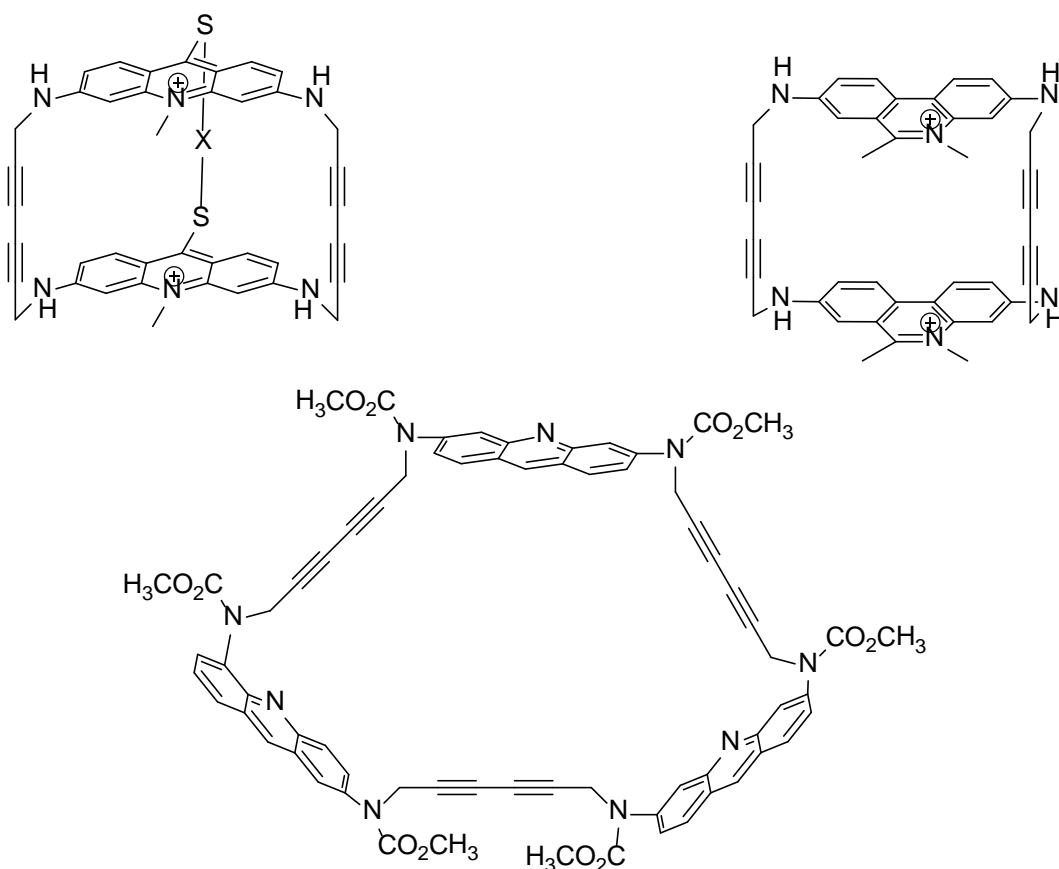
Scheme 14: The first Glaser coupling [73]

The original conditions are still frequently used for homo-coupling, however for hetero-coupling conditions the demand is still high. Of particular interest to this report are the conditions which use copper salts. For the oxidative coupling the mechanism proposed by Bohlmann and co-workers [74] provides a reasonable and widely accepted process shown in Scheme 15. There are few mechanistic examinations of catalyzed hetero-coupling which is probably due to the rapid rates of the reactions. [72]



Scheme 15: Oxidative coupling mechanism proposed by Bohlmann [72]

It would be impossible to review every example of the uses of acetylenic coupling, however one interesting example comes from the area of macrocyclic receptors. Lehn and co-workers were able to synthesise the receptors shown in Scheme 16 by homo-coupling of the propargyl derivatives using Eglinton conditions. [75] In these species the bridges serve as rigid spacers that provide the cavities for aromatic substrates and nucleotides that interact via intercalative π - π stacking.

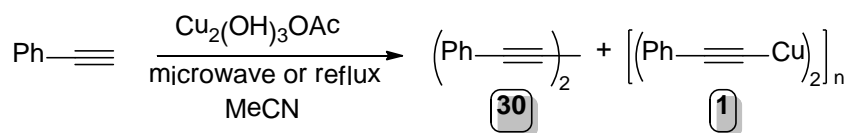


Scheme 16: Macrocyclic receptors prepared by Eglinton conditions by Lehn and co-workers [75]

Alkynyl Copper Ladder Polymers as Catalysts

Previous work within the Buckley-Dann group looked into various layered materials, such as $\text{Cu}_2(\text{OH})_3\text{NO}_3$ and $\text{Cu}_2(\text{OH})_3\text{OAc}$, for use as catalysts in organic synthesis. Whilst using copper hydroxyacetate in CuAAC reactions a bright yellow solid was isolated instead of the green layered material. This solid was later found to be a copper(I) alkynyl polymer. As previously discussed in the introduction dipolar cycloaddition reactions of terminal alkynes and organic azides are accelerated by the use of copper(I) catalysts. [25,26] This work then focused on gathering further experimental evidence on the mechanism of alkyne-azide click reaction.

Early studies examined the Eglinton-Glaser variation of acetylenic coupling, which uses copper(II) acetate. [75] The group determined it would be of use to investigate Glaser coupling reactions under conditions which were likely to generate a copper(I) catalytic species, which could then be used for CuAAC reactions. To begin with a suspension of copper(II) hydroxyacetate, a layered hydroxide of known purity as shown by its powder XRD pattern, and excess phenylacetylene in acetonitrile was exposed to microwave irradiation. This resulted in the formation of 1,4-diphenylbuta-1,3-diyne (**30**) in 95% yield, along with an insoluble yellow product (**1**), as shown in Scheme 17.



Scheme 17: Reaction of copper(II)hydroxyacetate and phenylacetylene, resulting in the formation of the yellow ladder polymer phenylethynyl copper(I)

Che and co-workers have determined the crystal structure of polymeric phenylethynylcopper(I) by powder XRD discussed previously in the introduction. [47] From a synthetic perspective it is of particular interest to note that the copper atoms are separated by distances of 2.49 Å and 2.83 Å. This means that they are ideally positioned to take part in the CuAAC reactions based on the transition state of the copper(I) alkyne proposed by Fokin and co-workers. [61] It has been shown that the insoluble yellow material (**1**) formed by the Glaser reaction shown in Scheme 17, is the phenylethynyl copper(I) ladder polymer by comparison of its XRD pattern (Figure 37), with that reported by Che and co-workers.

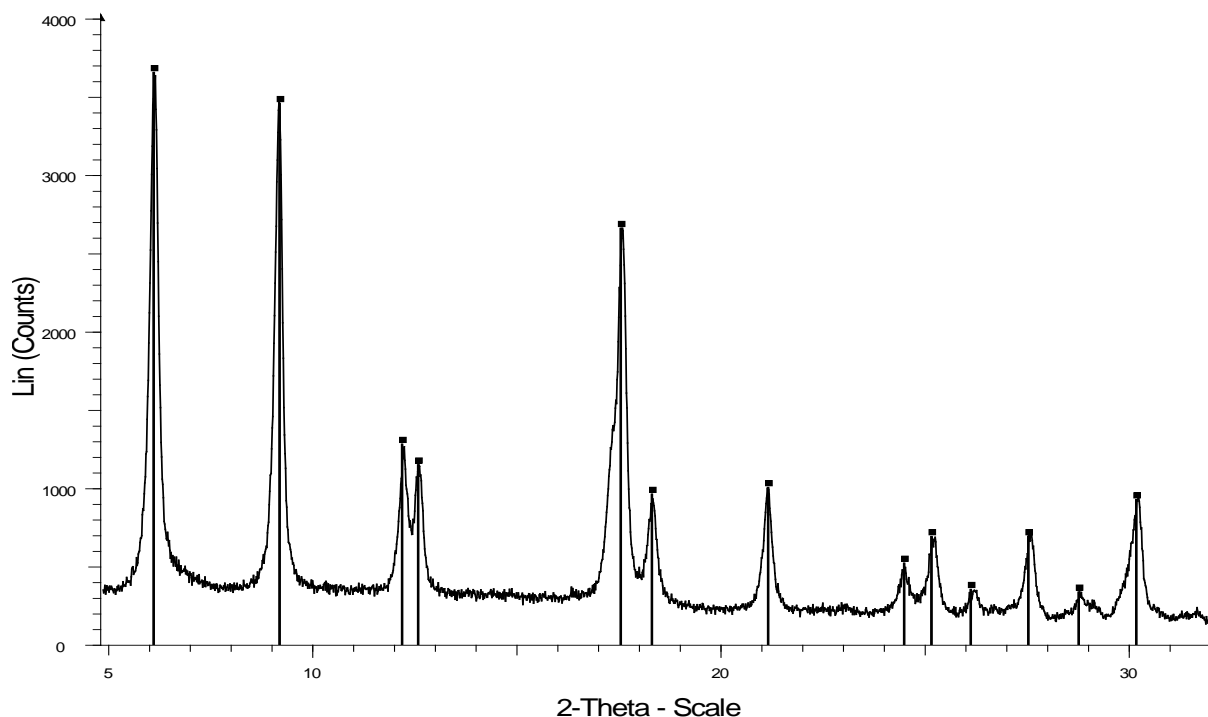
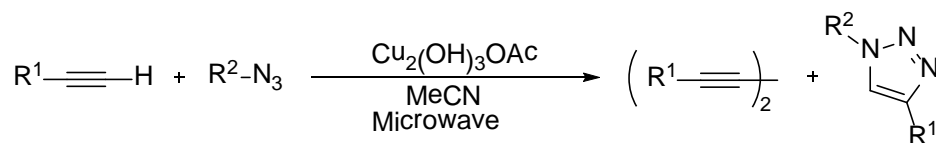


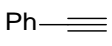
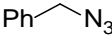
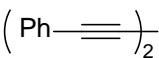
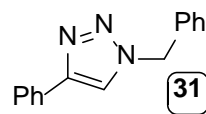
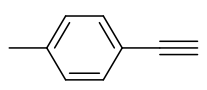
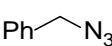
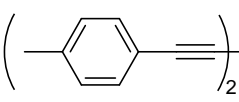
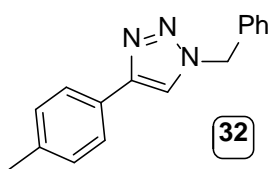
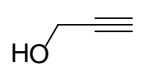
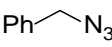
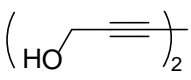
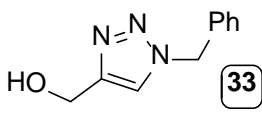
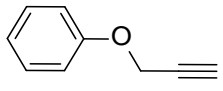
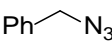
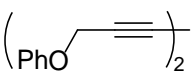
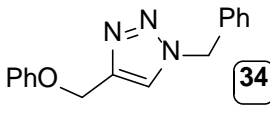
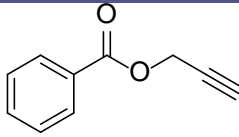
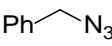
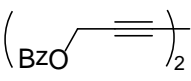
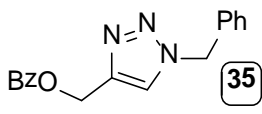
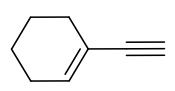
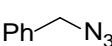
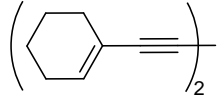
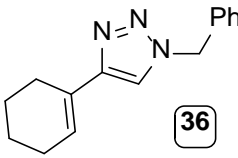
Figure 37: XRD pattern of the “yellow material” compared with the theoretical pattern (vertical ticks) from the structure of phenylethynyl copper(I) determined by Che and co-workers [47]

The research was then continued by examining the click reaction of benzyl azide with excess phenylacetylene using copper(II) hydroxyacetate as a catalyst. We observed the Glaser product 1,4-diphenylbuta-1,3-diyne, 77%, and the triazole product 1-benzyl-4-phenyltriazole, 92%, the phenylethynyl copper(I) was also formed 82% from the acetate. A series of experiments was then conducted using various alkynes, detailed in Table 7.



Scheme 18: General reaction scheme for the experiments shown in Table 7

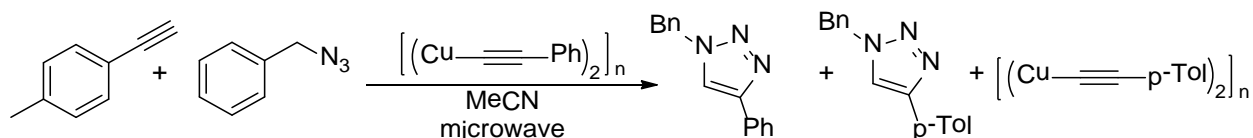
Table 7: Various reactions of alkynes and azides, with the corresponding glaser and 1,2,3-triazole products carried out with $\text{Cu}_2(\text{OH})_3\text{OAc}$ ^a

Alkyne	Azide	Glaser Product	Yield ^{b,c} (%)	Click Product	Yield ^b (%)
			77		92
			70		89
			74		79
			81		73
			79		85
			87		86

^a General conditions: $\text{Cu}_2(\text{OH})_3\text{OAc}$ (10 mol%), alkyne (1.5 eq.), azide (1.0 eq.), MeCN, 100°C microwave, 10 min. ^b single isolated yield. ^c Calculated w.r.t. mol% Cu added.

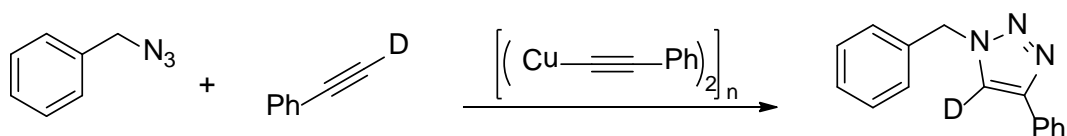
This was followed by a series of experiments to investigate the function of the phenylethynyl copper(I) ladder polymer. A click reaction was carried out between phenylacetylene and benzylazide in acetonitrile using the phenylethynyl copper(I) ladder polymer as the catalyst, this produced 1-benzyl-4-phenyltriazole in 86% yield. Re-using the ladder polymer in further reactions provides similar yields.

A click reaction of *p*-tolylacetylene and benzylazide catalysed by 10 mol% phenylethynyl copper(I) ladder polymer gave two different triazole products, 1-benzyl-4-phenyltriazole 10% and 1-benzyl-4-*p*-tolyltriazole 85%, shown in Scheme 19.



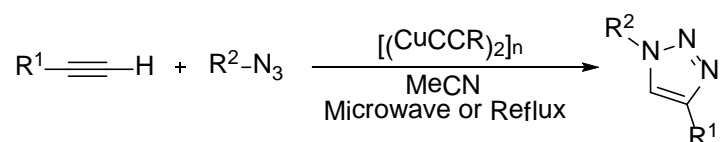
Scheme 19: By using a different acetylene and ladder polymer a mixture of products are obtained, and the R group on the ladder polymer is completely substituted

This suggests that the alkyne attached to the copper in the ladder polymer can be replaced during the reaction. To further understand the mechanism a reaction of 1-^[2H]-2-phenylethyne with benzylazide, using the phenylethynyl-copper(I) ladder as the catalyst, this produced 1-benzyl-4-phenyl-5-^[2H]-triazole as the product with a 65% yield with a quantitative incorporation of deuterium, shown in Scheme 20.



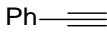
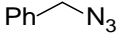
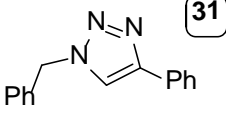
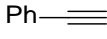
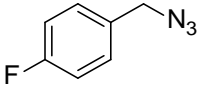
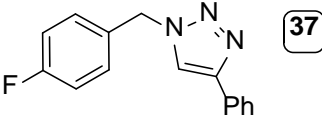
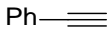
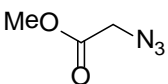
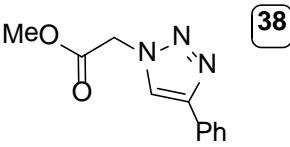
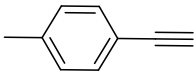
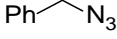
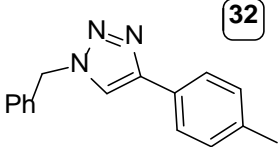
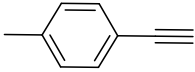
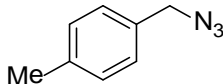
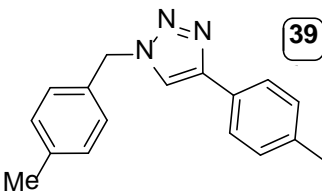
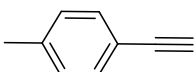
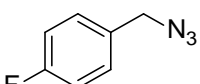
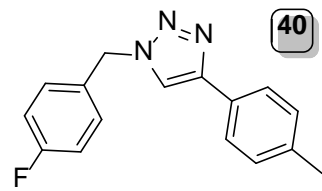
Scheme 20: By using a deuterated acetylene it was possible to observe the source of the proton in the triazole product as terminal proton of the acetylene

This experiment proved that under our reaction conditions the proton source for the triazole product comes from the alkyne starting material. Finally a series of reactions were carried out using phenylacetylene or *p*-tolylacetylene with a variety of different azides to show the scope of the reaction using our conditions, these are shown in Table 8.



Scheme 21: General reaction scheme for the experiments shown in Table 8

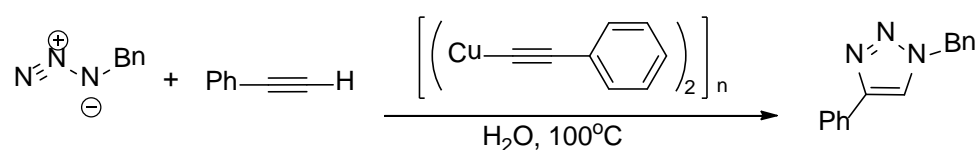
Table 8: A range of alkynes and azides reacted together with a copper(I) ladder polymer catalyst to give various triazole products carried out with $[(\text{CuCCR})_2]_n$ ^a

Catalyst	Alkyne	Azide	Product	Yield (%)
$[(\text{CuCCPh})_2]_n$ (10mol%)			 31	86
$[(\text{CuCCPh})_2]_n$ (10mol%)			 37	82
$[(\text{CuCCPh})_2]_n$ (10mol%)			 38	88
$[(\text{CuCC-pTol})_2]_n$ (10mol%)			 32	75
$[(\text{CuCC-pTol})_2]_n$ (10mol%)			 39	74
$[(\text{CuCC-pTol})_2]_n$ (10mol%)			 40	88

^a General conditions: $[(\text{CuCCR})_2]_n$ (10 mol%), alkyne (1.5 eq.), azide (1.0 eq.), MeCN, 100°C microwave, 10 min. ^b single isolated yield.

Click “on Water” Reactions

Organic synthesis “on water” has been of growing interest. The advantages of using water as a solvent include; improved safety due to water's high heat capacity and unique stability, and simplicity of product isolation. Therefore, using these alkynyl copper(I) ladderane polymers as catalysts for a range of azide-alkyne reactions “on water” was of particular interest. To begin a reaction was carried out between phenylacetylene (1.2 mmol), benzylazide (1.0 mmol), and 10 mol% phenylethynylcopper(I) as the catalyst in water (5 mL). These conditions were used to optimise the conditions for the click reaction, see Scheme 22.



Scheme 22: Reaction of benzyl azide and phenylacetylene using water as a solvent, and phenylethynyl copper(I) as the catalyst, to generate a 1,2,3-triazole product.

The first reactions were performed at room temperature and stirred overnight, changing the order of addition of each of the starting materials, to see if the order of addition made any difference to the product yield. It was observed that when the phenylacetylene and benzylazide were added to water followed by the catalyst a slight increase in yield was achieved so this method was continued for the following reactions.

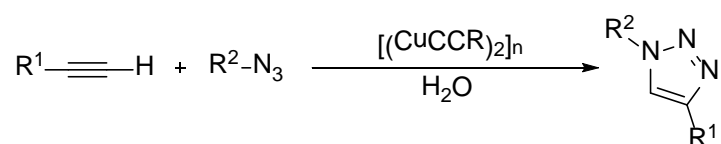
The effects of temperature on the reactions were then determined by performing one reaction in a water bath at 50°C overnight (61 % yield), and one reaction in the microwave at 100°C for 10 min (49 % yield), whilst the 50°C reaction gave the better yield this was attributed to the length of time allowed for the reaction. An examination of the optimum reaction time for the click reaction “on water” in the microwave was undertaken, where it was found that when left for 3 x 10 min the yield (61 %) improved to become similar to the 50°C reaction. Further optimisation was carried out, and found that by increasing the volume of water to 20 mL and the excess of phenylacetylene to 2.1 mmol it was possible to obtain a yield of 91 % for the crude 1,2,3-triazole product.

Lower loadings of the catalyst resulted in lower yields of the product for example 81 % when using 2.5 mol%, and 68 % when using 1 mol%. However by increasing the

irradiation time of the 2.5 mol% loading to 6 x 10 min the product was observed in an 89 % yield, which is within experimental error for the reaction of 10 mol% for 3 x 10 min.

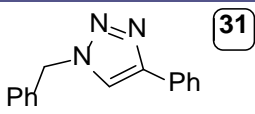
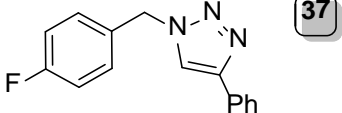
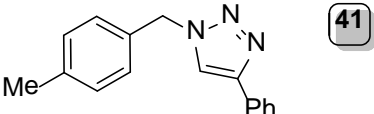
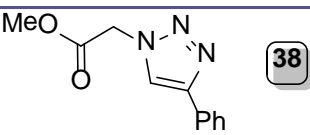
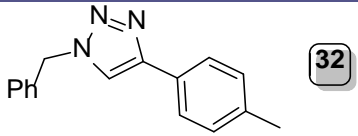
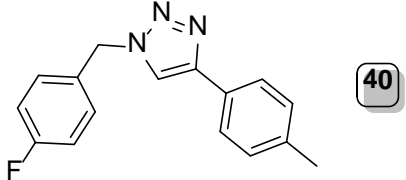
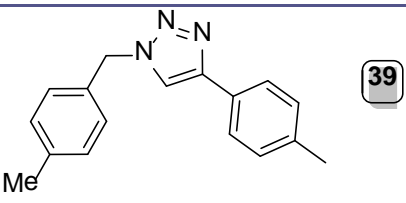
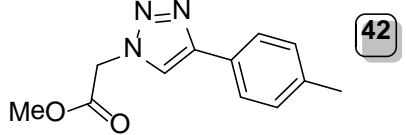
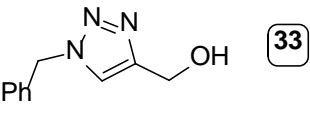
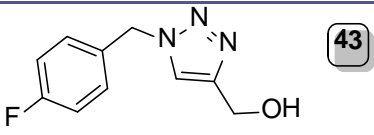
Since the reaction was performed “on water”, which is considered environmentally green, an equally green work-up rather than the previously used solvent dichloromethane, was sought. Sublimation was considered as a method of green work-up, requiring no solvent whatsoever. After the reaction was performed in the microwave the water was removed by filtration and the remaining solid heated on the kugler to 150°C for approximately 30 min, at which point it was observed that yellow globules of product and polymer had broken down to leave a layer of yellow solid on the bottom, and white crystals on the top half of the RBF. ¹H NMR spectroscopic analysis of the white crystals revealed there to be the purified click product, however since the separation had remained in a single flask an accurate yield of purified product was not obtained. So although this has proven to be a greener method of work-up, further work was not carried out in this manner, however with a stronger vacuum it may have been possible to achieve complete separation.

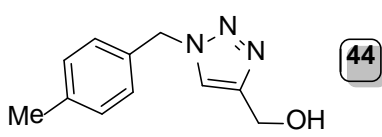
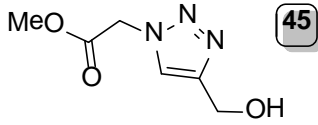
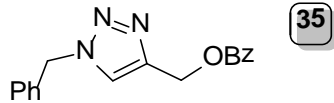
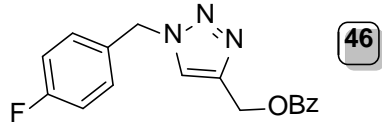
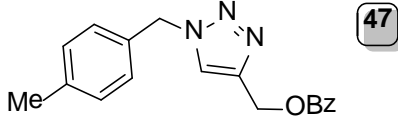
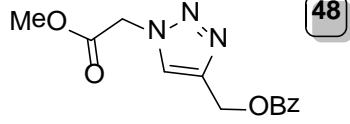
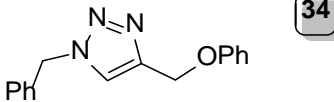
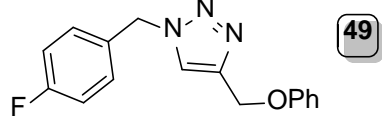
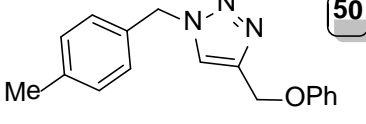
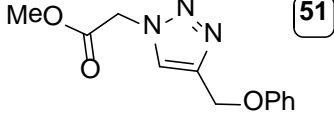
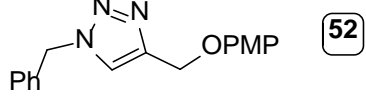
Using these optimised conditions a range of azides and acetylenes were used to generate a variety of 1,2,3-triazoles by “click on water”, these are shown in Table 9.

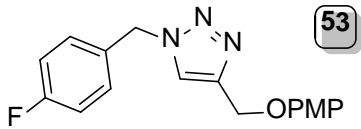
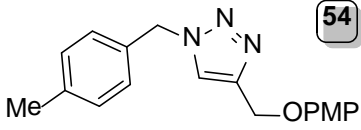
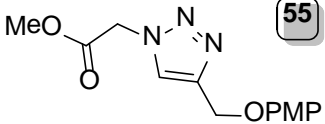


Scheme 23: General reaction scheme for the experiments in Table 3

Table 9: Results for the click “on water” series of reactions carried out under general conditions ^a

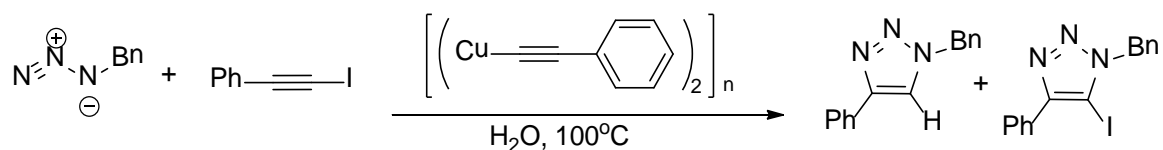
Catalyst	Click Product	Yield ^b (%)
[[CuCCPh] ₂] _n (10mol%)	 31	91
[[CuCCPh] ₂] _n (10mol%)	 37	99
[[CuCCPh] ₂] _n (10mol%)	 41	86
[[CuCCPh] ₂] _n (10mol%)	 38	82
[[CuCC- <i>p</i> Tol] ₂] _n (10mol%)	 32	88
[[CuCC- <i>p</i> Tol] ₂] _n (10mol%)	 40	79
[[CuCC- <i>p</i> Tol] ₂] _n (10mol%)	 39	83
[[CuCC- <i>p</i> Tol] ₂] _n (10mol%)	 42	98
[[CuCCCH ₂ OH] ₂] _n (10mol%)	 33	69
[[CuCCCH ₂ OH] ₂] _n (10mol%)	 43	98

Catalyst	Click Product	Yield ^b (%)
[[CuCCCH ₂ OH] ₂] _n (10mol%)	 44	87
[[CuCCCH ₂ OH] ₂] _n (10mol%)	 45	51
[[CuCCCH ₂ OBz] ₂] _n (10mol%)	 35	68
[[CuCCCH ₂ OBz] ₂] _n (10mol%)	 46	78
[[CuCCCH ₂ OBz] ₂] _n (10mol%)	 47	73
[[CuCCCH ₂ OBz] ₂] _n (10mol%)	 48	57
[[CuCCCH ₂ OPh] ₂] _n (10mol%)	 34	71
[[CuCCCH ₂ OPh] ₂] _n (10mol%)	 49	87
[[CuCCCH ₂ OPh] ₂] _n (10mol%)	 50	83
[[CuCCCH ₂ OPh] ₂] _n (10mol%)	 51	89
[[CuCCCH ₂ OPMP] ₂] _n (10mol%)	 52	67

Catalyst	Click Product	Yield ^b (%)
[[CuCCCH ₂ OPMP] ₂] _n (10mol%)	 53	66
[[CuCCCH ₂ OPMP] ₂] _n (10mol%)	 54	68
[[CuCCCH ₂ OPMP] ₂] _n (10mol%)	 55	66

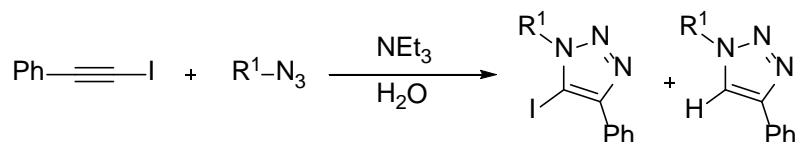
^a General conditions: [[CuCCR]₂]_n (10 mol%), alkyne (2.1 eq.), azide (1.0 eq.), H₂O, 100°C microwave, 3 x 10 min.
^b single isolated yield.

Reactions of 1-iodoalkynes and azides catalysed by copper(I) iodide, in the presence of an amine ligand are comparable to the CuAAC reactions of terminal alkynes, but with significant enhancements. Previous work has shown that the alkynyl copper(I) ladderane complexes could be used to catalyse the reactions rather than copper(I) iodide. It was therefore of interest to see if these reactions could be carried out “on water”, in similar microwave assisted reactions to the terminal alkynes discussed previously, see Scheme 24.



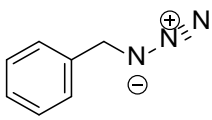
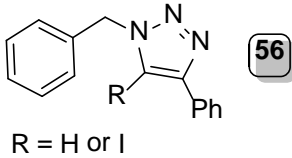
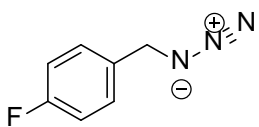
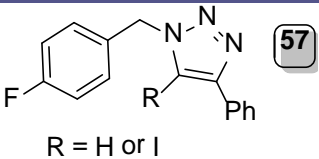
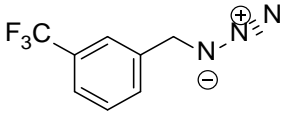
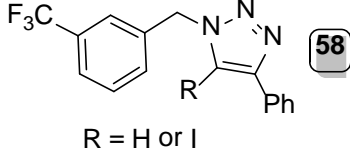
Scheme 24: Click reaction of iodoacetylene and benzylazide, using “on water” conditions, generates two possible 1,2,3-triazole products.

To begin three different azides (1 mmol) were reacted with iodoacetylene (1 mmol) using triethylamine (2 mmol) as a base and phenylethynylcopper(I) (10 mol%) as the catalyst in water (20 mL), in the microwave for 3 x 10 min at 100°C. The results of these reactions are shown in Table 10. The ratio of protonated to iodinated products was obtained from the NMR data.



Scheme 25: General reaction scheme for the experiments shown in Table 10

Table 10: Various azides reacted with iodoacetylene **a, showing the ratio of protonated to iodinated products and the overall yield of the reactions.**

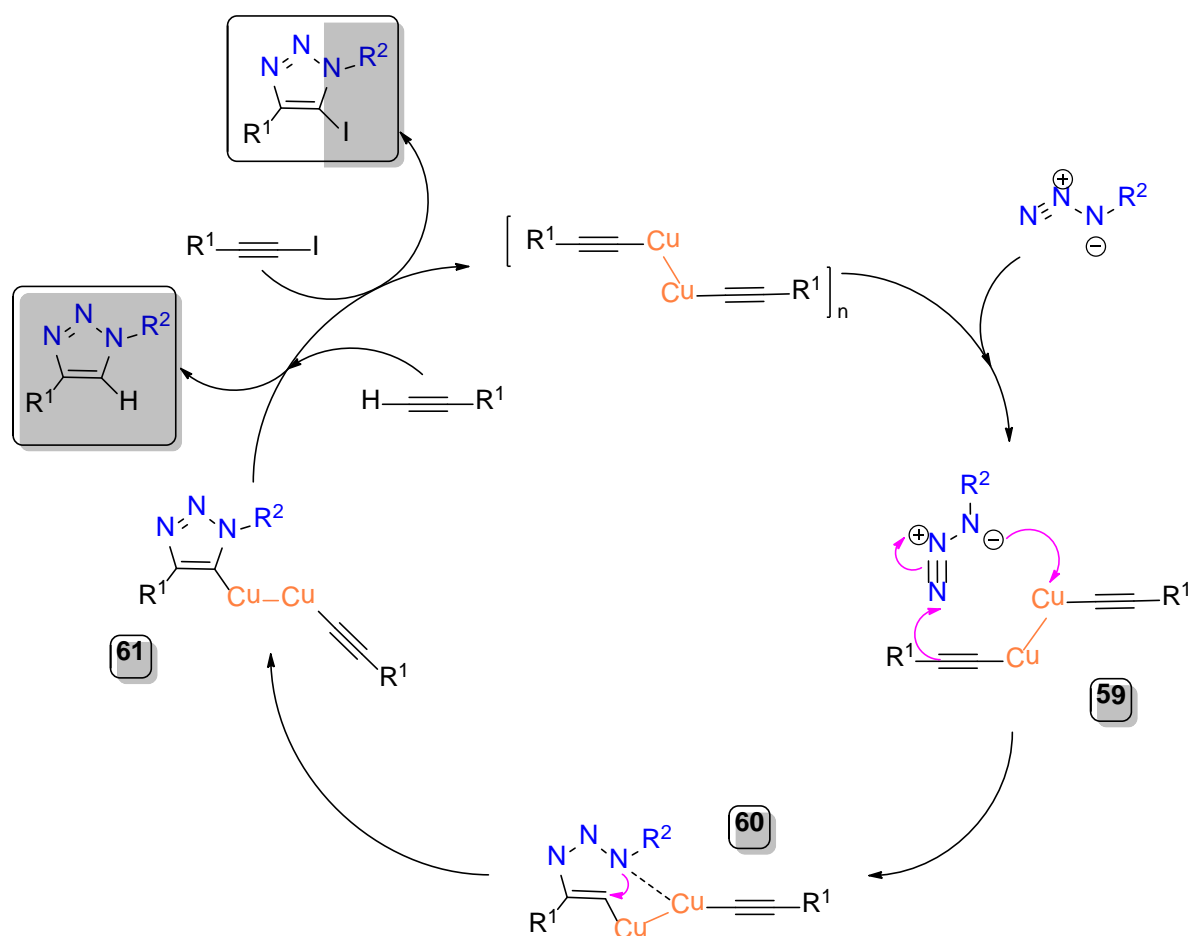
Azide	Product	Ratio (H : I) ^b	Total Yield (%) ^c
	 R = H or I	1 : 3 20% : 40%	60%
	 R = H or I	1 : 2.8 18% : 33%	51%
	 R = H or I	1 : 1.9 30% : 39%	69%

^a General conditions: [(CuCCPh)₂]_n (10 mol%), iodoalkyne (1.0 eq.), azide (1.0 eq.), triethylamine (2.0 eq.), H₂O, 100°C microwave, 3 x 10 min. ^b ratio of products determined by ¹H NMR. ^c combined yield of protonated and iodinated species

A variety of reactions were then carried out changing the quantity and type of base used in the reaction, using the 3-(trifluoromethyl)benzyl azide as it gave the best yield of the previous azides examined. By changing the quantity of triethylamine used (from 2 mmol to 4 mmol) resulted in an overall increase in the yield from 30 % and 39 % to 73 % and 26 % (protonated % and iodinated % respectively). When the base was changed to N,N,N',N',N''-pentamethyldiethylenetriamine PMDETA (2 mmol) a further increase in the amount of protonated product was observed with yields of 62 % and 12 % (H % and I % respectively). When DMAP (2 mmol) was used a yield of 43 % was observed for both protonated and iodinated species. Finally a reaction was performed using no base at all, which resulted in the formation of 44 % and 20 % (H % and I % respectively) which suggests that under microwave conditions protolysis of iodophenylacetylene occurs, but the 5-cupro-1,2,3-triazoles do not undergo proteolysis.

Mechanistic Discussion

From these results the following mechanism is proposed, (Scheme 26).



Scheme 26: Our groups proposed mechanism for the click reactions of azides with terminal, and iodo-alkynes

The reaction mechanism begins with the activation and co-ordination of the azide group to the copper ladder polymer (**59**). This is followed by a cyclisation to form the first carbon - nitrogen bond, which is stabilised by the presence of the second copper atom from the copper ladder (**60**). This retains the copper - copper bond from the copper(I) alkynyl ladder polymer, unlike the transition state shown in Figure 36, where the second copper interaction was described as interacting strongly with the acetylide carbon. The second carbon - nitrogen bond is made forming the five membered ring (**61**) with the copper now in an external position. Finally a σ -bond metathesis using excess alkyne material protonates the ring, and disconnecting the ladder polymer forming the triazole product. The copper(I) alkynyl ladder polymer (**1**) is regenerated allowing it to go on to further catalyse the reaction.

Flow Chemistry

Flow chemistry is the process of running a chemical reaction in a continuously flowing stream rather than in batch production. There are many benefits to using flow chemistry, some of the most valuable include the ability to perform multi-step reactions in a continuous sequence, which is handy if any intermediate species formed are unstable, or add further reagents to the reaction stream at specific points in time when required to prevent earlier side reactions from occurring. It can also allow you to pass the reaction stream over a catalyst which can then be recycled and used again. Figure 38 shows a Uniqsis FlowSyn reactor used for trial with click chemistry. The two parts of the system to take particular note of include the coil (right) which can be used to heat the reaction flow to high temperatures, and the heat block (left) where a tube filled with a solid material can also be heated and the reaction flow passed through.

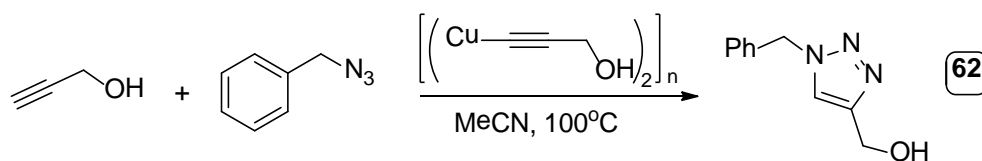


Figure 38: Picture of the Uniqsis FlowSyn system used in the flow reactions (obtained from uniqsis website: <http://www.uniqsis.com>)

The use of a flow reactor would allow the click reaction using an alkynyl copper(I) ladder polymer (Scheme 27) to be performed on a large scale. The reaction to be examined was between benzyl azide (2 M solⁿ, 10 mL) and propargyl alcohol (3 M solⁿ, 10 mL), which were made up in acetonitrile to reduce viscosity, and allow them to be pumped easily through the system.

It was possible to enter a specific flow rate of the reagents (1 mL/min), which would allow a precise quantity of starting material to react over a given time, and therefore allow for quantification of the end product. The starting materials were then passed through a mixer, and then through the heating coil, which allowed them to reach reaction temperature before reaching the catalyst. The catalyst was pre-packed into a column, with a known quantity, this could then be heated to reaction temperature in another self-contained oven.

The reaction flow then passed over the catalyst, the amount of contact between reagents and catalyst could be determined by the set flow rate.



Scheme 27: Flow reaction of propargyl alcohol and benzyl azide

The end material was collected and analysed by GC-MS, and was found to contain both the desired product and remaining starting materials. This suggests that alkynyl copper(I) ladder polymers could be used to catalyse large scale click reactions under flow conditions. However, time constraints with the instrument prevented further optimisation of the process.

Chapter 2 Conclusion

The work carried out in this chapter has demonstrated the use of copper(I) alkynyl ladder polymers as catalysts in CuAAC reactions, which showed very good yields and also tolerates a variety of substrates. Standard microwave conditions were optimised for the click reactions with phenylacetylene and benzylazide. It was found that using a two equivalent excess of acetylene to azide, with 10 mol% catalyst for 30 minutes in the microwave afforded the best results.

The reaction has also been shown to be possible when carried out in greener conditions, such as using “on water” rather than conventional solvents whilst maintaining overall high yields.

The click reaction was also carried out using iodoalkynes, whilst still using the copper(I) alkynyl ladder polymers as catalysts. It was shown to be possible to obtain the 1,2,3-triazole product with an iodo functional group, which is highly desirable as it provides a tether for further functionalisation of the product if necessary. A reaction mechanism has been proposed based on these results, which is similar to current literature ^[71] with regards to the presence of two copper atoms within the reaction intermediates.

Scale up of the CuAAC reaction using flow chemistry has also been shown to be a future possibility. If the conditions could be further optimised, flow would allow easy recycling of the catalyst, and minimal solvent requirements, making the reaction much greener than it already can be.

Chapter 2 Experimental

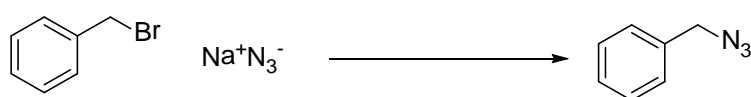
General Experimental Details

Infrared spectra were obtained using a Perkin-Elmer Paragon 1000 FT-IR spectrophotometer. ^1H and ^{13}C NMR spectra were measured at 400.13 and 100.62 MHz by using a Bruker DPX 400 MHz spectrometer or a Bruker Avance 400 MHz spectrometer. The solvent used for NMR spectrometry was CDCl_3 unless stated otherwise, with TMS (tetramethylsilane) as the internal reference. Chemical shifts are given as parts per million (ppm) and the J values are given in hertz (Hz). GCMS analysis was performed by using a Fisons GC 8000 series (AS 800), with a 15m x 0.25mm DB-5 column and electron-impact low-resolution mass spectrometer. Melting points were recorded by using a Stuart Scientific melting point apparatus (SMP3) and are uncorrected. Microanalysis were performed using an Exeter Analytical CE-440 Elemental Analyser. XRD data were recorded by using a Bruker Avance powder diffractometer operating with monochromated $\text{Cu}_{\text{K}\alpha 1}$ radiation over the 2θ range 5-60° with a 0.0147 2θ step unless stated otherwise. Mass spectra were recorded by using a Thermo Fisher Exactive with an ion max source and ESI probe fitted with Advion traversa nanomate.

Preparation of Azides

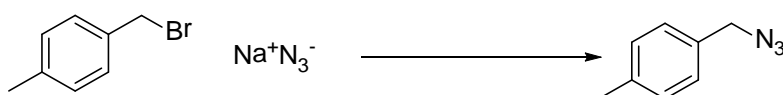
Representative method for the preparation of organic azides

Preparation of benzyl azide ^[76]



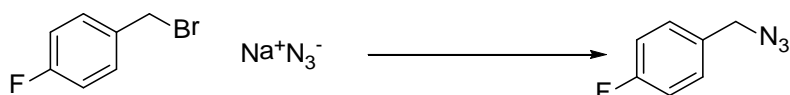
Benzyl bromide (28.0 mL, 235.4 mmol) was added to acetone:water (3:1, 160 mL). Sodium azide (29.3 g, 450.3 mmol) was added and the reaction mixture stirred at room temperature for 24 hours. The reaction was then extracted with dichloromethane (100 mL), and then washed with water (100 mL), followed by brine (100 mL). The organic layer was dried, filtered, and evaporated under reduced pressure to afford the title compound as a pale yellow oil (28.2 g, 90%). IR (thin film): $\nu = 1256.0, 1455.5, 1497.0, 2098.0, 2251.8, 3033.8$. ^1H NMR (400 MHz, CDCl_3): $\delta = 4.24$ (s, 2H, CH_2), 7.24-7.35 (m, 5H, CH Arom.). ^{13}C NMR (100 MHz, CDCl_3): $\delta = 55.0$ (CH_2), 128.3 (CH Arom.), 128.4 (2x CH Arom.), 128.9 (2x CH Arom.), 135.5 (qC), in agreement with the literature. ^[76]

Preparation of p-methylbenzyl azide [76]



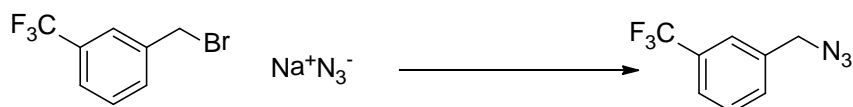
Prepared using the representative procedure from p-methylbenzyl bromide (5.0 g, 27.0 mmol) and sodium azide (3.6 g, 56 mmol). Pale yellow oil (4.4 g, 89%). IR (thin film): $\nu = 1255.0, 1516.0, 2100.5, 2253.2, 3155.1$. $^1\text{H NMR}$ (400 MHz, CDCl_3): $\delta = 2.35$ (s, 3H, CH_3), 4.27 (s, 2H, CH_2) 7.17 (s, 4H, CH Arom.). $^{13}\text{C NMR}$ (100 MHz, CDCl_3): $\delta = 21.2$ (CH_3), 54.7 (CH_2), 128.3 (2x CH Arom.), 129.5 (2x CH Arom), 132.3 (qC), 138.2 (qC), in agreement with the literature. [76]

Preparation of p-fluorobenzyl azide [76]



Prepared using the representative procedure from p-fluorobenzyl bromide (10.0 g, 53 mmol) and sodium azide (6.8 g, 105 mmol). Pale yellow oil (7.5 g, 94%). IR (thin film): $\nu = 1227.4, 1511.1, 1603.0, 2101.0, 2253.0, 3045.8$. $^1\text{H NMR}$ (400 MHz, CDCl_3): $\delta = 4.24$ (s, 2H, CH_2), 7.02 (t, $J = 12$ Hz, 2H, CH Arom.), 7.2 (t, $J = 8$ Hz, 2H, CH Arom.). $^{13}\text{C NMR}$ (100 MHz, CDCl_3): $\delta = 54.0$ (CH_2), 115.6 (CH Arom.), 115.8 (CH Arom.), 130.1 (2x CH Arom.), 131.4 (qC), 162.7 (qC, d, $^1J_{\text{CF}} = 240$ Hz), in agreement with the literature. [76]

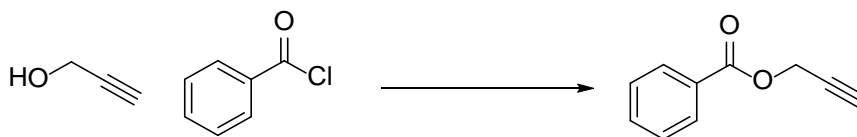
Preparation of 3-(trifluoromethyl)benzyl azide [76]



Prepared using the representative procedure from 3-(trifluoromethyl)benzyl bromide (5.9 g, 25 mmol) and sodium azide (3.3 g, 51 mmol). Yellow oil (4.5 g, 91%). $^1\text{H NMR}$ (400 MHz, CDCl_3): $\delta = 4.42$ (s, 2H, CH_2), 7.50-7.53 (m, 2H, CH Arom.), 7.58-7.61 (m, 2H, CH Arom.), in agreement with the literature. [76]

Preparation of Acetylenes

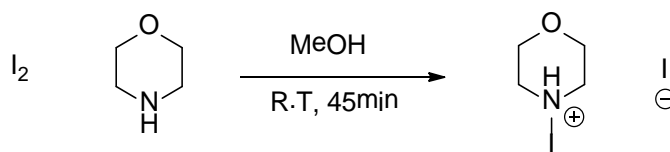
Preparation of propargyl benzoate ^[77]



Dichloromethane (250 mL) was added to a dry 500mL RBF under nitrogen. Propargyl alcohol (13.6 mL, 236 mmol), triethylamine (42 mL, 295 mmol), DMAP (2.4 g, 19.6 mmol) were added and the reaction was cooled in an ice bath for 45 min. Benzoyl chloride (23.2 mL, 196 mmol) was then added dropwise with stirring. The reaction was left to stir in the ice bath for a further 15 min. The reaction mixture was then brought back to room temperature and left to stir for a further 4 hours. The reaction was quenched with ice water (300 mL), and washed with aq. HCl (1 M, 2 x 300 mL), water (300 mL), and brine (300 mL). The organic layer was dried and evaporated under reduced pressure. The crude product was purified by distillation (200°C). Pale yellow oil (22.5 g, 70%). IR (thin film): $\nu = 1315.9, 1370.3, 1452.6, 1602.0, 1725.0, 2254.2, 3307.4$. ¹H NMR (400 MHz, CDCl₃): $\delta = 2.55$ (s, 1H, CH), 4.90 (s, 2H, CH₂), 7.42 (t, J = 8 Hz, 2H, CH Arom.), 7.54 (t, J = 8 Hz, 1H, CH Arom.), 8.04 (d, J = 8 Hz, 2H, CH Arom.). ¹³C NMR (100 MHz, CDCl₃): $\delta = 52.4$ (CH₂), 75.2 (qC), 77.8 (CH), 128.4 (2x CH Arom.), 129.4 (2x CH Arom.), 129.8 (qC), 133.3 (CH Arom.), 165.7 (qC), in agreement with the literature.

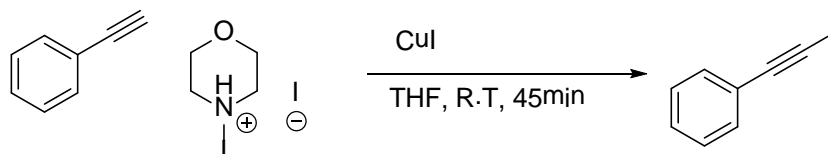
[77]

Preparation of 4-iodomorpholin-4-ium iodide [78]



A solution of iodine (25.4 g, 100 mmol) in methanol (400 mL) was treated dropwise with morpholine (8.71 mL, 100 mmol). The solution was stirred for 45 min, and the solid which formed was then isolated by suction filtration. This solid was then transferred to an RBF and dried under vacuum. An orange crystalline product (30.3 g, 89 %) was obtained.

Preparation of iodophenylacetylene [78]

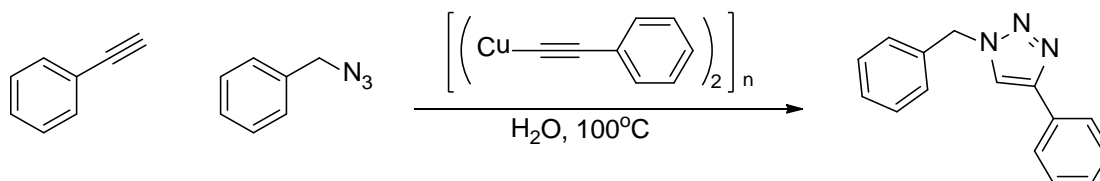


Phenylacetylene (4.1 g, 40 mmol) was dissolved in THF (200 mL) and treated with copper iodide (0.38 g, 2 mmol) and 4-iodomorpholin-4-ium iodide (15.0 g, 44 mmol). The reaction mixture was stirred at r.t. for 45 min. A fine white precipitate formed. The suspension was then poured onto a pad of neutral alumina and washed with DCM. The filtrate and organic fractions were combined and the solvent removed under reduced pressure. A dark orange oil (8.9 g, 97 %). IR (thin film): $\nu = 610.8, 1443.3, 1488.8, 2250.9, 3063.7$. 1H NMR (400 MHz, $CDCl_3$): $\delta = 7.20-7.50$ (m, 5H, CH Arom). ^{13}C NMR (100 MHz, $CDCl_3$): $\delta = 94.4$ (qC), 123.2 (qC), 128.4 (2x CH Arom.), 129.0 (CH Arom.), 132.5 (2x CH Arom.), 147.8 (qC), in agreement with the literature. [75]

Click Reactions

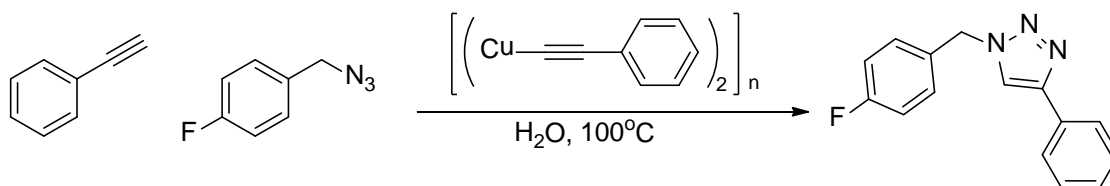
Representative synthesis of the click on water triazole synthesis

Preparation of 1-benzyl-4-phenyl-1H-1,2,3-triazole - (31) [60]



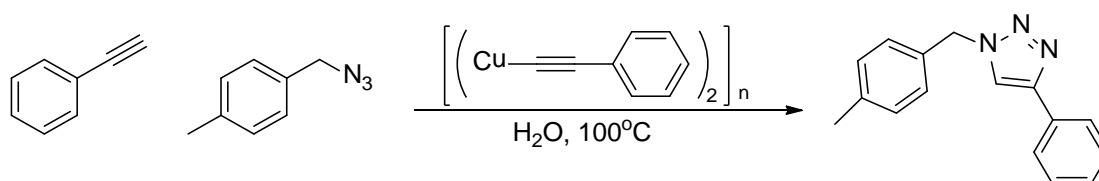
Water (20 mL) was added to a large microwave tube fitted with stirrer bar. Phenylacetylene (0.21 g, 2.1 mmol), benzylazide (0.13 g, 1.0 mmol), and copper ladder polymer (0.0166 g, 0.1 mmol) were added. The reaction was then put in the microwave for 3 x 10min @ 100°C with pre-stirring for 10 s. The reaction was then allowed to cool. The water was removed by gravity filtration, and the remaining solid washed with ethyl acetate. This was dried with magnesium sulfate, filtered and the solvent removed under reduced pressure. White solid (0.22 g, 91 %) was collected. IR (thin film): $\nu = 734.4, 908.8, 2253.0, 3035.1, 3583.9$. ^1H NMR (400 MHz, CDCl_3): $\delta = 5.58$ (s, 2H, CH_2), 7.19-7.35 (m, 8H, CH Arom.), 7.60 (s, 1H, CH), 7.74 (d, 2H, $J = 1.4$ Hz, CH Arom.). ^{13}C NMR (100 MHz, CDCl_3): $\delta = 54.2$ (CH_2), 119.6 (2x CH Arom.), 125.7 (CH Arom.), 127.5 (2x CH Arom.) 128.1 (2x CH Arom.), 128.2 (CH), 128.8 (CH Arom.), 129.2 (2x CH Arom.), 130.6 (qC), 134.7 (qC), 148.3 (qC), in agreement with the literature. [59]

Preparation of 1-(4-fluorobenzyl)-4-phenyl-1H-1,2,3-triazole - (37) [79]



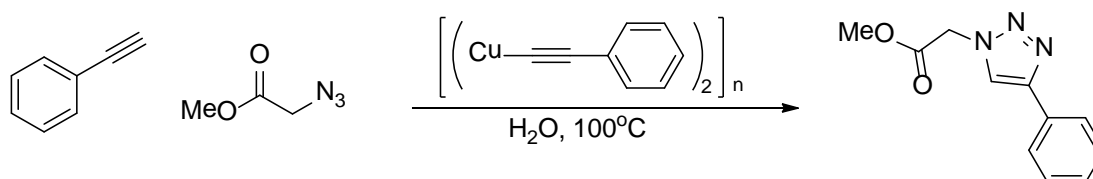
Prepared using the representative procedure from phenylacetylene (0.21 g, 2.0 mmol), p-fluorobenzyl azide (0.15 g, 1.0 mmol), and 10 % ladder polymer. Pale yellow solid (0.25 g, 99 %) was collected. Elemental analysis: Found C 70.78 %, H 4.84 %, N 16.33 % ($\text{C}_{15}\text{H}_{12}\text{N}_3\text{F}$ requires C 71.13 %, H 4.78 %, N 16.59 %). IR (thin film): $\nu = 1422.4, 1512.3, 2305.8, 2986.0, 3054.2$. ^1H NMR (400 MHz, CDCl_3): $\delta = 5.55$ (s, 2H, CH_2), 7.06-7.10 (m, 3H, CH Arom.), 7.26-7.41 (m, 4H, CH Arom.), 7.79 (s, 1H, CH), 7.81 (d, 2H, $J = 1.6$ Hz, CH Arom.). ^{13}C NMR (100 MHz, CDCl_3): $\delta = 53.5$ (CH_2), 116.1 (2x CH Arom, d, $^2J_{\text{CF}} = 8.4$ Hz), 119.4 (2x CH Arom.), 128.3 (CH), 128.9 (CH Arom.), 129.9 (2x CH Arom.), 130.2 (2x CH Arom, d, $^3J_{\text{CF}} = 8.4$ Hz), 130.5 (qC, d, $^4J_{\text{CF}} = 3.3$ Hz), 130.6 (qC), 148.3 (qC), 162.9 (qC, d, $^1J_{\text{CF}} = 250$ Hz), in agreement with the literature. [79]

Preparation of 1-(4-methylbenzyl)-4-phenyl-1H-1,2,3-triazole - (41) ^[80]



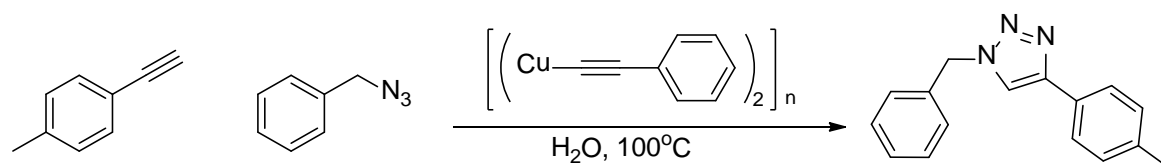
Prepared using the representative procedure from phenylacetylene (0.20 g, 2.0 mmol), p-methylbenzyl azide (0.15 g, 1.0 mmol), and 10% ladder polymer. White solid (0.22 g, 86 %) was collected. ¹H NMR (400 MHz, CDCl₃): δ = 2.35 (s, 3H, CH₃), 5.22 (s, 2H, CH₂), 7.18-7.41 (m, 7H, CH Arom.), 7.63 (s, 1H, CH), 7.78 (d, 2H, J = 7.2 Hz, CH Arom.). ¹³C NMR (100 MHz, CDCl₃): δ = 21.2 (CH₃), 54.0 (CH₂), 119.5 (2x CH Arom.), 125.7 (2x CH Arom.), 128.12 (2x CH Arom.), 128.14 (CH), 128.8 (CH Arom.), 129.8 (2x CH Arom.), 130.7 (qC), 131.7 (qC), 138.7 (qC), 148.1 (qC), in agreement with the literature. ^[80]

Preparation of methyl 2-(4-phenyl-1H-1,2,3-triazol-1-yl)acetate - (38)



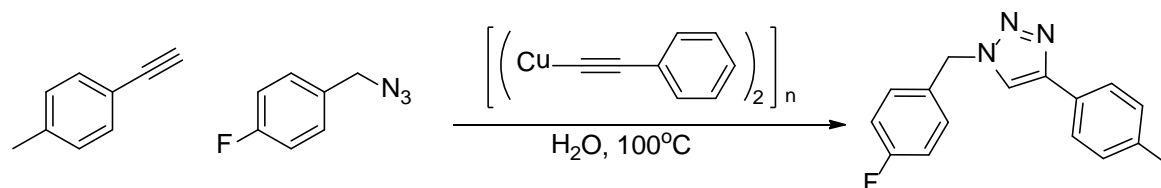
Prepared using the representative procedure from phenylacetylene (0.21 g, 2.0 mmol), methyl 2-azidoacetate (0.12 g, 1.0 mmol), and 10% ladder polymer. White solid (0.18 g, 82 %, m.p 81.4-82.3°C) was collected. Elemental analysis: Found C 60.58 %, H 5.13 %, N 19.08 % (C₁₁H₁₂N₃O₂ requires C 60.82 %, H 5.10 %, N 19.34 %) m/z found 218.0929 (C₁₁H₁₂N₃O₂ [M+H]⁺ requires 218.0924). IR (thin film): ν = 1439.1, 1756.0, 2934.7, 3053.1. ¹H NMR (400 MHz, CDCl₃): δ = 3.82 (s, 3H, CH₃), 5.22 (s, 2H, CH₂), 7.35 (t, 1H, J = 72 .Hz, CH Arom.), 7.43 (t, 2H, J = 7.2 Hz, CH Arom.), 7.84 (d, 2H, J = 0.4 Hz, CH Arom.), 7.92 (s, 1H, CH). ¹³C NMR (100 MHz, CDCl₃): δ = 50.8 (CH₃), 53.1 (CH₂), 121.0 (CH), 128.0 (2x CH Arom), 128.3 (CH Arom.), 128.9 (2x CH Arom), 130.3 (qC), 148.3 (qC), 166.8 (qC).

Preparation of 1-benzyl-4-p-tolyl-1H-1,2,3-triazole - (32) ^[81]



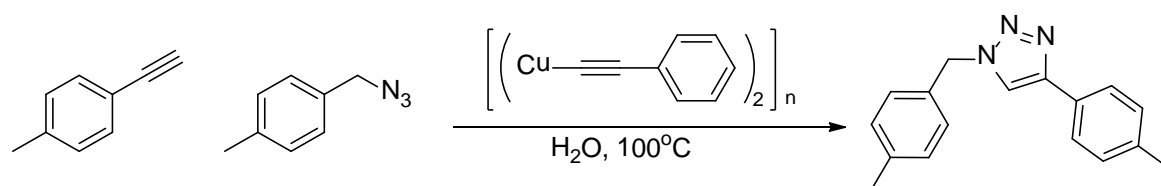
Prepared using the representative procedure from p-tolylacetylene (0.24 g, 2.1 mmol), benzyl azide (0.13 g, 1.0 mmol), and 10 % ladder polymer. White solid (0.22 g, 88 %) was collected. ¹H NMR (400 MHz, CDCl₃): δ = 2.36 (s, 3H, CH₃), 5.57 (s, 2H, CH₂), 7.20 (d, 2H, J = 7.9 Hz, CH Arom.), 7.25-7.38 (m, 5H, CH Arom.), 7.67 (s, 1H, CH), 7.68 (d, 2H, J = 8.2 Hz, CH Arom.). ¹³C NMR (100 MHz, CDCl₃): δ = 21.3 (CH₃), 54.2 (CH₂), 119.2 (2x CH Arom.), 125.6 (2x CH Arom.), 127.7 (2x CH Arom.), 128.1 (CH), 128.9 (CH Arom.), 129.1 (2x CH Arom.), 129.5 (qC), 134.7 (qC), 138.0 (qC), 148.3 (qC), in agreement with the literature. ^[81]

Preparation of 1-(4-fluorobenzyl)-4-p-tolyl-1H-1,2,3-triazole - (40)



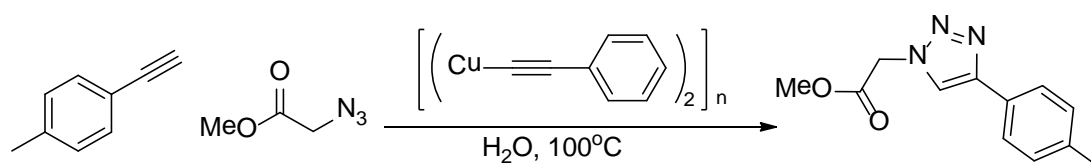
Prepared using the representative procedure from p-tolylacetylene (0.24 g, 2.1 mmol), p-fluorobenzyl azide (0.16 g, 1.0 mmol), and 10 % ladder polymer. Pale yellow solid (0.22 g, 79 %, m.p 150.1-151.3°C) was collected. Elemental analysis: Found C 71.71 %, H 5.27 %, N 15.44 % (C₁₆H₁₅N₃F requires C 71.89 %, H 5.28 %, N 15.72 %) m/z found 268.1248 (C₁₆H₁₅N₃F [M+H]⁺ requires 268.1250). IR (thin film): ν = 1264.9, 1422.0, 3053.3. ¹H NMR (400 MHz, CDCl₃): δ = 2.37 (s, 3H, CH₃), 5.54 (s, 2H, CH₂), 7.12-7.32 (m, 6H, CH Arom.), 7.61 (s, 1H, CH), 7.69 (d, 2H, J = 8.1 Hz, CH Arom.). ¹³C NMR (100 MHz, CDCl₃): δ = 21.3 (CH₃), 53.5 (CH₂), 116.2 (2x CH Arom, d, ²J_{CF} = 20 Hz), 119.0 (2x CH Arom.), 125.6 (2x CH Arom.), 129.5 (CH), 129.9 (qC), 130.3 (2x CH Arom, d, ³J_{CF} = 8 Hz), 131.7 (qC, d, ⁴J_{CF} = 3 Hz), 138.1 (qC), 148.4 (qC), 162.8 (qC, d, ¹J_{CF} = 250 Hz).

Preparation of 1-(4-methylbenzyl)-4-p-tolyl-1H-1,2,3-triazole - (39) ^[82]



Prepared using the representative procedure from p-tolylacetylene (0.24 g, 2.1 mmol), p-methylbenzyl azide (0.15 g, 1.0 mmol), and 10 % ladder polymer. White solid (0.22 g, 83 %) was collected. ¹H NMR (400 MHz, CDCl₃): δ = 2.35 (s, 6H, 2xCH₃), 5.50 (s, 2H, CH₂), 7.11-7.26 (m, 6H, CH Arom.), 7.59 (s, 1H, CH), 7.68 (d, 2H, J = 7.6 Hz, CH Arom.). ¹³C NMR (100 MHz, CDCl₃): δ = 21.2 (CH₃), 21.3 (CH₃), 54.0 (CH₂), 119.1 (2x CH Arom.), 125.6 (2x CH Arom.), 127.9 (2x CH Arom.), 128.1 (2x CH Arom.), 129.5 (CH), 129.8 (qC), 131.8 (qC), 137.9 (qC), 138.7 (qC), 148.0 (qC), in agreement with the literature. ^[82]

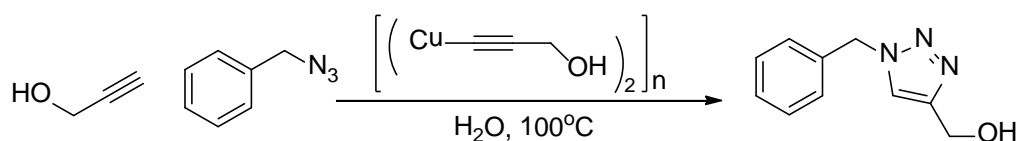
Preparation of methyl 2-(4-p-tolyl-1H-1,2,3-triazol-1-yl)acetate - (42)



Prepared using the representative procedure from p-tolylacetylene (0.24 g, 2.1 mmol), methyl 2-azidoacetate (0.12 g, 1.0 mmol), and 10 % ladder polymer. White solid (0.23 g, 98 %, m.p 116.1-117.0°C) was collected. Elemental analysis: Found C 62.33 %, H 5.69 %, N 17.80 % (C₁₂H₁₄N₃O₂ requires C 62.54 %, H 5.67 %, N 18.17 %) m/z found 232.1084 (C₁₂H₁₄N₃O₂ [M+H]⁺ requires 232.1086). IR (thin film): ν = 1439.1, 1756.0, 2934.7, 3053.1. ¹H NMR (400 MHz, CDCl₃): δ = 2.37 (s, 3H, CH₃), 3.80 (s, 3H, CH₃), 5.20 (s, 2H, CH₂), 7.22 (d, 2H, J = 8.1 Hz, CH Arom.), 7.72 (d, 2H, J = 8.1 Hz, CH Arom.), 7.87 (s, 1H, CH). ¹³C NMR (100 MHz, CDCl₃): δ = 21.3 (CH₃), 50.8 (CH₃), 53.1 (CH₂), 120.7 (CH), 125.7 (2x CH Arom.), 127.5 (2x CH Arom.), 129.5 (qC), 138.2 (qC), 148.3 (qC), 166.8 (qC).

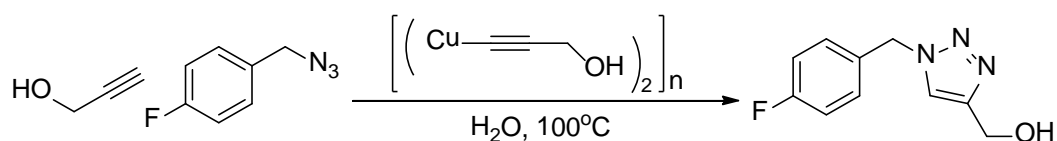
Preparation of (1-benzyl-1H-1,2,3-triazol-4-yl)methanol - (33) [83]

Modified representative synthesis of the click on water triazole synthesis



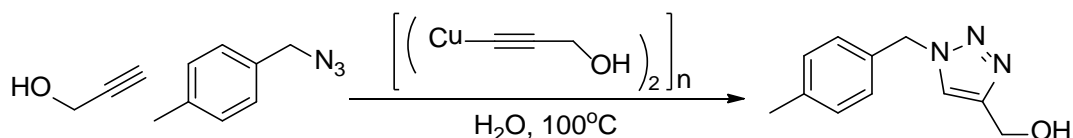
Water (20 mL) was added to a large microwave tube fitted with stirrer bar. Propargyl alcohol (0.12 g, 2.1 mmol), benzylazide, and 10 % copper ladder polymer (0.0143 g, 0.1 mmol) were added. The reaction was put in the microwave for 3 x 10 min @100°C with pre-stirring for 10 s. The reaction was then allowed to cool. The water removed by gravity filtration, and the solid washed with ethyl acetate. The water was extracted with ethyl acetate, then the extracts dried with magnesium sulfate, filtered, and the remaining solvent removed under reduced pressure. White solid (0.19 g, 72 %, m.p 80.5°C) was collected. Elemental analysis: Found C 63.31 %, H 5.85 %, N 21.67 % (C₁₀H₁₁N₃O requires C 63.48 %, H 5.86 %, N 22.21 %) m/z found 190.0970 (C₁₀H₁₁N₃O [M+H]⁺ requires 190.0975). IR (thin film): ν = 649.3, 733.1, 906.2, 1046.7, 1123.5, 1224.4, 1383.5, 1459.1, 2252.2, 3341.1. ¹H NMR (400 MHz, CDCl₃): δ = 4.71 (s, 2H, CH₂), 5.46 (s, 2H, CH₂), 7.23-7.25 (m, 2H, CH Arom.), 7.33-7.35 (m, 3H, CH Arom.), 7.47 (s, 1H, CH). ¹³C NMR (100 MHz, CDCl₃): δ = 54.1 (CH₂), 56.0 (CH₂), 121.9 (CH), 128.1 (2x CH Arom.), 128.8 (CH Arom.), 129.1 (2x CH Arom.), 134.5 (qC), 148.3 (qC), in agreement with the literature. [83]

Preparation of (1-(4-fluorobenzyl)-1H-1,2,3-triazol-4-yl)methanol - (43)



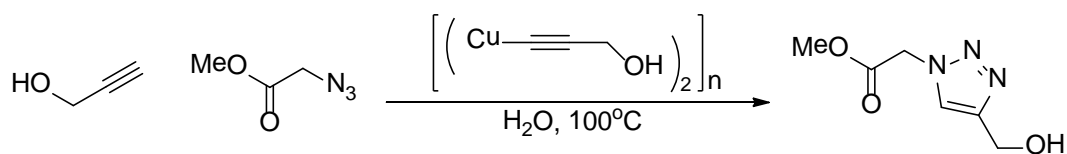
Prepared using the representative procedure from propargyl alcohol (0.12 g, 2.2 mmol), p-fluorobenzyl azide (0.16g, 1.0 mmol), and 10 % ladder polymer. Creamy white solid (0.21 g, 98 %, m.p 66.9°C) was collected. Elemental analysis: Found C 57.97 %, H 4.86 %, N 19.71 % (C₁₀H₁₀FN₃O requires C 57.97 %, H 4.86 %, N 20.28 %) m/z found 208.0874 (C₁₀H₁₀FN₃O [M+H]⁺ requires 208.0881). IR (thin film): ν = 649.4, 733.1, 907.2, 1046.3, 1229.6, 1512.9, 1607.4, 2252.2, 3341.2. ¹H NMR (400 MHz, CDCl₃): δ = 4.66 (s, 2H, CH₂), 5.44 (s, 2H, CH₂), 7.01 (t, ³J_{HF} = 8.4 Hz, 2H, CH Arom.), 7.24 (t, ⁴J_{HF} = 6.8 Hz, 2H, CH Arom.), 7.51 (s, 1H, CH). ¹³C NMR (100 MHz, CDCl₃): δ = 53.4 (CH₂), 55.9 (CH₂), 116.1 (2x CH Arom, d, ²J_{CF} = 21.6 Hz), 122.0 (CH), 130.1 (2x CH Arom, d, ³J_{CF} = 8.3 Hz), 130.5 (qC, d, ⁴J_{CF} = 3.3 Hz), 148.5 (qC) 162.8 (qC, ¹J_{CF} = 247 Hz).

Preparation of (1-(4-methylbenzyl)-1H-1,2,3-triazol-4-yl)methanol - (44)



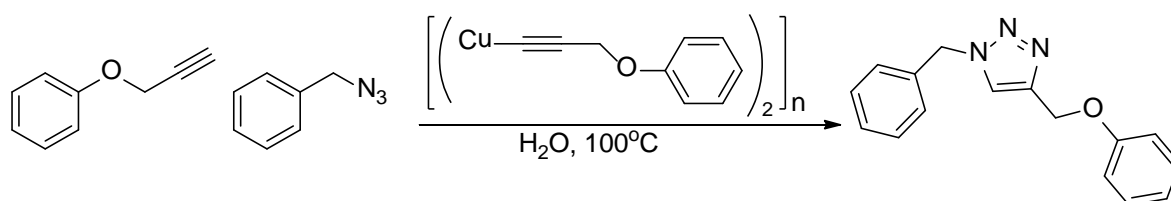
Prepared using the representative procedure from propargyl alcohol (0.12 g, 2.1 mmol), p-methylbenzyl azide (0.16 g, 1.0 mmol), and 10 % ladder polymer. Creamy white solid (0.18 g, 87 %, m.p 90.7°C) was collected. Elemental analysis: Found C 64.99 %, H 6.41 %, N 20.30 % (C₁₁H₁₃N₃O requires C 65.01 %, H 6.45 %, N 20.68 %) m/z found 204.1126 (C₁₁H₁₃N₃O₂ [M+H]⁺ requires 204.1131). IR (thin film): ν = 649.2, 743.7, 907.4, 1046.1, 1121.8, 1223.6, 1382.2, 1461.7, 1515.5, 2252.0, 3328.9. ¹H NMR (400 MHz, CDCl₃): δ = 2.32 (s, 3H, CH₃), 4.69 (s, 2H, CH₂), 5.41 (s, 2H, CH₂), 7.14 (s, 4H, CH Arom.), 7.45 (s, 1H, CH). ¹³C NMR (100 MHz, CDCl₃): δ = 21.2 (CH₃), 53.9 (CH₂), 56.0 (CH₂), 121.8 (CH), 128.2 (2x CH Arom.), 129.7 (2x CH Arom.), 131.5 (qC), 138.7 (qC), 148.3 (qC).

Preparation of methyl 2-(4-(hydroxymethyl)-1H-1,2,3-triazol-1-yl)acetate - (45)



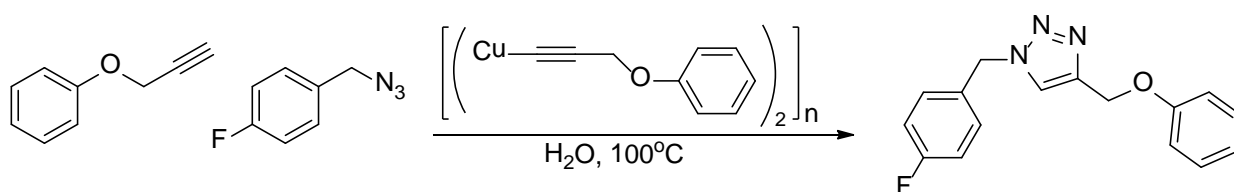
Prepared using the representative procedure from propargyl alcohol (0.11 g, 2.0 mmol), methyl 2-azidoacetate (0.12 g, 1.0 mmol), and 10 % ladder polymer. Brown oil (0.09 g, 51 %) was collected. m/z found 172.0712 ($C_6H_9N_3O_3$ $[M+H]^+$ requires 172.0717). IR (thin film): $\nu = 649.0, 733.0, 907.3, 1048.4, 1225.5, 1441.1, 1756.1, 2252.6, 2955.6, 3357.4$. 1H NMR (400 MHz, $CDCl_3$): $\delta = 3.69$ (s, 3H, CH_3), 4.63 (s, 2H, CH_2), 5.09 (s, 2H, CH_2), 7.63 (s, 1H, CH). ^{13}C NMR (100 MHz, $CDCl_3$): $\delta = 50.7$ (CH_2), 53.0 (CH_3), 55.8 (CH_2), 123.8 (CH), 148.3 (qC), 167.1 (qC).

Preparation of 1-benzyl-4-(phenoxyethyl)-1H-1,2,3-triazole - (34) [60]



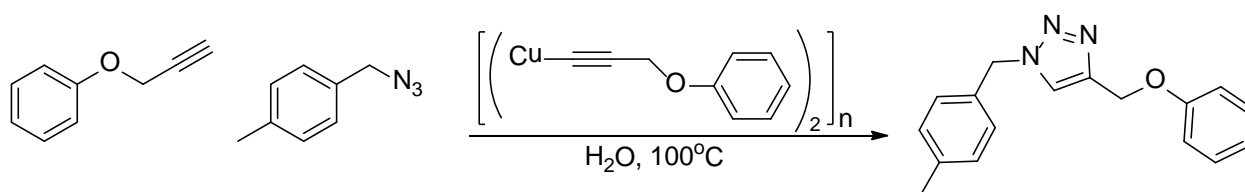
Prepared using the representative procedure from phenyl propargylether (0.31 g, 2.4 mmol), benzyl azide (0.14 g, 1.1 mmol), and 10 % ladder polymer. Product was purified by column chromatography, eluted in 10:1 petrol:ethyl acetate. White solid (0.20 g, 71 %, m.p 121.1°C) was collected. Elemental analysis: Found C 72.18 %, H 5.66 %, N 15.63 % ($C_{16}H_{15}N_3O$ requires C 72.43 %, H 5.70 %, N 15.84 %) m/z found 266.1285 ($C_{16}H_{15}N_3O$ $[M+H]^+$ requires 266.1288). IR (thin film): $\nu = 645.9, 732.2, 907.5, 1048.4, 1238.0, 1459.3, 1491.0, 1597.3, 2252.6, 3152.2$. 1H NMR (400 MHz, $CDCl_3$): $\delta = 5.17$ (s, 2H, CH_2), 5.51 (s, 2H, CH_2), 6.94-6.97 (m, 3H, CH Arom.), 7.25-7.27 (m, 4H, CH Arom.), 7.34-7.40 (m, 3H, CH Arom.), 7.52 (s, 1H, CH). ^{13}C NMR (100 MHz, $CDCl_3$): $\delta = 54.2$ (CH_2), 62.1 (CH_2), 114.8 (2x CH Arom.), 121.3 (CH Arom.), 122.6 (CH), 128.1 (2x CH Arom.), 128.8 (2x CH Arom.), 129.0 (CH Arom.), 129.6 (2x CH Arom.), 133.8 (qC), 144.7 (qC), 158.2 (qC), in agreement with the literature. [59]

Preparation of 1-(4-fluorobenzyl)-4-(phenoxyethyl)-1H-1,2,3-triazole - (49)



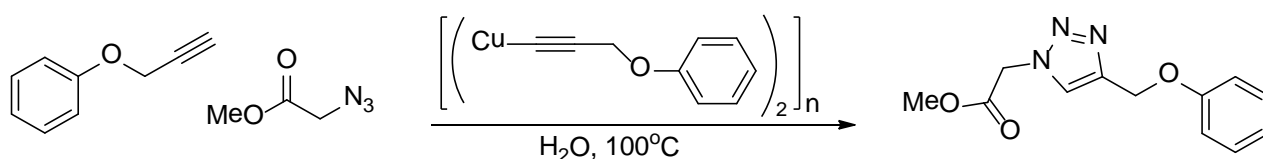
Prepared using the representative procedure from phenyl propargylether (0.28 g, 2.1 mmol), p-fluorobenzyl azide (0.16 g, 1.1 mmol), and 10 % ladder polymer. Product was purified column chromatography, eluted in 10:1 petrol:ethyl acetate. Light brown solid (0.26 g, 87 %, m.p 82.3°C) was collected. Elemental analysis: Found C 67.71 %, H 4.95 %, N 14.51 % (C₁₆H₁₄FN₃O requires C 67.83 %, H 4.98 %, N 14.83 %) m/z found 284.1183 (C₁₆H₁₄FN₃O [M+H]⁺ requires 284.1194). IR (thin film): ν = 907.0, 1049.2, 1230.7, 1494.1, 1512.1, 1599.8, 1710.2, 2251.6. ¹H NMR (400 MHz, CDCl₃): δ = 5.14 (s, 2H, CH₂), 5.44 (s, 2H, CH₂), 6.92-6.96 (m, 3H, CH Arom.), 7.01 (t, ³J_{HF} = 8.8 Hz, 2H, CH Arom.), 7.20-7.28 (m, 4H, CH Arom.), 7.54 (s, 1H, CH). ¹³C NMR (100 MHz, CDCl₃): δ = 53.4 (CH₂), 61.9 (CH₂), 114.8 (2x CH Arom.), 116.1 (2x CH Arom, d, ²J_{CF} = 21.7 Hz), 121.3 (CH Arom.), 122.7 (CH), 129.6 (2x CH Arom.), 130.2 (2x CH Arom, d, ³J_{CF} = 8.1 Hz), 130.5 (qC, ⁴J_{CF} = 3.3 Hz), 144.7 (qC), 158.2 (qC), 162.9 (qC, ¹J_{CF} = 247 Hz).

Preparation of 1-(4-methylbenzyl)-4-(phenoxyethyl)-1H-1,2,3-triazole - (50)



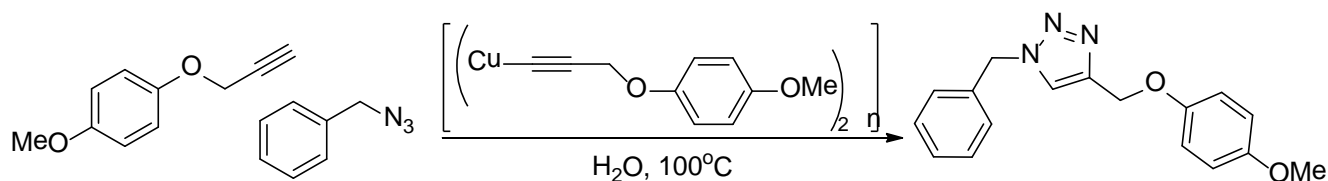
Prepared using the representative procedure from phenyl propargylether (0.28 g, 2.1 mmol), p-methylbenzyl azide (0.15 g, 1.0 mmol), and 10 % ladder polymer. Product was purified by column chromatography, eluted in 10:1 petrol:ethyl acetate. White solid (0.23 g, 83 %, m.p 88.0°C) was collected. Elemental analysis: Found C 72.94 %, H 6.08 %, N 14.44 % ($\text{C}_{17}\text{H}_{17}\text{N}_3\text{O}$ requires C 73.10 %, H 6.13 %, N 15.04 %) m/z found 280.1435 ($\text{C}_{17}\text{H}_{17}\text{N}_3\text{O}$ $[\text{M}+\text{H}]^+$ requires 280.1444). IR (thin film): $\nu = 909.2, 1049.2, 1265.3, 1494.3, 1597.8$. ^1H NMR (400 MHz, CDCl_3): $\delta = 2.30$ (s, 3H, CH_3), 5.12 (s, 2H, CH_2), 5.40 (s, 2H, CH_2), 6.94 (t, $J = 7.7$ Hz, 3H, CH Arom.), 7.12 (s, 4H, CH Arom.), 7.22 (t, $J = 4.5$ Hz, 2H, CH Arom.), 7.50 (s, 1H, CH). ^{13}C NMR (100 MHz, CDCl_3): $\delta = 21.0$ (CH_3), 54.0 (CH_2), 62.0 (CH_2), 114.8 (2x CH Arom.), 121.3 (CH Arom.), 122.8 (CH), 128.2 (2x CH Arom.), 129.3 (2x CH Arom.), 129.7 (2x CH Arom.), 131.6 (qC), 138.7 (qC), 144.5 (qC), 158.3 (qC).

Preparation of methyl 2-(4-(phenoxyethyl)-1H-1,2,3-triazol-1-yl)acetate - (51)



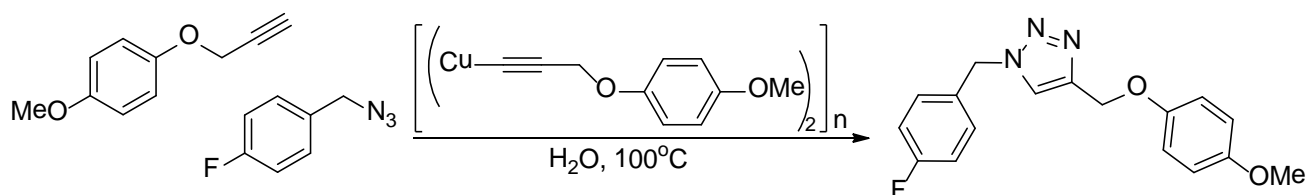
Prepared using the representative procedure from phenyl propargylether (0.27 g, 2.0 mmol), methyl 2-azidoacetate (0.18 g 1.0 mmol), and 10 % ladder polymer. Product was purified by column chromatography, eluted in 10:1 petrol:ethyl acetate. White solid (0.22 g, 89 %, m.p 87.8°C) was collected. Elemental analysis: Found C 58.26 %, H 5.26 %, N 16.60 % ($\text{C}_{12}\text{H}_{13}\text{N}_3\text{O}_3$ requires C 58.29 %, H 5.30 %, N 16.99 %) m/z found 248.1021 ($\text{C}_{12}\text{H}_{13}\text{N}_3\text{O}_3$ $[\text{M}+\text{H}]^+$ requires 248.1030). IR (thin film): $\nu = 733.1, 907.6, 1049.1, 1228.1, 1493.1, 1597.0, 1756.4, 2252.0, 2955.5, 3153.6$. ^1H NMR (400 MHz, CDCl_3): $\delta = 3.81$ (s, 3H, CH_3), 5.19 (s, 2H, CH_2), 5.25 (s, 2H, CH_2), 6.98 (t, $J = 8.4$ Hz, 3H, CH Arom.), 7.30 (m, 2H, CH Arom.), 7.76 (s, 1H, CH). ^{13}C NMR (100 MHz, CDCl_3): $\delta = 51.0$ (CH_2), 53.0 (CH_3), 61.7 (CH_2), 115.0 (2x CH Arom.), 121.3 (CH Arom.), 124.5 (CH), 129.6 (2x CH Arom.), 144.4 (qC), 158.2 (qC), 166.9 (qC).

Preparation of 1-benzyl-4-((4-methoxyphenoxy)methyl)-1H-1,2,3-triazole - (52)



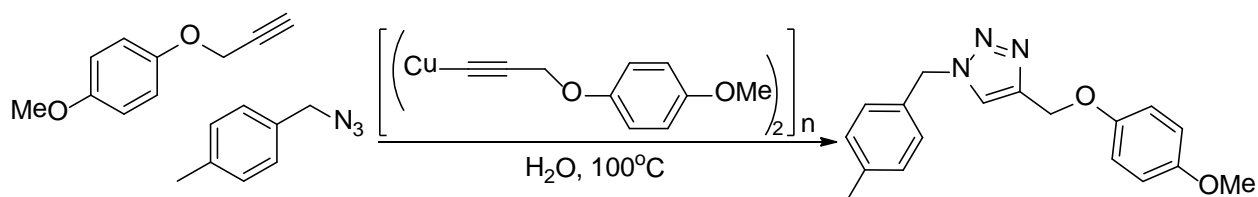
Prepared using the representative procedure from 1-methoxyphenyl propargylether (0.33 g, 2.1 mmol), benzylazide (0.14 g, 1.0 mmol), and 10 % ladder polymer. Product was purified using column chromatography, eluted in 10:1 petrol:ethyl acetate. Creamy white solid (0.20 g, 67 %, m.p 95.7°C) was collected. Elemental analysis: Found C 69.08 %, H 5.75 %, N 14.04 % ($\text{C}_{17}\text{H}_{17}\text{N}_3\text{O}_2$ requires C 69.14 %, H 5.80 %, N 14.23 %), m/z found 296.1382 ($\text{C}_{17}\text{H}_{17}\text{N}_3\text{O}_2$ [M+H]⁺ requires 296.1394). IR (thin film): $\nu = 650.2, 732.2, 908.1, 1048.7, 1230.8, 1462.7, 1508.0, 2253.2, 2836.7, 2953.9, 3155.9$. ¹H NMR (400 MHz, CDCl₃): $\delta = 3.72$ (s, 3H, CH₃), 5.01 (s, 2H, CH₂), 5.48 (s, 2H, CH₂), 6.81 (dt, J = 9.2, 2.4 Hz, 2H, CH Arom.), 6.87 (dt, J = 9.2, 2.4 Hz, 2H, CH Arom.), 7.22-7.26 (m, 2H, CH Arom.), 7.32-7.36 (m, 3H, CH Arom.), 7.52 (s, 1H, CH). ¹³C NMR (100 MHz, CDCl₃): $\delta = 54.2$ (CH₂), 55.7 (CH₃), 62.8 (CH₂), 114.3 (2x CH Arom.), 115.9 (2x CH Arom.), 122.7 (CH Arom.), 128.1 (CH), 128.9 (2x CH Arom.), 129.1 (2x CH Arom.), 134.3 (qC), 144.8 (qC) 152.3 (qC), 154.2 (qC).

Preparation of 1-(4-fluorobenzyl)-4-((4-methoxyphenoxy)methyl)-1H-1,2,3-triazole - (53)



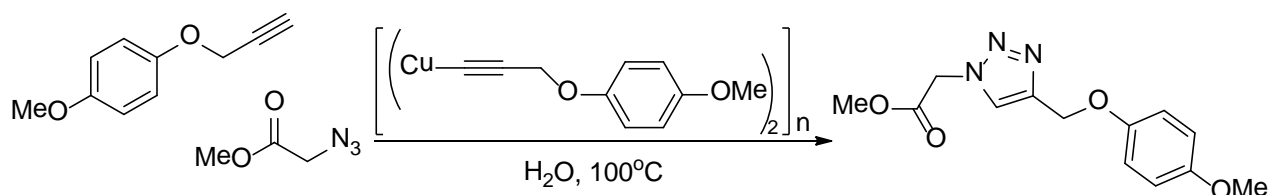
Prepared using the representative procedure from 1-methoxyphenyl propargylether (0.33 g, 2.0 mmol), p-fluorobenzyl azide (0.16 g, 1.0 mmol), and 10 % ladder polymer. Product was purified using column chromatography, eluted in 10:1 petrol:ethyl acetate. Creamy white solid (0.21 g, 66 %, m.p 108.7°C) was collected. Elemental analysis: Found C 64.94 %, H 5.09 %, N 13.22 % ($C_{17}H_{16}FN_3O_2$ requires C 65.17 %, H 5.15 %, N 13.41 %) m/z found 314.1286 ($C_{17}H_{16}FN_3O_2$ $[M+H]^+$ requires 314.1299). IR (thin film): $\nu = 649.8, 742.0, 911.6, 1046.2, 1230.8, 1465.2, 1507.6, 1607.3, 2253.2, 2836.7, 3003.8, 3155.9$. 1H NMR (400 MHz, $CDCl_3$): $\delta = 3.74$ (s, 3H, CH_3), 5.11 (s, 2H, CH_2), 5.47 (s, 2H, CH_2), 6.82 (dt, $J = 9.2, 2.4$ Hz, 2H, CH Arom.), 6.86 (dt, $J = 9.2$ Hz, 2.4 Hz, 2H, CH Arom.), 7.01 (t, $J = 8.4$ Hz, 2H, CH Arom.), 7.23 (m, 2H, CH Arom.) 7.54 (s, 1H, CH). ^{13}C NMR (100 MHz, $CDCl_3$): $\delta = 53.4$ (CH_2), 55.7 (CH_3), 62.7 (CH_2), 114.6 (2x CH Arom.), 115.8 (2x CH Arom.), 116.1 (2x CH Arom, d, $^2J_{CF} = 21.6$ Hz), 122.6 (CH), 129.9 (2x CH Arom, d, $^3J_{CF} = 8.3$ Hz), 134.4 (qC, $^4J_{CF} = 3.3$ Hz), 144.9 (qC), 152.3 (qC), 154.2 (qC), 162.9 (qC, d, $^1J_{CF} = 247$ Hz).

Preparation of 4-((4-methoxyphenoxy)methyl)-1-(4-methylbenzyl)-1H-1,2,3-triazole - (54)



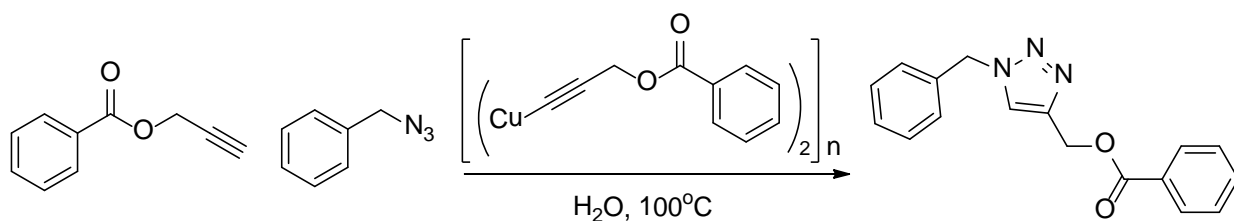
Prepared using the representative procedure from 1-methoxyphenyl propargylether (0.33 g, 2.1 mmol), p-methylbenzyl azide (0.16 g, 1.1 mmol), and 10 % ladder polymer. Product was purified using column chromatography, eluted in 10:1 petrol:ethyl acetate. Creamy white solid (0.22 g, 68 %, m.p 98.3°C) was collected. Elemental analysis: Found C 69.74 %, H 6.20 %, N 13.48 % ($C_{18}H_{19}N_3O_2$ requires C 69.88 %, H 6.19 %, N 13.58 %) m/z found 310.1538 ($C_{18}H_{19}N_3O_2$ $[M+H]^+$ requires 310.1550). IR (thin film): $\nu = 731.3, 910.1, 1051.6, 1230.4, 1466.3, 1508.5, 2251.0, 2834.5, 2953.7, 3152.4$. 1H NMR (400 MHz, $CDCl_3$): $\delta = 2.32$ (s, 3H, CH_3), 3.72 (s, 3H, CH_3), 5.08 (s, 2H, CH_2), 5.43 (s, 2H, CH_2), 6.80 (dt, $J = 9.2, 2.4$ Hz, 2H, CH Arom.), 6.86 (dt, $J = 9.2, 2.4$ Hz, 2H, CH Arom.), 7.14 (s, 4H, CH Arom.), 7.50 (s, 1H, CH). ^{13}C NMR (100 MHz, $CDCl_3$): $\delta = 21.2$ (CH_3), 54.0 (CH_2), 55.7 (CH_3), 62.7 (CH_2), 114.7 (2x CH Arom.), 115.9 (2x CH Arom.), 122.6 (CH), 128.4 (2x CH Arom.), 129.5 (2x CH Arom.), 131.6 (qC), 138.7 (qC), 144.7 (qC), 152.4 (CH Arom.), 154.2 (CH Arom.).

Preparation of methyl 2-(4-((4-methoxyphenoxy)methyl)-1H-1,2,3-triazol-1-yl)acetate - (55)



Prepared using the representative procedure from 1-methoxyphenyl propargylether (0.33 g, 2.1 mmol), methyl 2-azidoacetate (0.12 g, 1.1 mmol), and 10 % ladder polymer. Product was purified using column chromatography, eluted in 10:1 petrol:ethyl acetate. Creamy white solid (0.20 g, 66 %, m.p 96.2°C) was collected. Elemental analysis: Found C 56.13 %, H 5.40 %, N 14.92 % ($\text{C}_{13}\text{H}_{15}\text{N}_3\text{O}_4$ requires C 56.31 %, H 5.45 %, N 15.15 %) m/z found 278.1125 ($\text{C}_{13}\text{H}_{15}\text{N}_3\text{O}_4$ $[\text{M}+\text{H}]^+$ requires 278.1135). IR (thin film): $\nu = 732.3, 826.2, 907.9, 1040.1, 1226.8, 1439.7, 1466.0, 1508.3, 1754.9, 2253.2, 2835.6, 2957.0, 3003.1, 3153.4$. ^1H NMR (400 MHz, CDCl_3): $\delta = 3.74$ (s, 3H, CH_3), 3.77 (s, 3H, CH_3), 5.14 (s, 2H, CH_2), 5.15 (s, 2H, CH_2), 6.83 (dt, $J = 9.2, 2.4$ Hz, 2H, CH Arom.), 6.90 (dt, $J = 9.2, 2.4$ Hz, 2H, CH Arom.), 7.74 (s, 1H, CH). ^{13}C NMR (100 MHz, CDCl_3): $\delta = 50.7$ (CH_2), 53.0 (CH_3), 55.7 (CH_3), 62.6 (CH_2), 114.9 (2x CH Arom.), 115.9 (2x CH Arom.), 124.3 (CH), 144.7 (qC), 151.6 (qC), 154.2 (qC), 166.8 (qC).

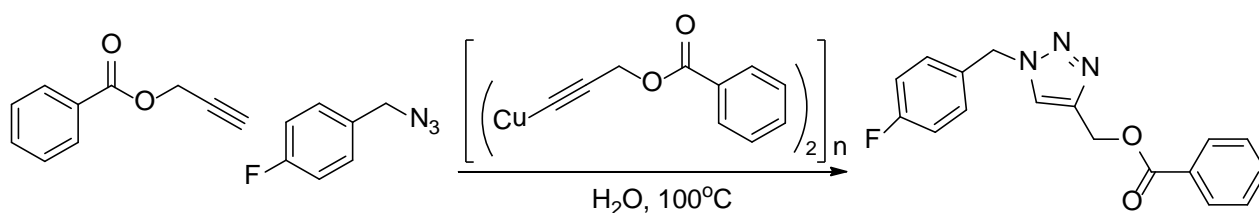
Preparation of (1-benzyl-1H-1,2,3-triazol-4-yl)methyl benzoate - (35) ^[84]



Prepared using the representative procedure from propargyl benzoate (0.33 g, 2.1 mmol), benzylazide (0.14 g, 1.1 mmol), and 10 % ladder polymer. Product was purified using column chromatography, eluted in 10:1 petrol:ethyl acetate. White solid (0.21 g, 68 %, m.p 121.7°C) was collected. Elemental analysis: Found C 69.14 %, H 5.19 %, N 14.06 % ($\text{C}_{17}\text{H}_{15}\text{N}_3\text{O}_2$ requires C 69.61 %, H 5.15 %, N 14.33 %) m/z found 294.1226 ($\text{C}_{17}\text{H}_{15}\text{N}_3\text{O}_2$ $[\text{M}+\text{H}]^+$ requires 294.1237). IR (thin film): $\nu = 649.3, 733.4, 907.5, 1111.2, 1272.6, 1454.0, 1716.1, 2252.9$. ^1H NMR (400 MHz, CDCl_3): $\delta = 5.43$ (s, 2H CH_2), 5.51 (s, 2H, CH_2), 7.26-7.28 (m, 2H, CH Arom.), 7.33-7.41 (m, 5H, CH Arom.), 7.51-7.55 (t, $J = 7.2$ Hz, 1H, CH Arom.), 7.62 (s, 1H, CH), 8.00-8.02 (d, $J = 8$ Hz, 2H, CH Arom.). ^{13}C NMR (100 MHz, CDCl_3): $\delta = 54.2$ (CH_2), 58.1 (CH_2), 123.8 (CH), 128.2 (CH Arom.), 128.4 (2x CH Arom.), 128.8 (2x CH Arom.), 128.9 (2x CH Arom.), 129.2 (2x CH Arom.), 129.7 (qC), 133.2 (CH Arom.), 134.4 (qC), 143.3 (qC), 166.4 (qC), in agreement with the literature.

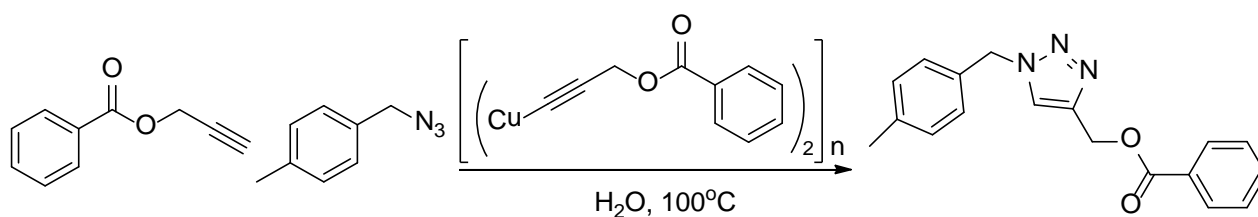
[84]

Preparation of (1-(4-fluorobenzyl)-1H-1,2,3-triazol-4-yl)methyl benzoate - (46)



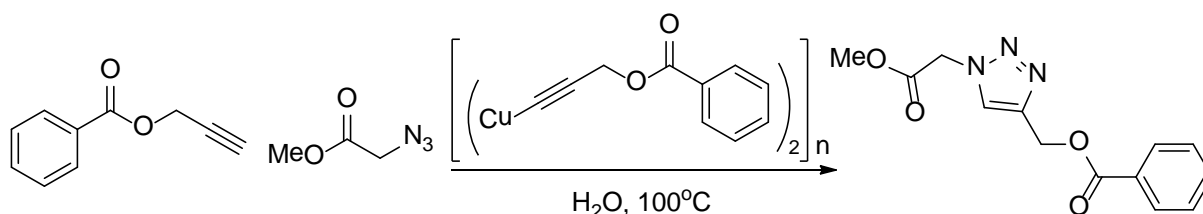
Prepared using the representative procedure from propargyl benzoate (0.35 g, 2.2 mmol), p-fluorobenzyl azide (0.15 g, 1.0 mmol), and 10 % ladder polymer. Product was purified using column chromatography, eluted in 10:1 petrol:ethyl acetate. White solid (0.25 g, 78 %, m.p 148.9°C) was collected. Elemental analysis: Found C 65.37 %, H 4.43 %, N 13.40 % ($\text{C}_{17}\text{H}_{14}\text{FN}_3\text{O}_2$ requires C 65.59 %, H 4.53 %, N 13.50 %) m/z found 312.1131 ($\text{C}_{17}\text{H}_{14}\text{FN}_3\text{O}_2$ $[\text{M}+\text{H}]^+$ requires 312.1143). IR (thin film): $\nu = 649.6, 734.3, 908.3, 1110.1, 1272.9, 1512.8, 1606.0, 1715.8, 2253.6$. ^1H NMR (400 MHz, CDCl_3): $\delta = 5.44$ (s, 2H, CH_2), 5.49 (s, 2H, CH_2), 7.05 (t, $J = 8.4$ Hz, 2H, CH Arom.), 7.27 (t, $J = 6$ Hz, 2H, CH Arom.), 7.41 (t, $J = 7.6$ Hz, 2H, CH Arom.), 7.54 (t, $J = 7.6$ Hz, 1H, CH Arom.), 7.63 (s, 1H, CH), 8.01 (d, $J = 7.2$ Hz, 2H, CH Arom.). ^{13}C NMR (100 MHz, CDCl_3): $\delta = 53.5$ (CH_2), 58.0 (CH_2), 116.2 (2x CH Arom, d, $^2J_{\text{CF}} = 21.7$ Hz), 123.8 (CH), 128.4 (2x CH Arom.), 129.70 (qC), 129.73 (2x CH Arom.), 130.1 (2x CH Arom, d, $^3J_{\text{CF}} = 8.4$ Hz), 130.3 (qC, d, $^4J_{\text{CF}} = 3.3$ Hz), 133.2 (CH Arom.), 143.5 (qC), 162.9 (qC, d, $^1J_{\text{CF}} = 247$ Hz), 166.4 (qC).

Preparation of (1-(4-methylbenzyl)-1H-1,2,3-triazol-4-yl)methyl benzoate - (47)



Prepared using the representative procedure from propargyl benzoate (0.33 g, 2.1 mmol), p-methylbenzyl azide (0.15 g, 1.0 mmol), and 10 % ladder polymer. Product was purified using column chromatography, eluted in 10:1 petrol:ethyl acetate. White solid (0.22 g, 73 %, m.p 94.2°C) was collected. Elemental analysis: Found C 70.24 %, H 5.60 %, N 13.57 % ($C_{18}H_{17}N_3O_2$ requires C 70.34 %, H 5.58 %, N 13.67 %) m/z found 308.1383 ($C_{18}H_{17}N_3O_2 [M+H]^+$ requires 308.1394). IR (thin film): $\nu = 650.7, 730.7, 907.5, 1110.4, 1273.4, 1716.3, 2254.4$. 1H NMR (400 MHz, $CDCl_3$): $\delta = 2.34$ (s, 3H, CH_3), 5.43 (s, 2H, CH_2), 5.47 (s, 2H, CH_2), 7.17 (s, 4H, CH Arom.), 7.40 (t, $J = 12$ Hz, 2H, CH Arom.), 7.54 (t, $J = 8$ Hz, 1H, CH Arom.), 7.59 (s, 1H, CH), 8.01 (d, $J = 8$ Hz, 2H, CH Arom.). ^{13}C NMR (100 MHz, $CDCl_3$): $\delta = 21.2$ (CH_3), 54.1 (CH_2), 58.1 (CH_2), 123.7 (CH), 128.2 (2x CH Arom.), 128.4 (2x CH Arom.), 128.9 (2x CH Arom.), 129.7 (qC), 129.8 (2x CH Arom.), 131.4 (qC), 133.2 (CH Arom.), 138.8 (qC), 143.3 (qC), 166.4 (qC).

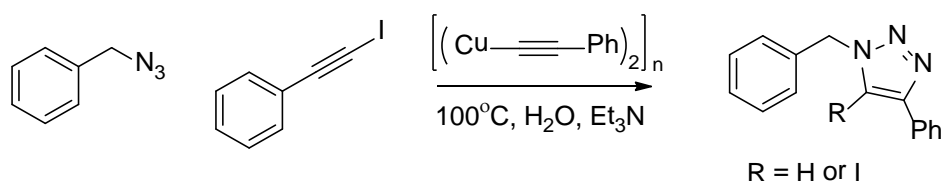
Preparation of (1-(2-methoxy-2-oxoethyl)-1H-1,2,3-triazol-4-yl)methyl benzoate - (48)



Prepared using the representative procedure from propargyl benzoate (0.34 g, 2.1 mmol), methyl 2-azidoacetate (0.12 g, 1.1 mmol), and 10 % ladder polymer. Product was purified using column chromatography, eluted in 10:1 petrol:ethyl acetate. Creamy white solid (0.17 g, 57 %, m.p 91.9°C) was collected. Elemental analysis: Found C 56.50 %, H 4.68 %, N 15.15 % ($C_{13}H_{13}N_3O_4$ requires C 56.72 %, H 4.76 %, N 15.27 %) m/z found 276.0970 ($C_{13}H_{13}N_3O_4 [M+H]^+$ requires 276.0979). IR (thin film): $\nu = 650.2, 732.2, 907.6, 1227.0, 1273.9, 1717.3, 1761.3, 2253.5$. 1H NMR (400 MHz, $CDCl_3$): $\delta = 3.80$ (s, 3H, CH_3), 5.19 (s, 2H, CH_2), 5.49 (s, 2H, CH_2), 7.42 (t, $J = 7.6$ Hz, 2H, CH Arom.), 7.55 (t, $J = 7.6$ Hz, 1H, CH Arom.), 7.85 (s, 1H, CH), 8.04 (d, $J = 7.6$ Hz, 2H, CH Arom.). ^{13}C NMR (100 MHz, $CDCl_3$): $\delta = 50.7$ (CH_2), 53.1 (CH_3), 58.0 (CH_2), 125.4 (CH), 128.4 (2x CH Arom.), 129.70 (qC), 129.74 (2x CH Arom.), 133.2 (CH Arom.), 143.4 (qC), 166.4 (qC), 166.6 (qC).

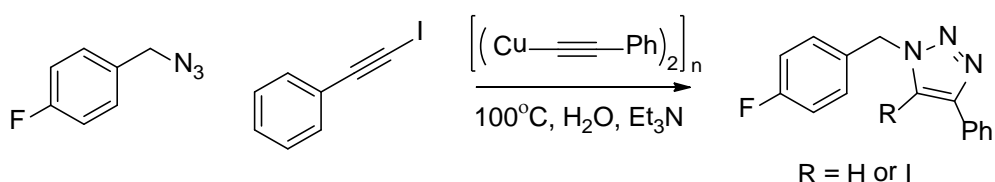
Representative method for the preparation of iodoalkynes

Preparation of 1-benzyl-5-iodo-4-phenyl-1H-1,2,3-triazole - (56)



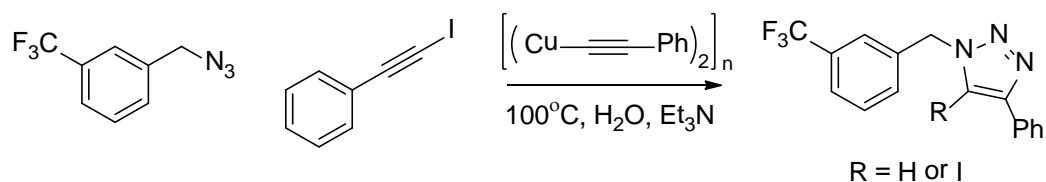
Water (20 mL) was added to a large microwave tube fitted with stirrer bar. Iodophenylacetylene (0.23 g, 1.0 mmol), benzyl azide (0.13 g, 1.0 mmol), triethylamine (0.20 g, 2.0 mmol), and copper ladder polymer (0.017 g, 0.1 mmol) were added. The reaction was put in the microwave for 3x10 min @100°C with pre-stirring for 10 s. The reaction was then allowed to cool to room temperature. The mixture was then filtered and washed with EtOAc (50 mL) and the filtrate washed extracted with EtOAc (3x10 mL). The organic fractions were combined and dried with magnesium sulphate, filtered, and the solvent removed under reduced pressure. Orange solid (0.19 g, 60 %) was collected. ¹H NMR (400 MHz, CDCl₃): δ = 5.47 (s, 2H, CH₂ - R=H), 5.57 (s, 2H, CH₂ - R=I), 7.17-7.43 (m, 16H, CH Arom. - R=H+I), 7.59 (s, 1H, CH - R=H), 7.71 (d, 2H, J=7.2 Hz, CH Arom. - R=H), 7.86 (d, 2H, J=7.2 Hz, CH Arom. - R=I).

Preparation of 1-(4-fluorobenzyl)-5-iodo-4-phenyl-1H-1,2,3-triazole - (57)



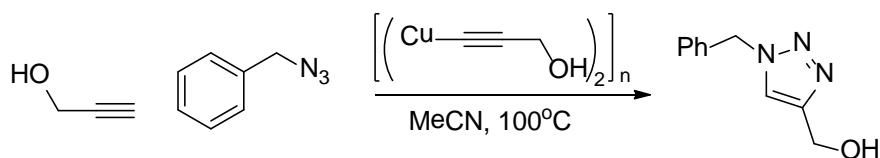
Prepared using the representative procedure from Iodophenylacetylene (0.23 g, 1.0 mmol), p-fluorobenzyl azide (0.16 g, 1.0 mmol), triethylamine (0.20 g, 2.0 mmol), and copper ladder polymer (0.016 g, 0.1 mmol). Orange solid (0.17 g, 51 %) was collected. ¹H NMR (400 MHz, CDCl₃): δ = 5.53 (s, 2H, CH₂ - R=H), 5.56 (s, 2H, CH₂ - R=I), 7.27-7.49 (m, 14H, CH Arom. - R=H+I), 7.68 (s, 1H, CH - R=H), 7.80 (d, 2H, J=7.2 Hz, CH Arom. - R=H), 7.92 (d, 2H, J=7.2 Hz, CH Arom. - R=I).

Preparation of 5-iodo-4-phenyl-1-(3-(trifluoromethyl)benzyl)-1H-1,2,3-triazole - (58)



Prepared using the representative procedure from Iodophenylacetylene (0.25 g, 1.1 mmol), 3-trifluoromethylbenzyl azide (0.23 g, 1.1mmol), triethylamine (0.20 g, 2mmol), and copper ladder polymer (0.017 g, 0.1 mmol). Dark orange oil (0.27 g, 69 %) was obtained. ¹H NMR (400 MHz, CDCl₃): δ = 5.64 (s, 2H, CH₂ - R=H), 5.73 (s, 2H, CH₂ - R=I), 7.37-7.56 (m, 14H, CH Arom. - R=H+I), 7.73 (s, 1H, CH - R=H), 7.82 (d, 2H, J=7.2 Hz, CH Arom. - R=H), 7.93 (d, 2H, J=7.2 Hz, CH Arom. - R=I).

Flow Reaction - (62)



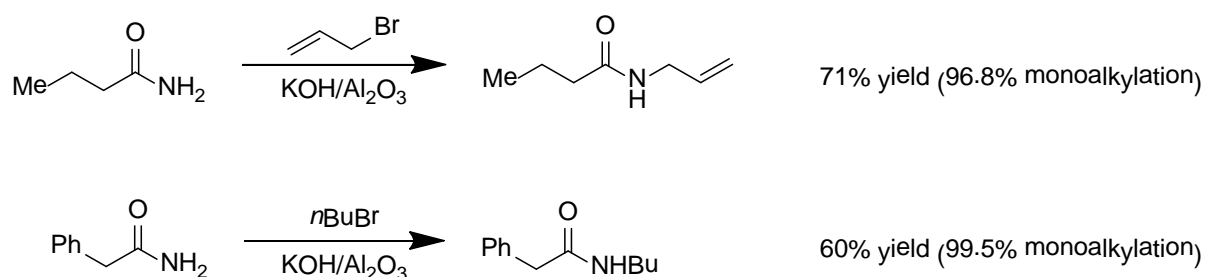
Propargyl alcohol (3 M solⁿ, 10 mL) and benzyl azide (2 M solⁿ, 10 mL) were passed through a FlowSyn reactor with a flow rate of 1 mL/min, at 100°C. The propargyl alcohol copper(I) ladder polymer was used as a catalyst. Collected material was analysed by GC-MS, observed mixture of starting material, (benzyl azide, retention time = 11 min, m/z found 133.0), and product (retention time = 23 min, m/z found 189.0).

Chapter 3

Solid Support Materials

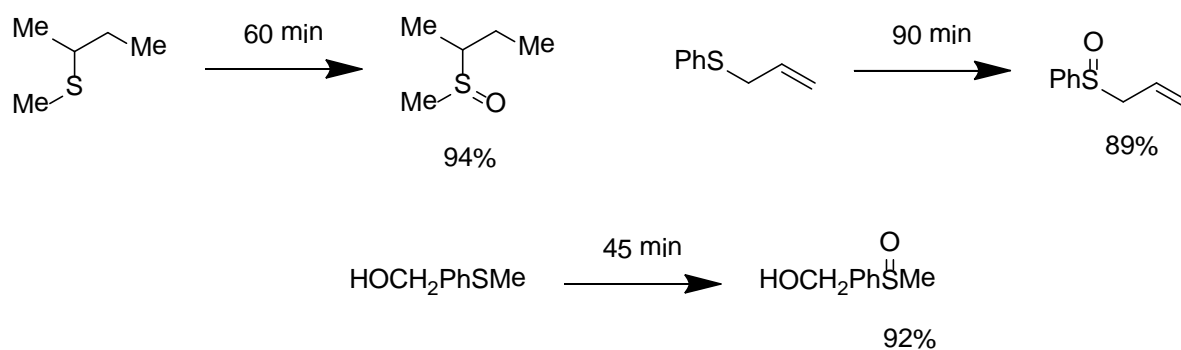
Introduction

Solid support media for catalysis of organic synthesis is an expanding area of chemistry that also takes advantage of the combination of organic and inorganic chemistry. By using a solid support material to disperse and immobilise a variety of precious metal catalysts, such as platinum or palladium, a greater active surface area per unit weight of the metal becomes available for catalysis, which improves the effectiveness of organic reactions. There are a variety of advantages to using solid support reagents, such as the ability to easily recover the material from the reaction by filtration, and the ability to finely tune the chemical properties of the catalyst by altering the characteristics of the support. [85] There are a series of characteristics which are desired for solid support materials including high surface area, inertness, porosity, and stability under reaction and regeneration conditions. [86] The most widely used materials alumina, silica and carbon optimally combine these characteristics. Some examples of the use of alumina as a solid support material for catalysis include the use of $\text{NaBH}_4/\text{Al}_2\text{O}_3$ for selective reductions, or $\text{KOH}/\text{Al}_2\text{O}_3$ for the selective monoalkylation of primary amides, [85] shown in Scheme 28.



Scheme 28: Examples of the use of $\text{KOH}/\text{Al}_2\text{O}_3$ for the selective monoalkylation of primary amides. [85]

There are also a variety of examples of the use of silica as a solid support material for catalysis for example magnesium monoperoxyphthalate on wet SiO_2 oxidises sulphides to sulfoxides without α -hydroxylating ketones, some examples are shown in Scheme 29.



Scheme 29: First examples of oxidation of sulphides with a carbonyl group with MMPP in aqueous media without Baeyer – Villiger reaction [85]

However, it is the use of carbon as a solid support which is currently receiving the most research interest. [87, 88, 89] One particular advantage of using carbon as a support is that the precious metal dispersed upon it can be easily recovered from the carbon support by burning the material away into a concentrated ash. [90] Carbon is also a unique material for support due to the variety of possible forms it can take, each of which possess distinct bulk and surface properties which can be tailored to provide specific characteristics.

Activated carbon is perhaps the most studied catalytic support due to its advantageous properties such as its high porosity, and large internal surface area. [91] Other types of carbon can, and have been used such as graphite, intercalation compounds, fullerenes and carbon nanotubes. [92] However, this review will go into most depth with the activated carbons in relation to the research carried out later in the chapter. Activated carbons have porous structures generally containing a small number of chemically bound heteroatoms, usually hydrogen and oxygen. The average structure of activated carbon is generally believed to consist of aromatic sheets and strips containing a variety of micropore gaps, [93] as shown in Figure 39.



Figure 39: Simplified diagram representing the aromatics strips and sheets of activated carbon. [93]

The raw material used in the preparation of the activated carbon can have a drastic effect on the morphology of the material. SEM images of wood (a), peat (b), and coconut shell (c) based activated carbons show characteristic traits carried over from the materials they were prepared from, [94] shown in Figure 40.

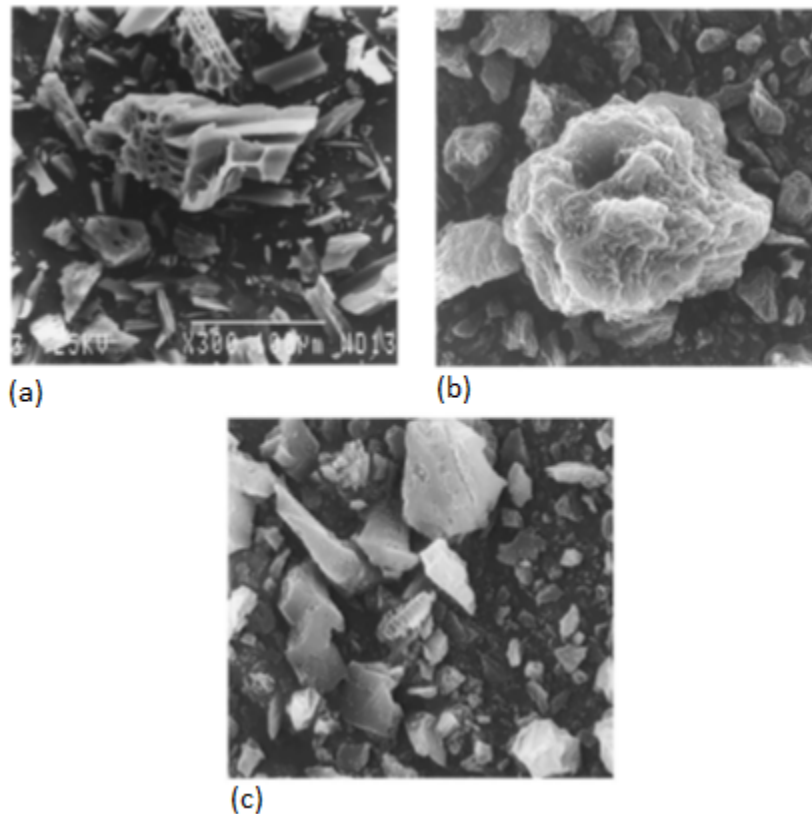


Figure 40: SEM images of wood (a), peat (b), and coconut shell (c) based activated carbons. [94]

The method of preparation can also affect the pore size of the material (Figure 41). [95]

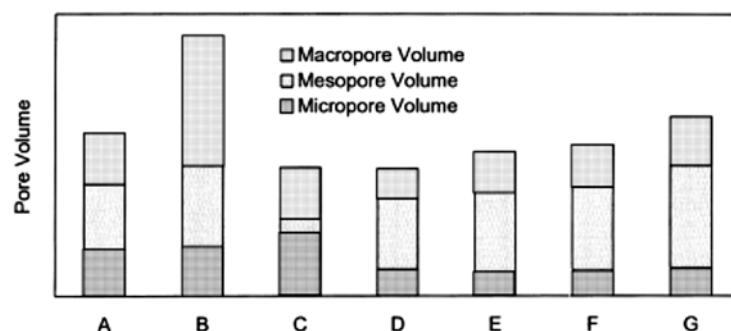


Figure 41: A variety of activated carbons prepared via different methods to provide a variety of pore sizes. [95]

It is important to optimise the pore size distribution for specific reaction dependant purposes, as pore size is directly responsible for surface area available for the

catalytically active materials, and also controls access to these metals from the substrate molecules of the reaction. A highly porous support provides the highest access to the metal catalyst, and therefore gives a higher catalytic activity. However, the larger pore size tends to lead to higher sensitivity to catalyst poisoning, as the poisons also have easier access to the metals.

According to IUPAC definitions there are three distinguishable groups of pores possible for activated carbons; macropores (>50 nm diameter), mesopores (2-50 nm diameter), and micropores (<2 nm diameter).^[96]

The surface chemistry of an activated carbon can also influence the performance of the catalyst. Whilst carbon is considered an inert material compared to supports such as alumina and silica, there are in fact a variety of functionalities present on its surface, shown in Figure 42. This functionality comes at the edges of the basal planes of the carbon where the unsaturated carbon atoms chemisorb oxygen into the structure. Since activated carbon has a highly disordered structure containing defects, dislocations, and discontinuities, there is more edge area available for oxygen chemisorption. These surface oxides are responsible for the acid/base and redox properties of activated carbon.^[97]

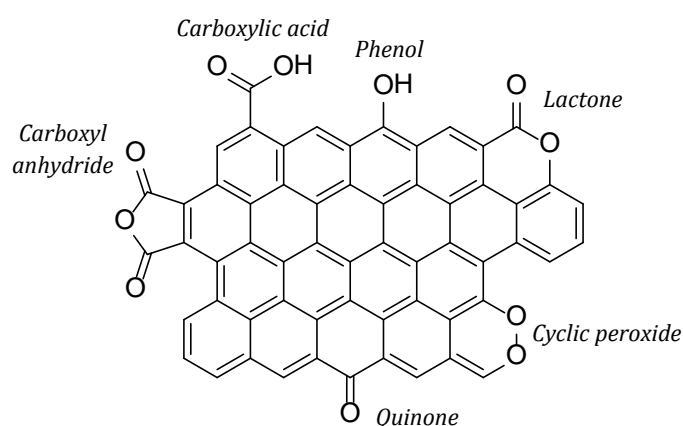


Figure 42: The variety of possible functionalisation present on the surface of activated carbons.^[97]

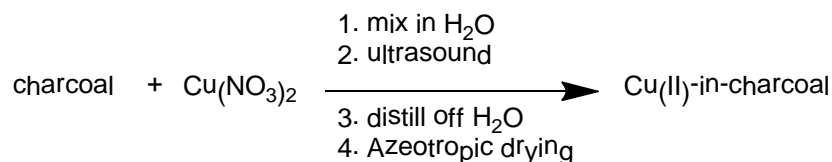
An example of the use of a solid supported catalyst is given by the Lipshutz group,^[98] who have used copper nanoparticles supported within the pores of activated carbon to act as a source of copper(I) for the heterogeneous catalysis of a series of Huisgen [3+2] cycloadditions. The group were able to show that they could obtain high yields of the

triazole products (over 90% in all cases presented). They also showed that the copper on carbon material was particularly robust, they were able to use a wide range of solvents at high temperature microwave conditions, with no solubility issues. The catalysts could also be reused with the group showing its use in at least three catalytic cycles without loss of catalytic activity. This material was prepared via a method of sonification, distillation of water followed by azeotropic drying with toluene to afford the catalyst. ^[99]

Their group characterized this material using a variety of methods. Firstly XPS spectral data were acquired and were reported to show the presence of CuO with lesser amounts of Cu₂O in the charcoal matrix. ^[100] Transmission electron microscopy (TEM) was also used to record 2D images of the carbon material, from which the group proposed a relatively even distribution of the copper nanoparticles within the charcoal matrix. ^[99] Finally quantitative inductively coupled plasma atomic emission spectrometry (ICP-AES) was used to determine the loading of copper within the charcoal, which was found to be 0.344mmol Cu/g catalyst, as well as the extent of copper bleed into solution during the reactions. ^[99] However, previous research ^[101] suggests the catalyst identity is questionable, therefore a further investigation into the copper on carbon material was conducted.

Preparation of Copper on Solid Support Materials

A sample of the copper nanoparticles on the carbon support media, Darko KB, was prepared according to the method given by the Lipshutz group, [98] shown in Scheme 30.



Scheme 30: Preparation of Cu/C via the Lipshutz method [97]

The material was compared by powder XRD to the copper in charcoal, 3 wt. %, material prepared in the same manner and sold by Sigma Aldrich. The two materials were found to be a direct match to each other. Both contained a quantity of copper hydroxynitrate, with a small quantity of an, as yet, unidentified impurity. Figure 43 shows the results of the powder XRD for the material prepared, compared to samples of copper hydroxynitrate and the copper nitrate starting material.

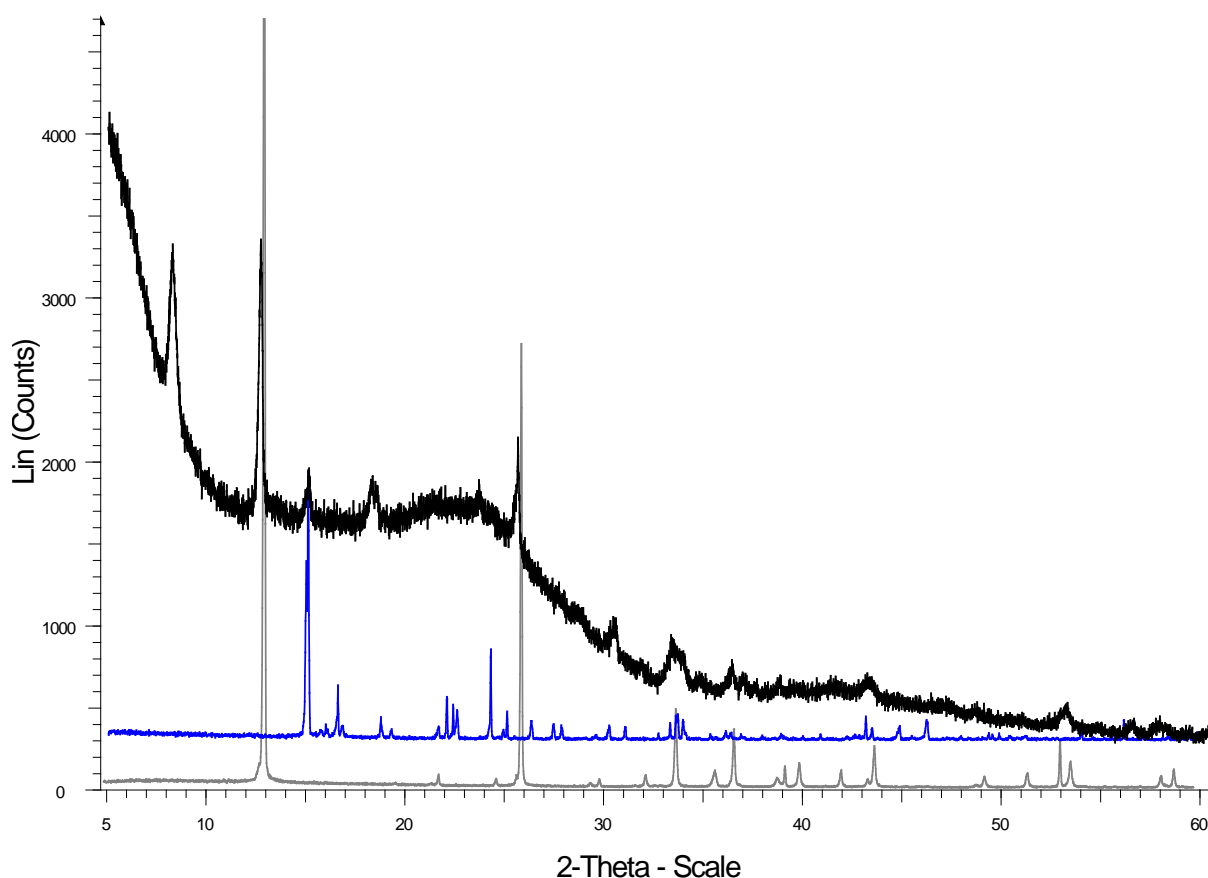


Figure 43: XRD results for the copper on carbon material (top) compared to copper nitrate starting material (blue) and $\text{Cu}_2(\text{OH})_3(\text{NO}_3)$ (grey)

These results showed that rather than the catalyst being a suspension of copper particles bound to the surface of the solid support, what was actually prepared was a sample of copper hydroxynitrate ($\text{Cu}_2(\text{OH})_3\text{NO}_3$) with carbon. Following the initial results for copper 'on' carbon, a series of copper 'on' various support materials were prepared via the Lipshutz method. Silica, alumina, and titania materials were prepared for comparison with the previous results for carbon.

<i>Copper on Carbon</i>	(62)
<i>Copper on Silica</i>	(63)
<i>Copper on alumina</i>	(64)
<i>Copper on titania</i>	(65)

After the samples had been prepared and dried they were analysed by powder XRD. Each of the samples showed the same distinct reflections which correspond to copper hydroxynitrate, shown in Figure 44.

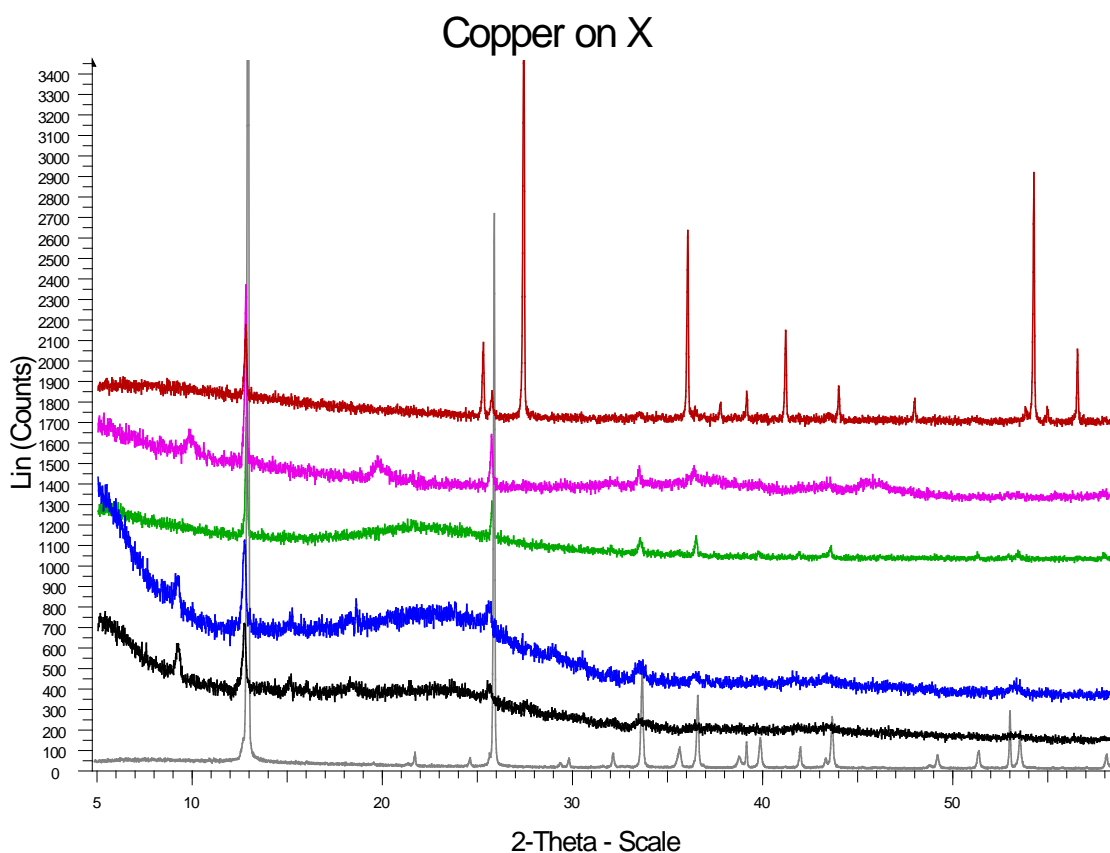
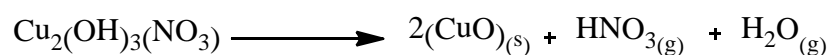


Figure 44: XRD results for the copper on X series of materials; titanium (red), alumina (pink), silica (green), Sigma Aldrich carbon (blue), synthesised copper on carbon (black), compared to $\text{Cu}_2(\text{OH})_3(\text{NO}_3)$ (grey).

A series of TGA experiments were carried out for each of the samples. The clearest pattern was observed for the titanium support, (Figure 45). The first step 40°C - 140°C corresponding to approximately 8% weight loss was attributed to the loss of water from the sample. The second interval corresponds to the thermal decomposition of copper hydroxynitrate, the most commonly accepted method for this degradation is shown in Scheme 31. [24]



Scheme 31: Thermal degradation of $\text{Cu}_2(\text{OH})_3(\text{NO}_3)$

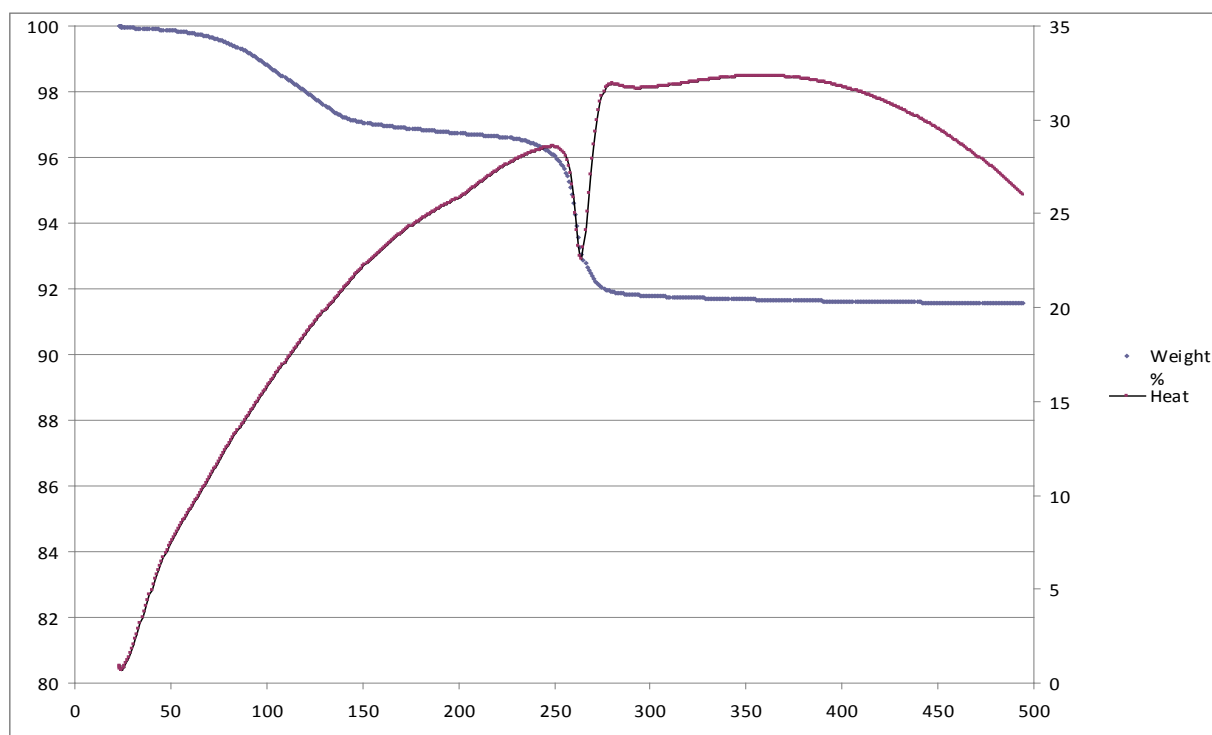


Figure 45: TGA trace for copper on titanium species, shows distinct weight loss at $\approx 250^\circ\text{C}$

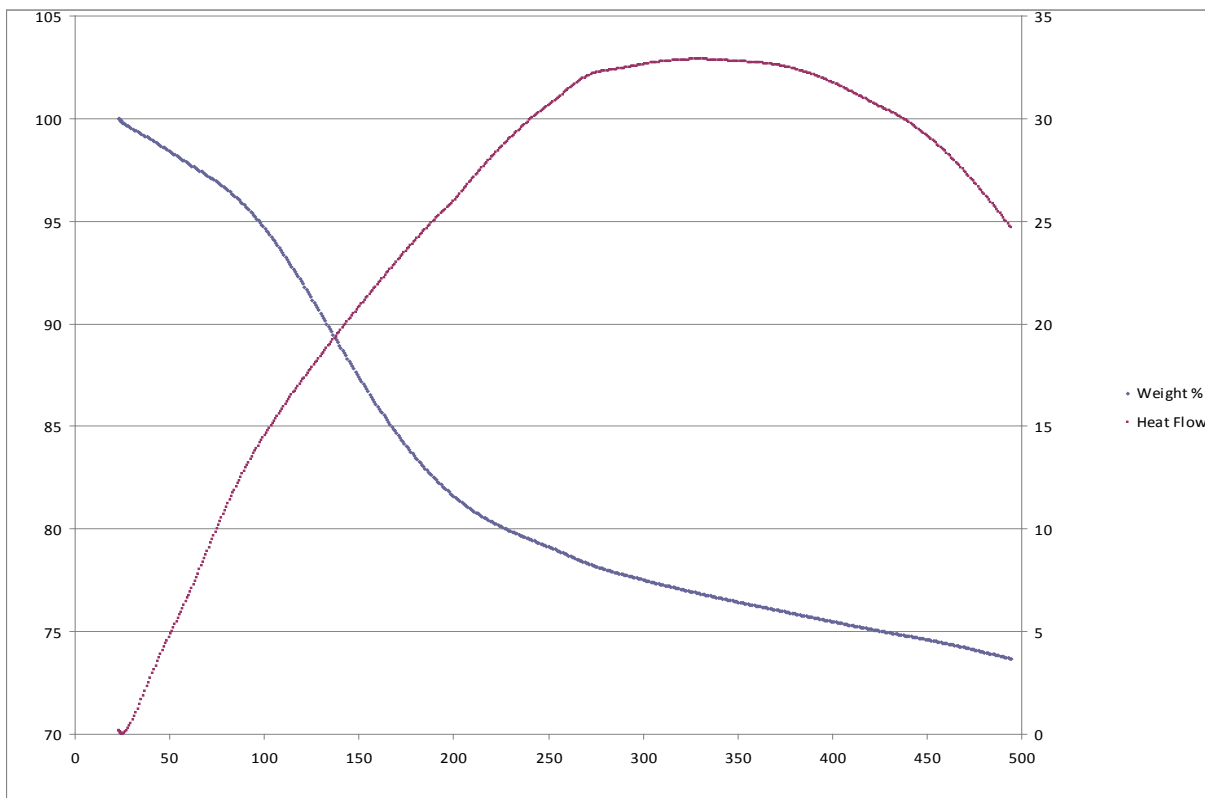


Figure 46: TGA trace for the prepared copper on carbon showing a general dehydration pattern.

The TGA traces for the other materials did not show the same level of detail, for example the carbon supports (Figure 46) show a broad weight loss from dehydration but nothing in the 250°C region to suggest the degradation of copper hydroxynitrate.

Identification of the Impurity Phase

After the range of solid support materials had been prepared, an impurity phase was observed in the XRD patterns of the Copper on Carbon (Darko KB) and Aldrich samples, but not in a Copper on Carbon using a different variation of carbon (Norit). This impurity had to be identified before any further catalysis work could be carried out.

A series of reactions were carried out to prepare the Copper 'on' Carbon (Darko KB) material with a higher loading of copper, where the copper nitrate starting material loading was increased to x2, x5, and x10 from the original reaction, the solid support materials prepared in this way can be seen in Figure 47. We believed the impurity was somehow coming from the source of copper and by increasing the amount of copper in the reaction we would see more of the impurity formed.

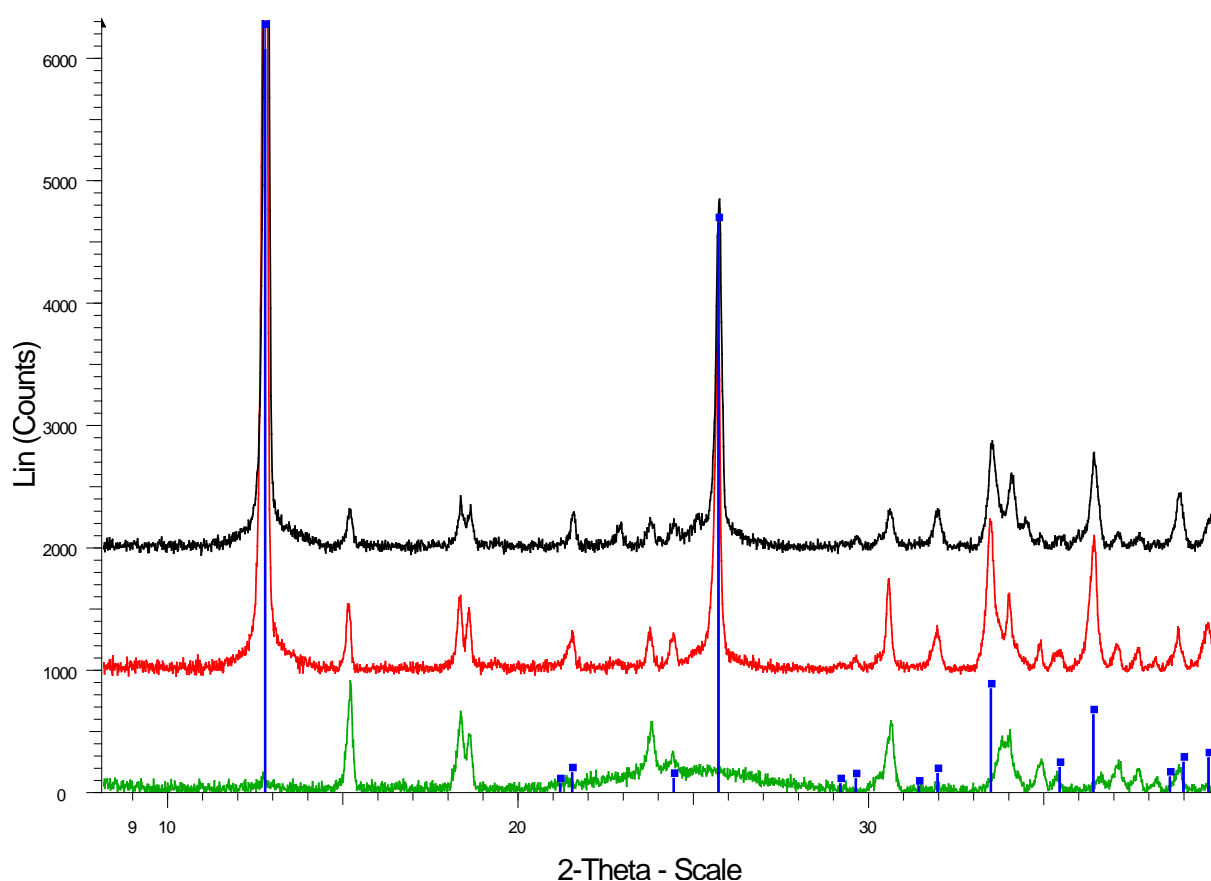


Figure 47: XRD pattern showing the results of the higher copper loading, x2 (Green), x5 (Red), and x10 (Black), Blue ticks correspond with Gerhardtite.

Surprisingly the different copper loadings did not show much variation on the quantity of the impurity that formed. However, the x2 loading did not form any of the expected copper hydroxynitrate, just impurity phase. It was later believed that this was due to the

reaction not quite reaching the temperature required. The lack of copper hydroxynitrate though proved to be an advantage, giving a clearer XRD pattern of just the impurity, which allowed a better library search of this unknown compound.

A perfect match was made with the mineral libethenite ($\text{Cu}_2(\text{PO}_4)\text{OH}$), a phosphorus containing species, which explains why the copper loading did not affect the quantity of the impurity formed. A synthetic sample of libethenite was then prepared independently from the support material in the laboratory for XRD analysis, and gave an even clearer match to the impurities present in the Darko and Aldrich copper on carbon support materials.

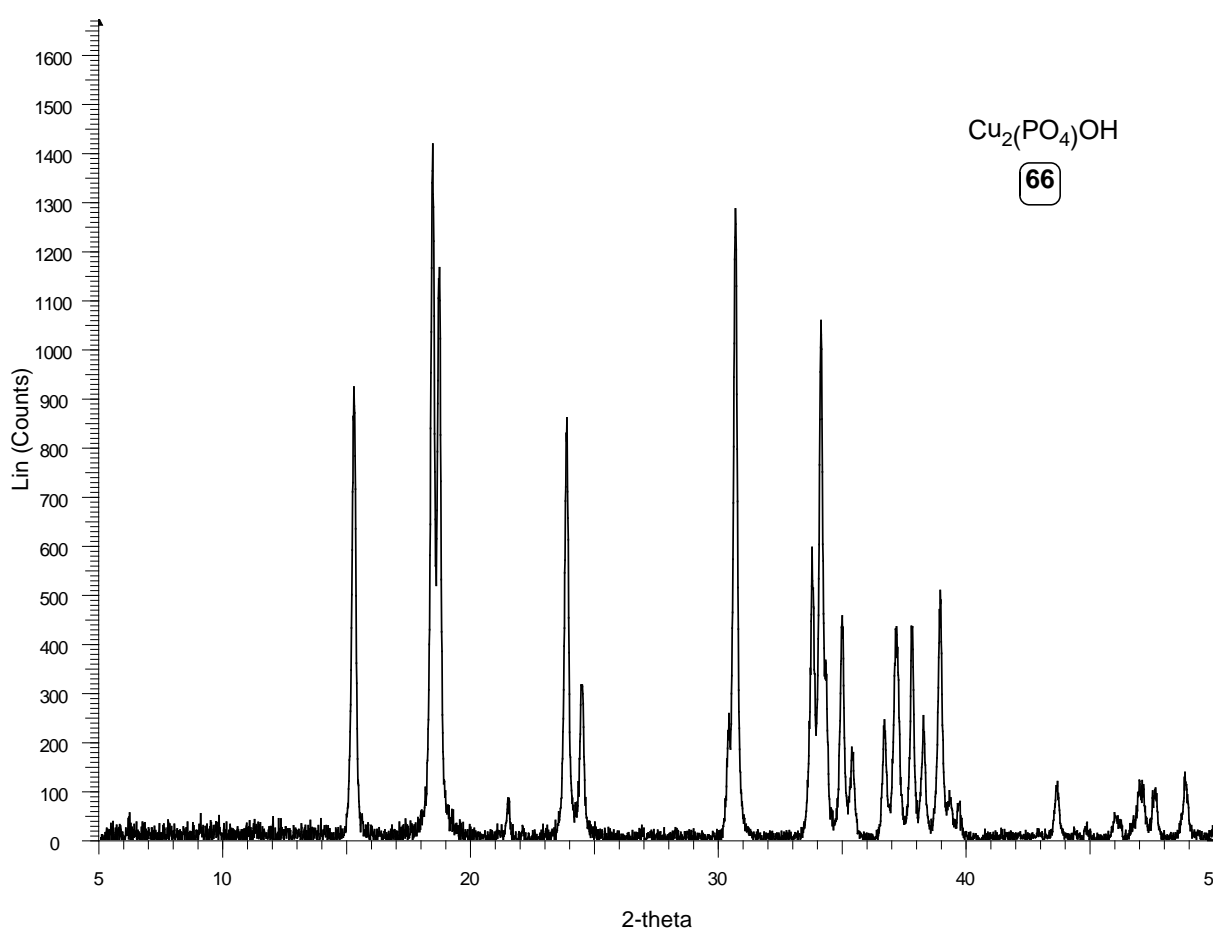


Figure 48: XRD pattern for the Libethenite sample prepared in our laboratory independently from the support materials.

Why this phosphorus containing impurity is found in the Darko carbon species and not the Norit carbon species is due to the method of activating each carbon. The Norit carbon is prepared via a method of steam activation, where-as the Darko carbon is prepared from bone ash, which would contain a low concentration of phosphorus. This could react with the copper nitrate starting material during the reaction to prepare the Copper on Carbon support material.

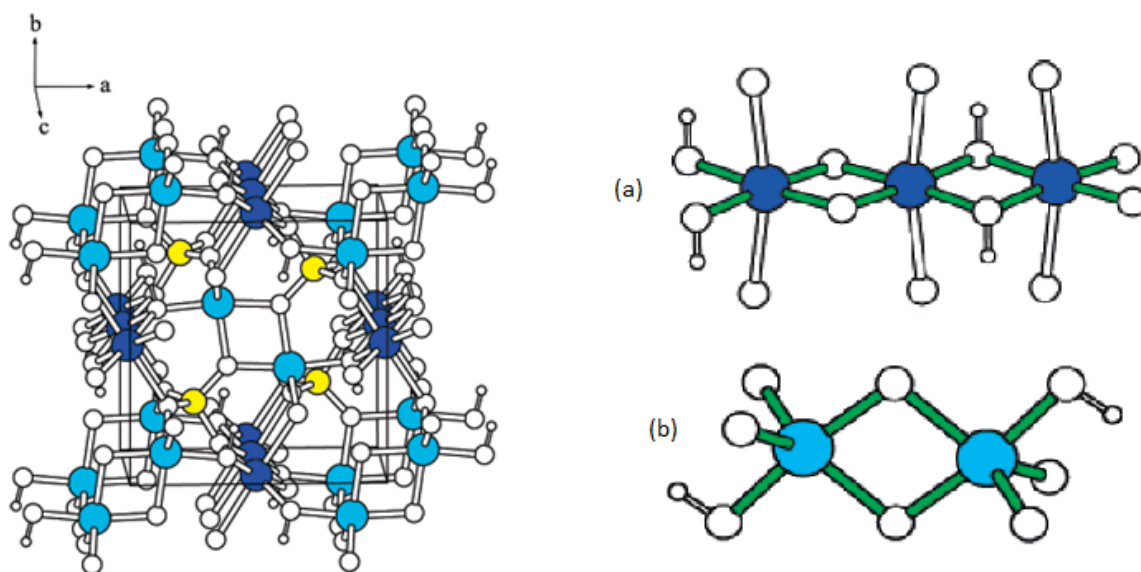
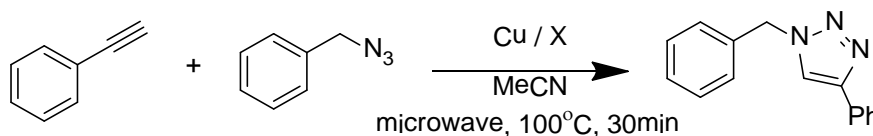


Figure 49: Perspective view of the crystal structure of Libethenite (left). (a) edge-sharing $[\text{Cu}_{12}\text{O}_6(\text{OH})_2]_{\infty}$ chain along the c axis, (b) edge-sharing $\text{Cu}_2\text{O}_6(\text{OH})_2$ dimer. ^[102]

Figure 49 shows the crystal structure of Libethenite, which unlike copper hydroxynitrate does not show a layer structure. It is believed that this will prevent the libethenite from catalysing reactions in the same way that the copper hydroxynitrate will.

Click Reactions

A series of click triazole reactions were then carried out to test the catalytic activity of the solid support materials (Scheme 32), as well as a click reaction with libethenite to show the reaction occurs due to the copper ladder species, rather than the impurity in the samples, the results are shown in Table 11.



Scheme 32: Click reaction using the Cu/X materials as catalyst

Table 11: Results of the click reaction using the Cu/X catalysts

Cu / X	Yield	Product Number
Cu/Darko Carbon	85%	(67)
Cu/Aldrich Carbon	54%	(68)
Cu/Norit Carbon	82%	(69)
Cu/Silica	98%	(70)
Cu/Alumina	89%	(71)
Cu/Titanium	93%	(72)
Libethenite	No rxn	(73)

It is believed that the triazole click reaction does not work with libethenite, due to the layer structure of the material being incompatible with the formation of the alkynyl copper(I) ladder polymer, and therefore not capable of catalysing the click reaction on its own.

The materials recovered post click reaction led to an interesting discovery. After each reaction the catalyst was recovered by filtration and dried in air. Of particular interest was the recovered copper on silica sample, which had changed colour from green to bright yellow. The material was analysed by XRD and the resulting pattern, shown in Figure 50, showed that the gerhardtite had acted as a source of copper to form the alkynyl copper(I) ladder polymer.

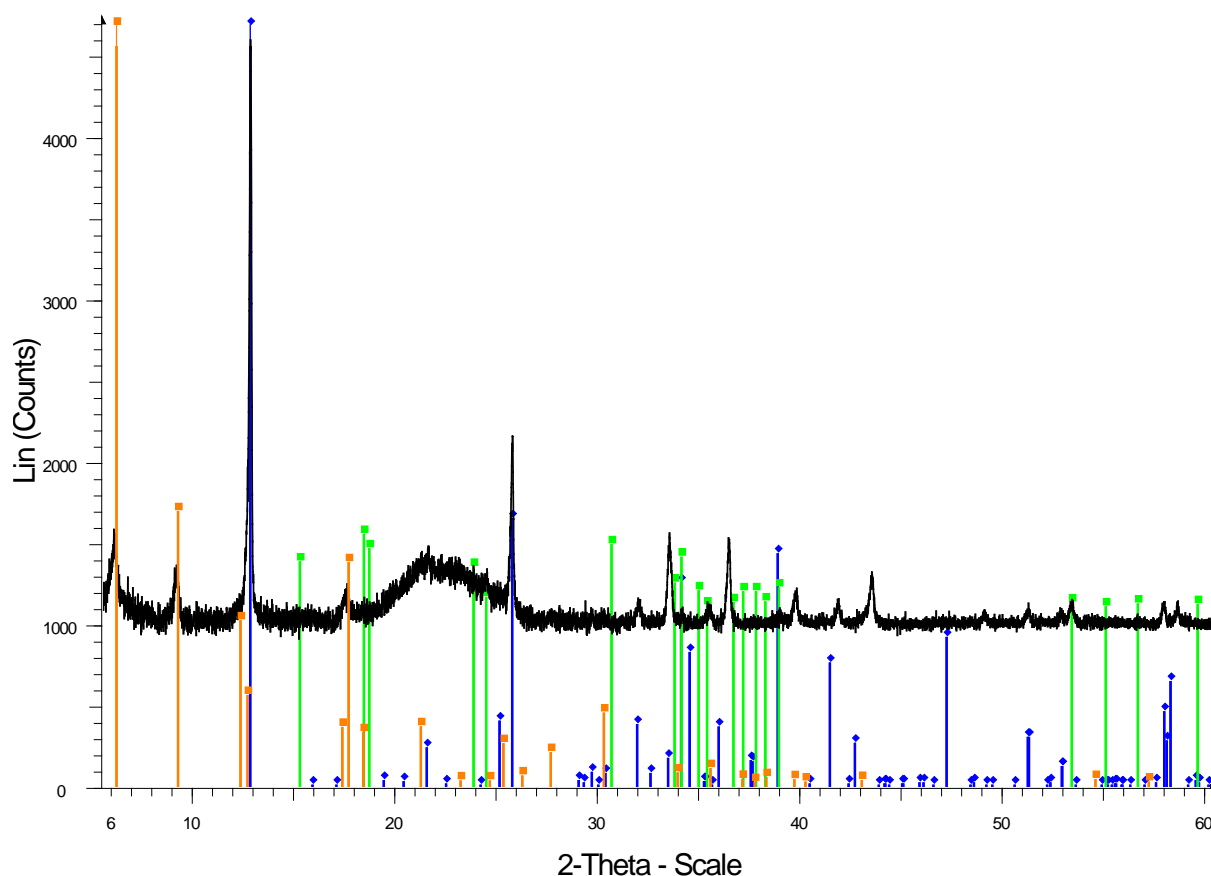
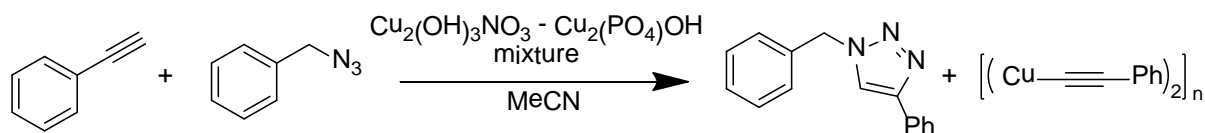


Figure 50: XRD pattern from the recovered Cu/Si material post click reaction, showing copper hydroxynitrate (blue ticks), and formed copper(I) ladder polymer (orange ticks), with libethenite shown for comparison (green ticks).

Whilst there was some conversion shown from copper hydroxynitrate to copper ladder polymer during the reaction, it was not a full conversion so a series of time controlled reactions were performed to try to drive the conversion of copper hydroxynitrate to ladder polymer. Using the conditions shown in Scheme 33, the click reaction was catalysed using a mixture of copper hydroxynitrate and libethenite without the solid support material present. We believed that this would help to remove some of the background noise from the XRD patterns making interpretation easier. The results are shown in Figure 51.



Scheme 33: Click reaction using NO₃/PO₄ mixture without the support material present.

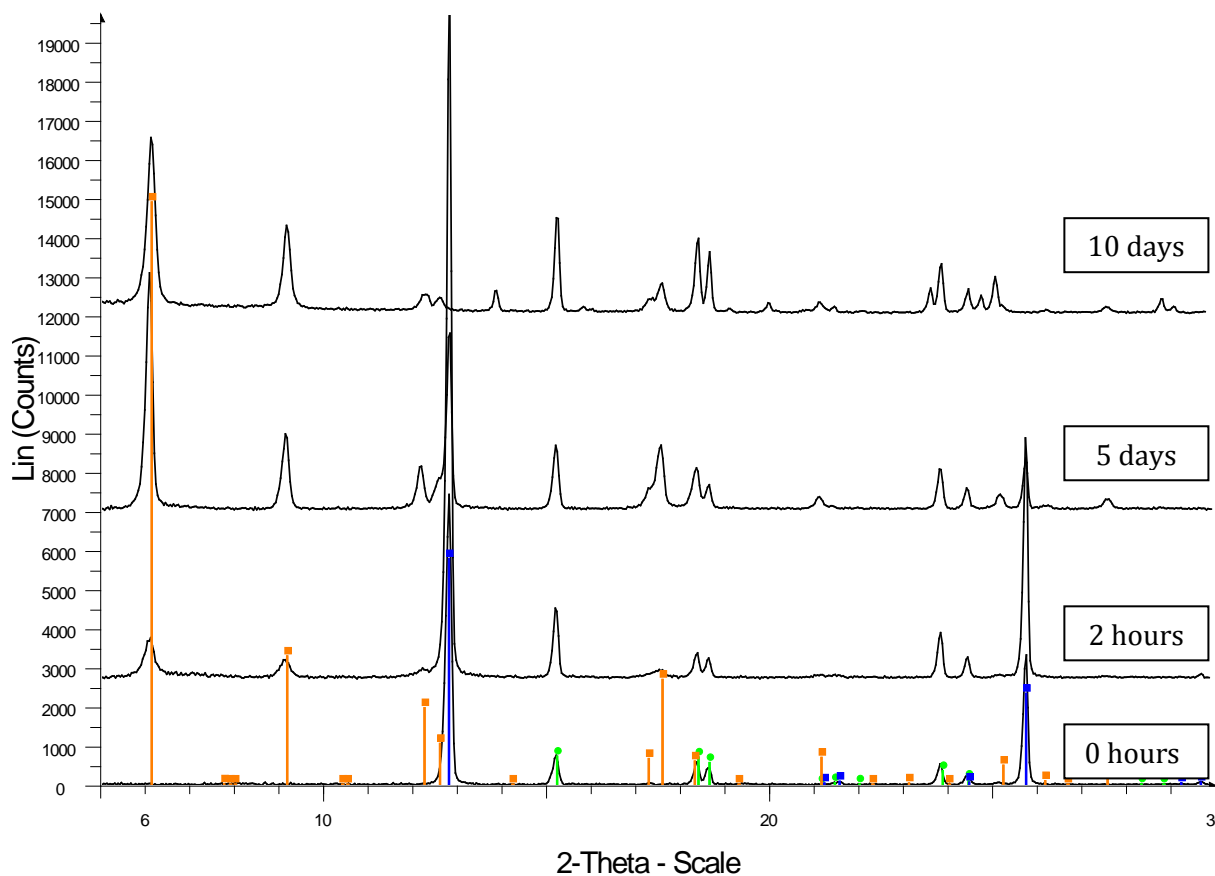


Figure 51: XRD results from the series of time controlled click reactions, showing the formation of the copper(I) ladder polymer (orange) from Gerhardtite (blue) not Libethenite (green)

The XRD patterns from 0 hours to 10 days show the gradual formation of the copper(I) ladder polymer corresponding the gradual disappearance of the copper hydroxynitrate as it is consumed during the formation of the ladder. The libethenite remains present in all XRD patterns, which proves that it has no impact on the formation of the copper(I) ladder polymer.

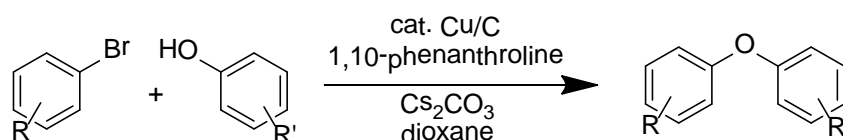
Further use of Copper on Carbon to Catalysis Organic Reactions

Further syntheses were carried out based on literature uses of copper on carbon materials to catalyse reactions. We believed that if the click reaction was forming the alkynyl copper(I) ladder polymer from the support material then it stood to reason that other reactions perhaps reacted the same way. The first reaction considered was the Ullmann copper based diaryl ether formation.

Ullmann Synthesis

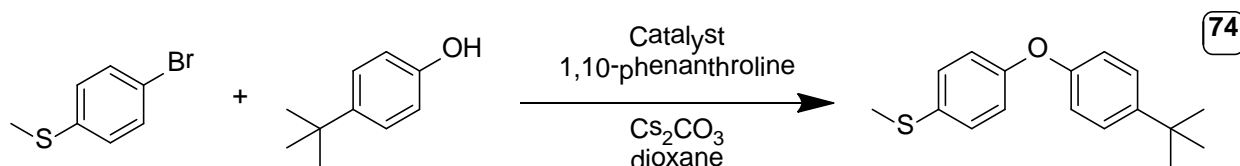
The Ullmann ether synthesis is a variation of the Ullmann reaction using a phenol to couple with an aryl halide to create a diaryl ether using a copper source. The reaction has recently received renewed interest in attempts to improve the reaction, from the use of milder conditions, ^[103] the use of copper nanoparticles as a catalyst, ^[104] or the effects of microwave heating on the reaction. ^[105] With the research into solid support materials we were conducting, we were particularly interested in the use of solid support materials, namely copper 'on' carbon as a catalysts for the Ullmann ether coupling.

The reaction was undertaken first by the Lipshutz group ^[106] who employed the use of copper on carbon to catalyse the synthesis of diaryl ethers shown in Scheme 34.



Scheme 34: Ullmann aryl ether coupling carried out by the Lipshutz group

The reaction was carried out using the same conditions and using the copper on carbon material prepared previously, shown in Scheme 35. Samples of Gerhardtite and Libethenite, as well as a reaction with no source of copper to act as a control, were carried out. The results of which can be seen in Table 12.



Scheme 35: Ullmann aryl ether coupling conditions.

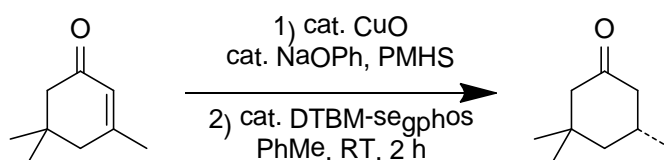
Table 12: Results of the Ullmann aryl ether coupling reactions.

Catalyst	Yield	Product Number
Cu/Carbon	49%	(74)
Gerhardtite	47%	(75)
Libethenite	44%	(76)
Control	32%	(77)

The Lipshutz group were able to obtain an 87% purified yield for the aryl ether we were attempting to replicate in synthesis ^[106], our yield was unfortunately lower, with the copper 'on' carbon catalysed reaction only giving a purified yield of 49%. However we observed little difference between the yields of the copper on carbon catalysed reaction and the other copper sources, copper hydroxynitrate and libethenite, which suggests that the solid support medium is not entirely necessary. When the reaction was carried out without any copper catalyst at all it was found that just using microwave conditions the reaction proceeded, but produced a reduced yield compared to the copper catalysed reactions.

Heterogeneous Copper-Catalysed Asymmetric Hydrogenation

Heterogeneous asymmetric catalysis remains a topic of intense research interest, predominantly due to the major synthetic challenge represented by the need to control enantioselectivity. Successful strategies to achieve this include a) adsorption of chiral modifiers onto an active metal surface, b) covalent tethering of homogeneous catalysts, and c) electrostatic interaction between a negatively charged framework and a cation, all of which have been reviewed. [107] We were again interested by the research of the Lipshutz group who were interested in implementing copper on carbon as a catalyst for asymmetric hydrogenation. [108] The catalyst used was copper 'on' carbon, the same as prepared previously in Scheme 30, and the ligand they found to work best was R-(-)-DTBM-segphos, which gave both a reasonable conversion time and high ee, shown in Figure 52.



Scheme 36: The Lipshutz groups conditions for the asymmetric hydrogenation

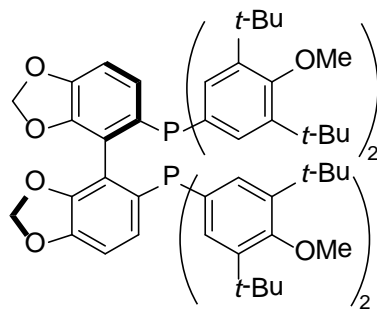
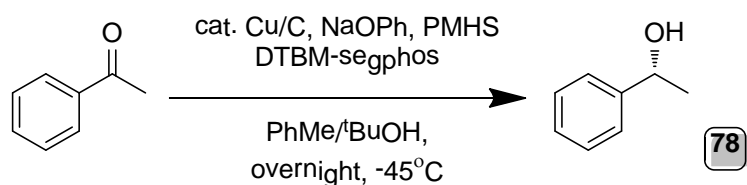


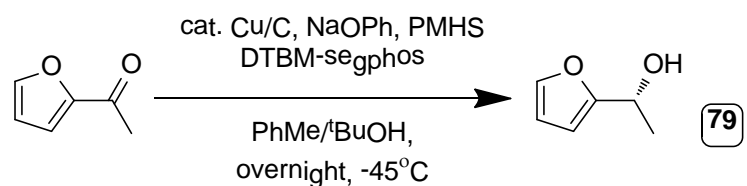
Figure 52: The ligand (R)-(-)-DTBM-segphos

Our group attempted to repeat the results of the asymmetric hydrogenation using Cu/C as a catalyst, we then envisioned continuing the investigation using the other solid support materials as catalysts. We began with the reduction of acetophenone, our reaction scheme is given in Scheme 37.



Scheme 37: Our conditions for the asymmetric hydrolysis of Acetophenone, product was obtained in a 43% yield and 86% ee.

After monitoring the reaction by TLC it was considered to contain an amount of starting material even after the 8 hours, so was left to react overnight. Even after leaving the reaction for this long there was still some starting material present in the TLC, so it was decided to continue with the procedure regardless. It is possible that this starting material is still present due to the lab equipment being capable of reaching -45°C rather than the colder -50°C that the Lipshutz group used. A 43% purified yield was obtained. This was followed by the reduction of 2-acetylfuran shown in Scheme 38.



Scheme 38: Our conditions for the asymmetric hydrolysis of 2-Acetylfuran, product was obtained in an 80% yield and 49% ee.

Using the same conditions as the acetophenone reduction this reduction worked slightly better affording the purified product in a yield of 80%.

Chapter 3 Conclusion

Through the work carried out in this chapter it has been shown that the solid support material Copper 'on' Carbon, is in fact actually a mixture of carbon and the layered material Gerhardtite. It is possible to prepare a variety of these materials by changing the carbon, not only with other types of carbon, but also with other materials such as silica and titanium.

When the material is prepared with the Norit carbon an additional compound of relatively small quantity is introduced, this was identified to be the phosphate containing mineral Libethenite.

We were then able to use these materials in the catalysis of triazole click reactions, all of which resulted in good yields. During these reactions it was discovered that the copper(I) alkynyl ladder polymer was being formed from the Gerhardtite present in the sample (not the Libethenite), and we believe that the formation of this polymer is what then catalyses the triazole click reaction.

Finally we were able to use the support materials to catalyse both a series of Ullman aryl ether couplings where we obtained a set of reasonable yields, as well as a couple of heterogeneous asymmetric hydrolyses which resulted in both good yields and ee's.

Chapter 3 Experimental

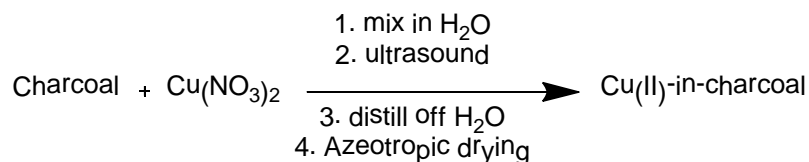
General Experimental Details

Infrared spectra were obtained using a Perkin-Elmer Paragon 1000 FT-IR spectrophotometer. ^1H and ^{13}C NMR spectra were measured at 400.13 and 100.62 MHz by using a Bruker DPX 400 MHz spectrometer or a Bruker Avance 400 MHz spectrometer. The solvent used for NMR spectrometry was CDCl_3 unless stated otherwise, with TMS (tetramethylsilane) as the internal reference. Chemical shifts are given as parts per million (ppm) and the J values are given in hertz (Hz). GCMS analysis was performed by using a Fisons GC 8000 series (AS 800), with a 15m x 0.25mm DB-5 column and electron-impact low-resolution mass spectrometer. Melting points were recorded by using a Stuart Scientific melting point apparatus (SMP3) and are uncorrected. Microanalysis were performed using an Exeter Analytical CE-440 Elemental Analyser. XRD data were recorded by using a Bruker Avance powder diffractometer operating with monochromated $\text{Cu}_{\text{K}\alpha 1}$ radiation over the 2θ range 5-60° with a 0.0147 2θ step unless stated otherwise. Mass spectra were recorded by using a Thermo Fisher Exactive with an ion max source and ESI probe fitted with Advion triversa nanomate. The enantiomeric excess was determined by chiral HPLC. A Eurocel 01 (manufactured by Knauer, ChiralOD equivalent) column was used, with the UV absorbtion detector set to 254 nm.

Preparation of solid support materials

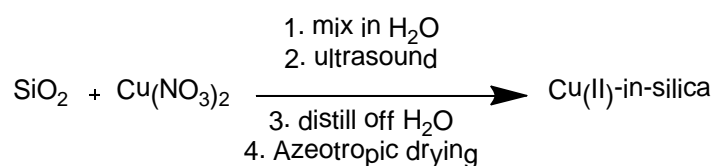
Representative synthesis of copper on support material

Preparation of Copper 'on' Carbon - (62)^[108]



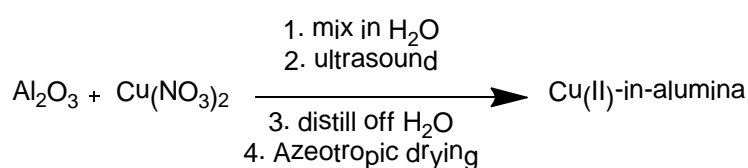
Darko KB activated carbon (15.2 g) was added to a 500 mL RBF fitted with stirrer bar. A solution of $\text{Cu}(\text{NO}_3)_2 \cdot 3\text{H}_2\text{O}$ (3.3 g, 13.8 mmol) in water (100 mL) was added to the flask, along with an additional (125 mL) water to rinse the sides of the flask. The reaction vessel was then purged with nitrogen for 30 min with vigorous stirring. The flask was then submerged in an ultrasonic bath fitted with a nitrogen balloon for 1 hour. The reaction mixture was then distilled at 175 -180°C with stirring. After the majority of the water was removed, toluene (75 mL) was added and the mixture was dried under Dean-Stark conditions overnight. A further distillation was carried out to remove the remaining solvent. A fine black powder (13.3 g recovered yield) was obtained. This solid was dried overnight in a vacuum oven at 100°C, and then stored in a desiccator. The material was then characterised by powder XRD.

Preparation of Copper 'on' Silica - (63)



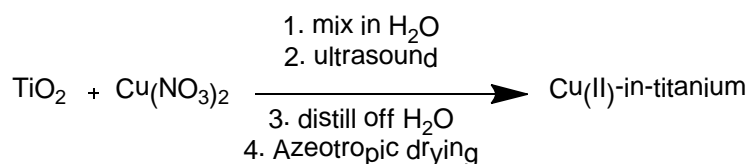
Prepared using the representative procedure from silica (15.1 g, column grade) and $\text{Cu}_2(\text{NO}_3)_2 \cdot 3\text{H}_2\text{O}$ (3.3 g, 13.8 mmol). A pale green solid was obtained (12.9 g recovered yield) and characterised by powder XRD.

Preparation of Copper 'on' Alumina - (64)



Prepared using the representative procedure from activated alumina oxide (15.0 g) and $\text{Cu}_2(\text{NO}_3)_2 \cdot 3\text{H}_2\text{O}$ (3.3 g, 13.8 mmol). A pale green solid was obtained (12.7 g recovered yield) and characterised by powder XRD.

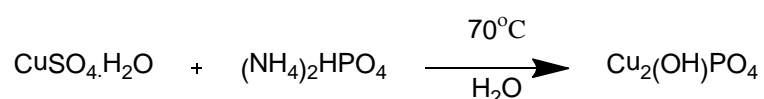
Preparation of Copper 'on' Titanium - (65)



Prepared using the representative procedure from titanium (IV) oxide (1.5 g, 18.9 mmol) and $\text{Cu}_2(\text{NO}_3)_2 \cdot 3\text{H}_2\text{O}$ (0.3 g, 1.38 mmol). A very pale green solid (1.2 g recovered yield) was obtained and characterised by powder XRD.

Libethenite

Preparation of Libethenite ($\text{Cu}_2(\text{OH})\text{PO}_4$) - (66)



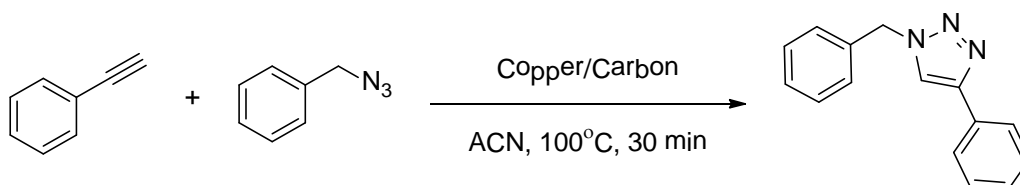
$\text{CuSO}_4 \cdot \text{H}_2\text{O}$ (1.1 g, 6.2 mmol) was added to a conical flask, water (20 mL) was then added in a separate conical flask $(\text{NH}_4)_2\text{HPO}_4$ (0.42 g, 3.2 mmol) dissolved in water (20 mL). The ammonium phosphate solution was then added to the copper sulphate solution, in a single addition, and neutralised with NH_3 (4-5 drops). The mixture was then heated to 70°C until the solution turned a light green colour. The mixture was allowed to cool, then filtered under suction and washed with H_2O (100 mL). The solid was then vacuum oven dried at 120°C for 1 hour. A light green powder was obtained (2.7 g, 90%), and identified by powder XRD.

Solid support materials in Click Reactions

Preparation of 1-benzyl-4-phenyl-1H-1,2,3-triazole using Copper on Carbon

(Darko) - (67) ^[101]

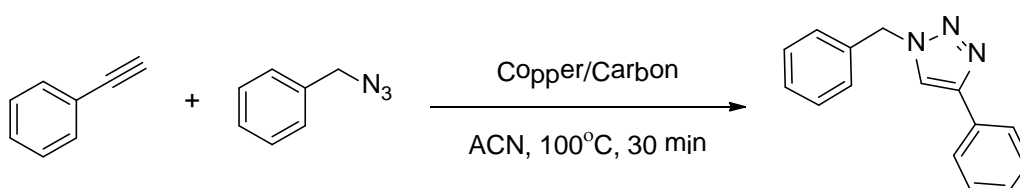
Representative click reaction using copper on support material catalyst



Benzyl azide (0.23 g, 1.7 mmol) and phenylacetylene (0.43 g, 4.2 mmol) were added to a 5 mL microwave tube fitted with magnetic stirrer bar. To this added Copper 'on' Carbon (Darko) (10 mol%) and the mixture suspended in acetonitrile (5 mL). The reaction was then heated in the microwave for 30 min at 100°C. The reaction was then allowed to cool to room temperature, the solid support material removed by gravity filtration, and washed with EtOAc (3 x 10 mL). The volatiles were removed by rotary evaporation to produce a pale off white (grey) solid (0.34 g, 85%). ¹H NMR (400 MHz, CDCl₃): δ = 5.54 (s, 2H, CH₂), 7.26-7.40 (m, 8H, CH Arom.), 7.67 (s, 1H, CH), 7.78 (d, 2H, J=7.6 Hz, CH Arom.), in agreement with the literature. ^[92]

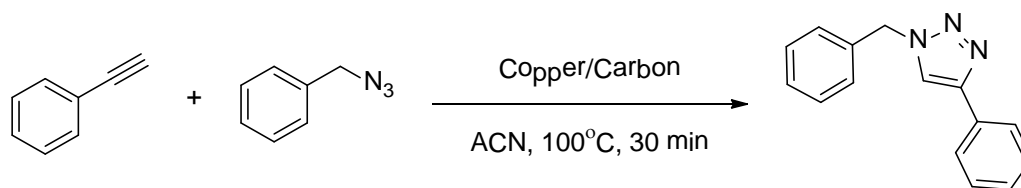
Preparation of 1-benzyl-4-phenyl-1H-1,2,3-triazole using Copper on Carbon

(Norit) - (69)



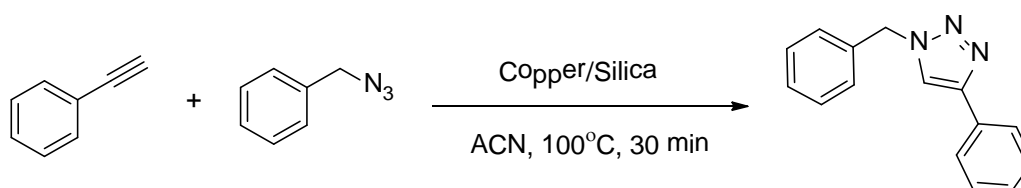
Prepared using the representative procedure from benzyl azide (0.21g, 1.6 mmol), phenylacetylene (0.41 g, 4.0 mmol) and Copper on Carbon(Nosit) (10 mol%). A pale off white (grey) solid (0.31 g, 82%) was produced. ¹H NMR (400 MHz, CDCl₃): δ = 5.54 (s, 2H, CH₂), 7.25-7.37 (m, 8H, CH Arom.), 7.69 (s, 1H, CH), 7.81 (d, 2H, J=7.6 Hz, CH Arom.).

Preparation of 1-benzyl-4-phenyl-1H-1,2,3-triazole using Copper on Carbon (Aldrich) - (68)



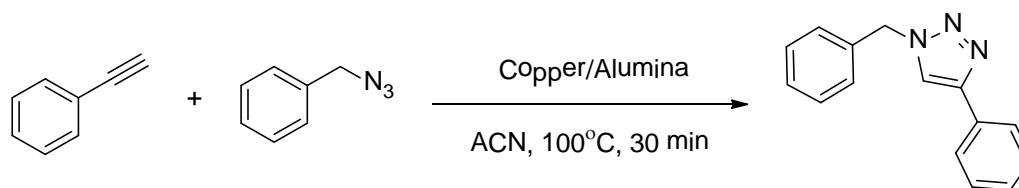
Prepared using the representative procedure from benzyl azide (0.16g, 1.2 mmol), phenylacetylene (0.27 g, 2.6 mmol) and Copper on Carbon(Nosit) (10 mol%). A pale off white (grey) solid (0.15 g, 54%) was produced. ¹H NMR (400 MHz, CDCl₃): δ = 5.57 (s, 2H, CH₂), 7.27-7.44 (m, 8H, CH Arom.), 7.68 (s, 1H, CH), 7.79 (d, 2H, J=7.6 Hz, CH Arom.)

Preparation of 1-benzyl-4-phenyl-1H-1,2,3-triazole using Silica on Carbon - (70)



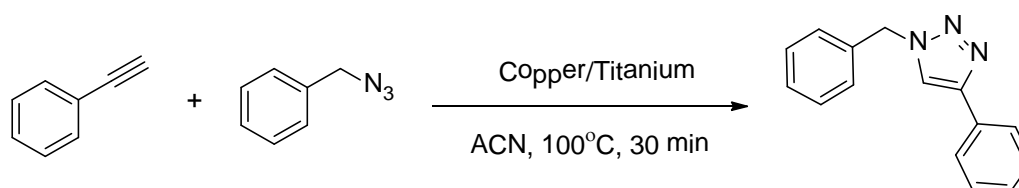
Prepared using the representative procedure from benzyl azide (0.16 g, 1.2 mmol), phenylacetylene (0.33 g, 3.2 mmol) and Copper on Silica (10 mol%). A pale creamy white solid (0.28 g, 98%) was produced. ¹H NMR (400 MHz, CDCl₃): δ = 5.58 (s, 2H, CH₂), 7.29-7.41 (m, 8H, CH Arom.), 7.70 (s, 1H, CH), 7.86 (d, 2H, J=7.6 Hz, CH Arom.)

Preparation of 1-benzyl-4-phenyl-1H-1,2,3-triazole using Alumina on Carbon - (71)



Prepared using the representative procedure from benzyl azide (0.14 g, 1.1 mmol), phenylacetylene (0.28 g, 2.7 mmol) and Copper on Alumina (10 mol%). A pale creamy white solid (0.22 g, 89%) was produced. ¹H NMR (400 MHz, CDCl₃): δ = 5.56 (s, 2H, CH₂), 7.29-7.39 (m, 8H, CH Arom.), 7.72 (s, 1H, CH), 7.82 (d, 2H, J=7.6 Hz, CH Arom.).

Preparation of 1-benzyl-4-phenyl-1H-1,2,3-triazole using Titanium on Carbon - (72)

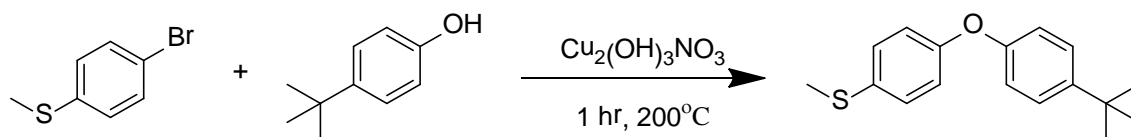


Prepared using the representative procedure from benzyl azide (0.15 g, 1.1 mmol), phenylacetylene (0.30 g, 2.9 mmol) and Copper on titania (10 mol%). A pale creamy white solid (0.24 g, 93%) was produced. ¹H NMR (400 MHz, CDCl₃): δ = 5.57 (s, 2H, CH₂), 7.29-7.41 (m, 8H, CH Arom.), 7.75 (s, 1H, CH), 7.81 (d, 2H, J=7.6 Hz, CH Arom.).

Solid support materials in Ullmann ether coupling Reactions

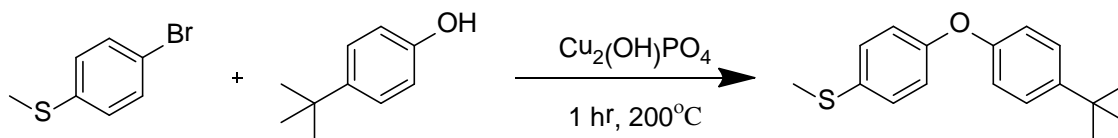
Preparation of (4-(4-(tert-butyl)phenoxy)phenyl)(methyl)sulfane using Gerhardtite - (75) ^[106]

Representative ether coupling reaction using copper on support material catalyst



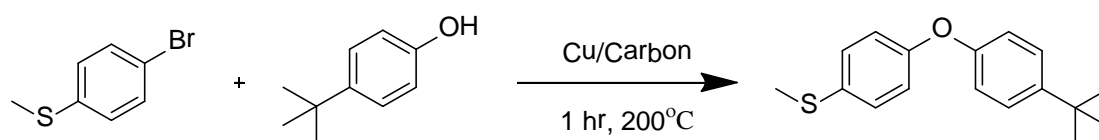
In a typical procedure $\text{Cu}_2(\text{OH})_3\text{NO}_3$ (0.03 g, 0.1 mmol) was added to an oven dry 5 mL microwave tube fitted with magnetic stirrer bar, followed by 1,10-phenanthroline (0.09 g, 0.5 mmol), caesium carbonate (0.39 g, 1.2 mmol), and 4-t-butylphenol (0.16 g, 1.0 mmol). To this mixture anhydrous dioxane (3 mL) was added by syringe and the solution turned a dark reddish purple, the resulting slurry was stirred at room temperature for 30 min. 4-bromothioanisole (0.31 g, 1.5 mmol) was added to the microwave tube, the mixture was then heated in the microwave with stirring for 1 hr at 200°C . The reaction was then allowed to cool to room temperature, filtered through celite, and washed with EtOAc (3x20 mL). The volatiles were removed by rotary evaporation. Purification by column chromatography produced a pale yellow oil (0.13 g, 47%). ^1H NMR (400 MHz, CDCl_3): δ = 1.32 (s, 9H, 3x CH_3), 2.47 (s, 3H, CH_3), 6.93 (t, 4H, $J=8.8$ Hz, CH Arom.), 7.25 (d, 2H, $J=8.8$ Hz, CH Arom.) 7.34 (d, 2H, $J=8.8$ Hz, CH Arom.). ^{13}C NMR (100 MHz, CDCl_3): δ = 17.4 (CH_3), 31.4 (3x CH_3), 34.4 (qC), 118.4 (2x CH Arom.), 119.5 (2x CH Arom.), 126.7 (2x CH Arom.), 129.4 (2x CH Arom.), 132.0 (qC), 146.3 (qC), 154.8 (qC) 155.8 (qC), in agreement with the literature. ^[97]

Preparation of (4-(4-(tert-butyl)phenoxy)phenyl)(methyl)sulfane using Libethenite - (76)



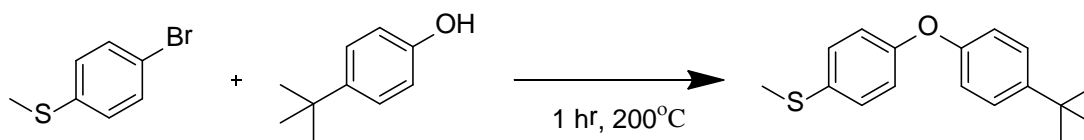
Prepared using the representative procedure from Libethenite (0.03 g, 0.15 mmol), 1,10-phenanthroline (0.09 g, 0.5 mmol), caesium carbonate (0.38 g, 1.2 mmol), 4-tert-butylphenol (0.15 g, 1.0 mmol), dioxane (3 mL) and 4-bromothioanisole (0.36 g, 1.8 mmol). Purification by column chromatography afforded a pale yellow oil (0.12 g, 44%). ^1H NMR (400 MHz, CDCl_3): δ = 1.32 (s, 9H, 3x CH_3), 2.47 (s, 3H, CH_3), 6.94 (t, 4H, $J=8.8$ Hz, CH Arom.), 7.25 (d, 2H, $J=8.8$ Hz, CH Arom.), 7.33 (d, 2H, $J=9.2$ Hz, Arom.).

Preparation of (4-(4-(tert-butyl)phenoxy)phenyl)(methyl)sulfane using Copper on Carbon - (74)



Prepared using the representative procedure from Copper on Carbon (10 mol%), 1,10-phenanthroline (0.09 g, 0.5 mmol), caesium carbonate (0.37 g, 1.1 mmol), 4-tert-butylphenol (0.16 g, 1.0 mmol), dioxane (3 mL) and 4-bromothioanisole (0.37 g, 1.8 mmol). Purification by column chromatography afforded a pale yellow oil (0.13 g, 49%). ^1H NMR (400 MHz, CDCl_3): δ = 1.21 (s, 9H, 3x CH_3), 2.33 (s, 3H, CH_3), 6.82 (t, 4H, $J=8.8$ Hz, CH Arom.), 7.12 (d, 2H, $J=8.8$ Hz, CH Arom.), 7.21 (d, 2H, $J=9.2$ Hz, CH Arom.).

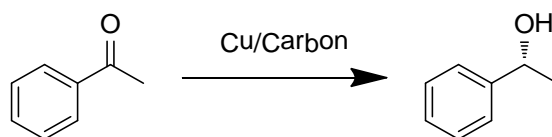
Preparation of (4-(4-(tert-butyl)phenoxy)phenyl)(methyl)sulfane - Control - (77)



Prepared using the representative procedure from 1,10-phenanthroline (0.09 g, 0.5 mmol), caesium carbonate (0.36 g, 1.1 mmol), 4-t-butylphenol (0.16 g, 1 mmol), dioxane (3 mL) and 4-bromothioanisole (0.36 g, 1.8 mmol). Purification by column chromatography afforded a pale yellow oil (0.09 g, 32%). ^1H NMR (400 MHz, CDCl_3): δ = 1.23 (s, 9H, 3x CH_3), 2.37 (s, 3H, CH_3), 6.85 (t, 4H, $J=8.8$ Hz, CH Arom.), 7.16 (d, 2H, $J=8.8$ Hz, CH Arom.), 7.24 (d, 2H, $J=8.8$ Hz, CH Arom.).

Solid support materials in Asymmetric Hydrolysatation Reactions

Preparation of 1-phenylethanol - (78) [108]



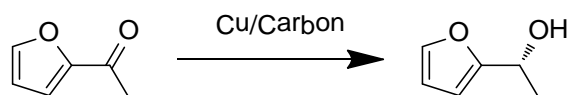
Copper on Carbon (10 mol%) was added to a flame dried 25 mL RBF, fitted with magnetic stirrer bar, followed by sodium phenolate (0.02 g) and DTBM-segphos (0.004 g), all of which was suspended in toluene (2 mL) and the mixture allowed to stir at room temperature for 90 min.

PMHS (0.24 mL) was then added and the mixture stirred at room temperature for a further 60 min. The reaction mixture was then cooled to -45°C and acetophenone (0.25 mL, 2.1 mmol) in $t\text{BuOH}$ (0.25 mL) was added dropwise. The reaction was then left to stir overnight at -45°C .

After the reaction had been allowed to warm to room temperature, the Cu/Carbon was removed by gravity filtration and washed with ether (3x5 mL). The filtrate was then neutralised with sodium hydroxide (3M, 15 mL) for 2 hours. The product was extracted with ether (50 mL), dried with magnesium sulphate, and the volatiles removed by rotary evaporation to produce a crude yellow oil.

Purification by column chromatography produced a pale yellow oil (0.11 g, 43%, 86% ee). IR (thin film): $\nu = 739.1, 1240.1, 1487.2, 1588.6, 2963.2, 3049.1$. $^1\text{H NMR}$ (400 MHz, CDCl_3): $\delta = 1.47$ (d, 3H, $J=6.4$ Hz, CH_3), 2.24 (s, broad, 1H, OH), 4.85 (q, 1H, $J=6.4$ Hz, CH), 7.35 (m, 5H, CH Arom.). $^{13}\text{C NMR}$ (100 MHz, CDCl_3): $\delta = 31.4$ (CH_3), 77.4 (CH), 126.7 (2x CH Arom.), 128.9 (CH Arom.), 129.4 (2x CH Arom.), 146.3 (qC), in agreement with the literature. [99]

Preparation of 1-(cyclopenta-1,3-dien-1-yl)ethanol - (79) [108]



Copper on Carbon (10 mol%) was added to a flame dried 25 mL RBF, fitted with magnetic stirrer bar, followed by sodium phenolate (0.02 g) and DTBM-segphos (0.008 g), all of which was suspended in toluene (2 mL) and the mixture allowed to stir at room temperature for 90 min.

PMHS (0.24 mL) was then added and the mixture stirred at room temperature for a further 60 min. The reaction mixture was then cooled to -45°C and 2-acetylfuran (0.22 g, 2 mmol) in $t\text{BuOH}$ (0.25 mL) was added dropwise. The reaction was then left to stir overnight at -45°C .

After the reaction had been allowed to warm to room temperature, the Cu/Carbon was removed by gravity filtration and washed with ether (3x5 mL). The reaction was then neutralised with sodium hydroxide (3M, 15 mL) for 2 hours. The product was extracted with ether (50 mL), dried with magnesium sulphate, and the volatiles removed by rotary evaporation to produce a crude yellow oil.

Purification by column chromatography produced a pale yellow oil (0.18 g, 80%, 49% ee). IR (thin film): $\nu = 650.5, 735.1, 908.8, 1082.3, 1260.8, 2165.6, 2254.0, 2972.5$. ^1H NMR (400 MHz, CDCl_3): $\delta = 1.51$ (d, 3H, $J=4.4$ Hz, CH_3), 3.63 (s, broad, 1H, OH), 4.10 (q, 1H, $J=7.2$ Hz, CH), 6.24 (m, 1H, CH Arom.), 6.32 (m, 1H, CH Arom.), 7.37 (m, 1H, CH Arom.). ^{13}C NMR (100 MHz, CDCl_3): $\delta = 30.1$ (CH_3), 62.3 (CH), 103.4 (CH Arom.), 108.4 (CH Arom.), 139.8 (CH Arom.), 155.6 (qC), in agreement with the literature. [99]

Conclusions

This thesis has demonstrated throughout the potential uses of copper(I) alkynyl ladder polymers as catalysts. Their structural characterisations have been investigated using a variety of techniques, and the differences in structure caused by the R group on the copper chain have been of particular interest. This work has shown that it is possible to tailor the copper ladder polymers by changing this R group to have specific characteristics desirable for catalysing various reactions. It has also shown preparation of mixed metal ladders are possible, which could be advantageous in the catalysis of multi component one pot reactions.

The application of the copper(I) alkynyl ladder polymers has also been investigated using the CuAAC reaction, where excellent yields were obtained. The reaction conditions can be easily altered for greener chemistry where desired. It is also possible by using iodoalkynes to introduce an iodo group tether, this can provide further interesting synthetic possibilities.

Finally a series of solid support materials were investigated, and it was discovered that the materials were composed largely of the material copper hydroxynitrate, rather than being truly solid supports. These materials are also capable of catalysing the CuAAC reaction as the Gerhardtite is able to form the copper(I) alkynyl ladder polymer in-situ which is then thought to catalyse the reactions.

Further Work

Whilst this project has detailed many of the structural characteristics of the copper(I) alkynyl ladder polymers, as well as their use as catalysts in click chemistry, there is still scope for further investigation into both the structural properties of the ladder polymers and also the range of uses as catalysts.

Further characterisation of the ladder structures is the first possibility for further work. Of most importance in this area would be the refinement of the powder XRD data for the range of synthesised ladder polymers. By determining the space groups of each species a better understanding of the structural packing and bond lengths could be determined. Another technique not yet attempted in this project would be the use of SEM to help with the structural characterisation of each ladder polymer, and would ideally provide information on both a dry and solvated state showing any particular visible differences of interest.

Finally a series of flow experiments could be conducted and monitored by XRD, although this would require a powerful instrument for example the diffractometers powered by the synchrotron at the Diamond Light Source institute. The experiment would consist of a flow cell maintained in a position that would allow a portion of the cell to be monitored by synchrotron powder XRD. The cell would contain one of the ladder polymer species or possibly their copper hydroxyacetate starting material. By passing a flow of the reactants through this cell it would be possible to monitor either the structural changes of the ladder polymers during catalysis, or even the formation of the ladder polymer followed by its use in catalysis in a single process. Since the instruments are capable of acquiring high resolution diffraction patterns in seconds it would be possible to track even the smallest changes in the ladder polymers structures.

An effort to introduce various different metals other than copper into the ladder polymer structure would be of significant value. Some work was undertaken within this project and it was proven that it was possible to introduce silver atoms into the backbone of the copper ladder polymer. However, full characterisation was not obtained, so it was unknown what arrangement the two metals took, or the quantity ratio between the two. Once full characterisation is achieved it could be possible to control both the ordering and the ratio of the metals via the method of preparation. This

would allow further tailoring of the ladder polymers to suit the needs of the reactions they catalysed. If further investigation into mixed copper silver ladder proved fruitful it may even be possible to introduce further metals such as gold.

Further work could also be continued on the range of reactions that the copper ladders could catalyse. Following on from the previous possibility of mixed metal ladders, if they were successfully synthesised, it may be possible to catalyse multistep one pot reactions using the ladder polymers, which would make them extremely synthetically viable.

Supplementary Work

The following manuscripts were published by the date of submission of this thesis.

Heterogeneous Catalytic Reactions “On Water” by Using Stable Polymeric Alkynylcopper(I) Pre-Catalysts: Alkyne/Azide Cycloaddition Reactions

Benjamin R. Buckley, Sandra E. Dann, Harry Heaney, Emma C. Stubbs

European Journal of Organic Chemistry

2011, Issue 4, pages 770–776

Dinuclear alkynylcopper(I) complexes have been found to be the active pre-catalysts in copper-catalysed cycloaddition of azides and terminal alkynes (CuAAC). These copper(I) ladderane polymers are used in “on water” CuAAC reactions, with loadings as low as 1 mol-%.

Alkynylcopper(I) polymers and their use in a mechanistic study of alkyne–azide click reactions

Benjamin R. Buckley, Sandra E. Dann, Daniel P. Harris, Harry Heaney, Emma C. Stubbs

Chemical Communications

2010, Issue 46, pages 2274-2276

Polymeric dinuclear alkynylcopper(I) complexes, for example phenylethynylcopper(I), can be prepared by a robust method involving the interaction of terminal alkynes with copper(II) salts in acetonitrile. The use of the ladder polymers provides heterogeneous catalysts for copper-catalyzed azide–alkyne cycloaddition (CuAAC) reactions and provides important mechanistic information.

References

- [1] H. Henning, J.F. Liebman, H.M. Perko. *PATAI's Chemistry of Functional Groups*. **2009**.
- [2] J.A. Fuerst. *Annual Review of Microbiology*. **2005**, 59, 299-328
- [3] X. Wang, K-C. Lau, W-K. Li. *J. Phys. Chem. A*. **2009**, 113, 3413-3419
- [4] R.N. Warrener, G. Abbenante, C.H.L. Kennard. *J. Am. Chem. Soc.* **1994**, 116, 3645-3646
- [5] G. Mehta, M.B. Viswanath. *J. Braz. Chem. Soc.* **1996**, 7, 219-224
- [6] L.R. MacGillivray, G.S. Papaefstathiou, T. Frišćić, T.D. Hamilton, D-K Bučar, Q. Chu, D.B. Varshney, I.G. Georgiev. *Acc. Chem. Res.* **2008**, 41, 280-291
- [7] H. Matsumoto, S. Kyushin, M. Unno, R. Tanaka. *J. Organomet. Chem.* **2000**, 611, 52-63
- [8] S. Ayyappan, X. Bu, A.K. Cheetham, S. Natarajan, C.N.R. Rao. *Chem. Commun.* **1998**, 2181-2182
- [9] S. Neeraj, S. Natarajan, C.N.R.Rao. *Chem Mater.* **1999**, 11, 1390-1395
- [10] P.W.R. Corefield, H.M.M Shearer. *Acta. Cryst.* **1966**, 21, 957-965
- [11] Y. Ide, N. Ochi, M. Ogawa. *Angew. Chem.* **2011**, 123, 680-682
- [12] K. Ladewig, Z.P. Xu, G.Q. Lu. *Expert opinion on drug delivery*. **2009**, 6, 907-922
- [13] F. Leroux, J-P. Besse. *Chem. Mater.* **2001**, 13, 3507-3515
- [14] M-Q Zhao, Q. Zhang, J-Q. Huang, J-Q. Nei, F. Wei. *Carbon*. **2010**, 48, 3260-3270
- [15] G.R. Williams, D. O'Hare. *J. Matter. Chem.* **2006**, 16, 3065-3074
- [16] G.G.C. Arizaga, K.G. Satyanarayana, F. Wypych. *Solid State Ionics*. **2007**, 178, 1143-1162
- [17] D.G. Costa, A.B. Rocha, W.F. Souza, S.S.X. Chiaro, A.A. Leitão. *J. Phys. Chem.* **2008**, 112, 10681-10687
- [18] C. Henrist, K. Traina, C. Hubert, G. Toussaint, A. Rulmont, R. Cloots. *J. Cryst. Growth*. **2003**, 254, 176
- [19] J. Zhang, F. Zhang, L. Ren, D.G. Evans, W. Duan. *Matter. Chem. Phys.* **2004**, 85, 207
- [20] H. Tanaka, S. Terada. *J. Thermal. Anal.* **1993**, 39, 1011
- [21] N. Guillou, M. Louër, D. Louër. *J. Solid.State. Chem.* **1994**, 109, 307
- [22] B. Bovio, S. Locchi. *J. Crystallogr. Spectr. Res.* **1982**, 12, 507
- [23] D.C. Pereira, D.L.A. de Farria, V.R.L. Constantino. *J. Braz. Chem. Soc.* **2006**, 17, 1651-1657

-
- [24] J. M. Aguirre, A. Gutiérrez, O. Giraldo. *J. Braz. Chem. Soc.* **2011**, *22*, 546-551
- [25] R.L. Frost, P. Leverett, P.A. Williams, M.L. Weier, K.L. Erickson. *J. Raman. Spectrosc.* **2004**, *35*, 991
- [26] E.A. Secco, G.G. Worth. *Can. J. Chem.* **1987**, *65*, 2504
- [27] P.M. Castro, P.W. Jagodzinski. *Spectrochim. Acta.* **1991**, *47A*, 1707
- [28] S. Iijima. *Nature.* **1991**, *354*, 56
- [29] C.L. Zhu, C.N. Chen, L.Y. Hao, Y. Hu, Z.Y. Chen. *J. Cryst. Growth.* **2004**, *263*, 473-479
- [30] V.W-W. Yam, W.K-M. Fung, M-T. Wong. *Organometallics.* **1997**, *16*, 1772-1778
- [31] G-J. Zhou, W-Y. Wong. *Chem. Soc. Rev.* **2011**, *40*, 2541-2566
- [32] J. Nishijo, C. Okabe, J. Bushiri, K. Kosugi, N. Nishi, and H. Sawa. *Eur. Phys. J. D.* **2005**, *34*, 219-222
- [33] V.W-W. Yam, K.K-W. Lo, K.M-C. Wong. *J. Organomet. Chem.* **1999**, *578*, 3-30
- [34] Y-P. Zhou, E-B. Liu, J. Wang, H-Y. Chao. *Inorg. Chem.* **2013**, *52*, 8629-8637
- [35] V.W-W. Yam, K.K-W. Lo. *Chem. Soc. Rev.* **1999**, *28*, 323-334
- [36] G.F. Manbeck, W.W. Brennessel, R.A. Stockland, Jr., R. Eisenberg. *J. Am. Chem. Soc.* **2010**, *132*, 12307-12318
- [37] C.E. Powell, M.G. Humphrey. *Coord. Chem. Rev.* **2004**, *248*, 725-756
- [38] M.C.B. Colbert, J. Lewis, N.J. Long, P.R. Raithby, M. Younus, A.J.P. White, D.J. Williams, N.N. Payne, L. Yellowlees, D. Beljonne, N. Chawdhury, R.H. Friend. *Organometallics.* **1998**, *17*, 3034-3043
- [39] N.J. Long, C.K. Williams. *Angew. Chem. Int. Ed.* **2003**, *42*, 2586-2617
- [40] M.I. Bruce, R. Clark, J. Howard, P. Woodward. *J. Organomet. Chem.* **1972**, *42*, 107
- [41] O.M. Alousalah, M.I. Bruce. *J. Chem. Soc. Dalton trans.* **1974**, 2302
- [42] P.J. Kim, H. Massai, K. Sonogashira, N. Hagihara. *Inorg. Nucl. Chem. Lett.* **1970**, *6*, 181
- [43] D.M.P. Mingos, R. Vilar. D. Rais. *J. Organomet. Chem.* **2002**, *641*, 126-133
- [44] W. Lu, N. Zhu, C.M. Che. *J. Organomet. Chem.* **2003**, *670*, 11-16
- [45] W. Lu, B.X. Mi, M.C.W. Chan, C.M. Che, N. Zhu, S.T. Lee. *J. Am. Chem. Soc.* **2004**, *126*, 4958-4971

-
- [46] P.K.M. Siu, S.W. Lai, W. Lu, N. Zhu, C.M. Che. *Eur. J. Inorg. Chem.* **2003**, 2749-2752
- [47] S.S.Y. Chui, M.F.Y. Ng, C.M. Che. *Chem. Eur. J.* **2005**, *11*, 1739-1749
- [48] W.H. Chan, Z.Z. Zhang, T.C.W. Mak, C.M. Che. *J. Organomet. Chem.* **1998**, *556*, 169-172
- [49] L. Naldini, F. Demartin, M. Manassero, M. Sansoni, G. Rassu, M.A. Zoroddu. *J. Organomet. Chem.* **1985**, *279*, C42-C44
- [50] J. Emsley. *The Elements, Clarendon, Oxford, UK.* **1989**, p.192
- [51] H. Schmidbaur. *Chem. Soc. Rev.* **1995**, *24*, 391-400
- [52] P. Thompson, I.G. Wood. *J. Appl. Cryst.* **1983**, *16*, 458-472
- [53] A. Al-Obaidi, G. Baranovič, J. Coyle, C.G. Coates, J.J. McGarvey, V. McKee, J. Nelson. *Inorg. Chem.*, **1998**, *37*, 3567-3574
- [54] I.A. Garbusova, V.T. Alexanjan, L.A. Leites, I.R. Golding, A.M. Sladkov. *J. Organomet. Chem.* **1973**, *54*, 341-344
- [55] S. W. Millward, H.D. Angew, B. Lai, S.S. Lee, J. Lim, A. Nag, S. Pitram, R. Rohde, J.R. Heath. *Integr. Biol.* **2013**, *5*, 87-95
- [56] G. de Almeida, E.M. Sletten, H. Nakamura, K.K. Palaniappan, C.R. Bertozzi. *Angew. Chem.* **2012**, *124*, 2493-2497
- [57] M. Savonnet, A. Camarata, J. Canivet, D. Bazer-Bachi, N. Bats, V. Lecocq, C. Pinel, D. Farrusseng. *Dalton Trans.* **2012**, *41*, 3945-3948
- [58] H.C. Kolb, M.G. Finn, K.B. Sharpless. *Angew. Chem. Int. Ed.* **2001**, *40*, 2004-2021
- [59] C.W. Tornøe, C. Christensen, M. Meldal. *J. Org. Chem.* **2002**, *67*, 3057-3062
- [60] V.V. Rostovtsev, L.G. Green, V.V. Fokin, K.B. Sharpless. *Angew. Chem. Int. Ed.* **2002**, *41*, 2596-2599
- [61] J.E. Hein, V.V. Fokin. *Chem. Soc. Rev.* **2010**, *39*, 1302-1315
- [62] G.C. Tron, T. Pirali, R.A. Billington, P.L. Canonico, G. Sorba, A.A. Genazzani. *Med. Res. Rev.* **2008**, *60*, 958-970
- [63] V.V. Fokin. *ACS Chem. Biol.* **2007**, *2*, 775-778
- [64] M. Meldal, C.W. Tornøe. *Chem. Rev.* **2008**, *108*, 2952-3015
- [65] A. Michael. *Journal für Praktische Chemie.* **1893**, *48*, 94-95
- [66] R. Huisgen. *Angew. Chem. Int. Ed. Engl.* **1963**, *2*, 565-598

-
- [67] F.Himo, T. Lovell, R. Hilgraph, V.V. Rostovtsev, L. Noodleman, K.B. Sharpless, V.V. Fokin. *J. Am. Chem. Soc.* **2005**, *127*, 210-216
- [68] M. Ahlquist, V.V Fokin. *Organometallics*. **2007**, *26*, 4389-4391
- [69] B.F Straub. *Chem. Commun.* **2007**, 2868-3870
- [70] J.E. Hein, J.C. Tripp, L.B. Krasnova, K.B. Sharpless, V.V. Fokin. *Angew. Chem. Int. Ed.* **2009**, *48*, 8018-8021
- [71] B.T. Worrell, J.A. Malik, V.V. Fokin. *Science*. **2013**, *340*, 457-460
- [72] P. Siemsen, R.C. Livingston, F. Diederich. *Angew. Chem. Int. Ed.* **2000**, *39*, 2632-2657
- [73] C. Glaser. *Ber. Dtsch. Chem. Ges.* **1869**, *2*, 422-424
- [74] F. Bohlmann, H. Schönowsky, E. Inhoffen, G. Grau. *Chem. Ber.* **1964**, *97*, 794-800
- [75] S. Claude, J.M. Lehn, F. Schmidt, J.P. Vigneron. *J. Chem. Soc. Chem. Commun.* **1991**, 1182-1185
- [76] L. S. Campbell-Verduyn, L. Mirfeizi, R. A. Dierckx, P. H. Elsinga, B. L. Feringa. *Chem. Commun.* **2009**, 2139-2141
- [77] T. Achard, A. Lepronier, Y. Gimbert, H. Clavier, L. Giordano, A. Tenaglia, G. Buono. *Angew. Chem. Int. Ed.* **2011**. *50*, 3552-3556
- [78] M. Koyama, N. Ohtani, F. Kai, I. Moriguchi, S. Inouye. *J. Med. Chem.* **1987**, *30*, 552-562
- [79] L.S. Campbell-Verduyn, L. Mirfeizi, R.A. Dierckx, P.H. Elsinga, B.L. Feringa, *Chem. Commun.*, **2009**, 2139
- [80] N. Kayambu, K. Mayilvasagam, P. Kasi, *Chem. Eur. J.* **2009**, *15*, 2755
- [81] M. G. Finn, V. V. Fokin, V. O. Rodionov, *Angew. Chem.*, **2005**, *117*, 2250; *Angew. Chem. Int. Ed.* **2005**, *44*, 2210
- [82] K. Kamata, Y. Nakagawa, K. Yamaguchi, N. Mizuno, *J. Am. Chem. Soc.* **2008**, *130*, 15304
- [83] H. A. Orgueira, D. Fokas, Y. Isome, P. C.-M. Chan, C. M. Baldino, *Tet. Lett.*, **2005**, *46*, 2911
- [84] L. Leeb, P. Gmeiner, S. Loeber, *QSAR & Combinatorial Science*, **2007**, *26*, 1145
- [85] Solid Supports and Catalysis in Organic Synthesis; Smith, K, Ed; Ellis Horwood and PTR Prentice Hall. New York **1992**.
- [86] Heterogeneous Catalysis in Practice; Satterfield C.N; McGraw-Hill. New York **1980**.

-
- [87] S. Yang, C. Shen, X. Lu, H. Tong, J. Zhu, X. Zhang, H-J. Gao. *Electrochimica Acta*, **2012**, 62, 242-249
- [88] K. Chizari, A. Deneuve, O. Ersen, I. Florea, Y. Liu, D. Edouard, I. Janowska, D. Begin, C. Pham-Huu. *ChemSusChem*, **2012**, 5, 102-108
- [89] J. Zhu, M. Lu, M. Li, J. Zhu, Y. Shan. *Mater. Chem. Phys.*, **2012**, 132, 316-323
- [90] C. Hagelücken. *Erzmetall*. **1996**, 49, 122
- [91] H. Marsh, F.R. Reinoso. *Activated Carbon, Elsevier*. **2006**
- [92] A. Dandekar, R.T.K. Baker, M.A. Vannice. *J. Catal.* **1999**, 183, 131-154
- [93] H.F. Stoeckli. *Carbon*. **1990**, 1, 28
- [94] E. Auer, A. Freund, J. Pietsch, T.Tacke. *Appl. Catal.* **1998**, 173, 259-271
- [95] L.R. Radovic. *Hem. Ind.* **1996**, 50, 225
- [96] www.norit.com/carbon-academy/introduction/
- [97] D.S. Cameron, S.J. Cooper, I.L. Dodgson, B. Harrison, J.W. Jenkins. *Catal. Today*. **1990**, 7, 113
- [98] B. H. Lipshutz, B.R. Taft. *Angew Chem*. **2006**, 198, 8415-8418
- [99] B.H. Lipshutz, B.A. Frieman, A.E. Tomas Jr. *Angew. Chem*. **2006**, 198, 1281-1286
- [100] C-T. Lee, S. Huang, B.H. Lipshutz. *Adv. Synth. Catal.* **2009**, 351, 3139-3142
- [101] B.R. Buckley, S.E. Dann, D.P. Harris, H.Heaney, E.C. Stubbs. *Chem Commun*. **2010**, 46, 2274-2276
- [102] A.A. Belik, H-J. Koo, M-H. Whangbo, N. Tsujii, P. Naumov, E. Takayama-Muromachi. *Inorg. Chem*. **2007**, 46, 8684-8689
- [103] H-J. Cristau, P.P Cellier, S. Hamada, J-F. Spindler, M. Taillefer. *Org. Lett.* **2004**, 6, 913-916
- [104] M. Kidwai, N.K. Mishra, V. Bansai, A. Kumar, S. Mozumdar. *Tet. Lett.* **2007**, 48, 8883-8887
- [105] N.D. D'Angelo, J.J Peterson, S.K. Booker, I.Fellows, C. Dominguez, R. Hungate, P.J. Reider, T-S. Kim. *Tet. Lett.* **2006**, 47, 5045-5048
- [106] B.H. Lipshutz, J.B. Unger, B.R. Taft. *Org. Lett.* **2007**, 9, 1089-1092
- [107] G.J. Hutchings. *Annual Review of Materials Research*, **2005**, 35, 143-166
- [108] B.H. Lipshutz, B.A. Frieman, A.E. Tomaso Jr. *Angew. Chem*. **2006**, 45, 1259-1264